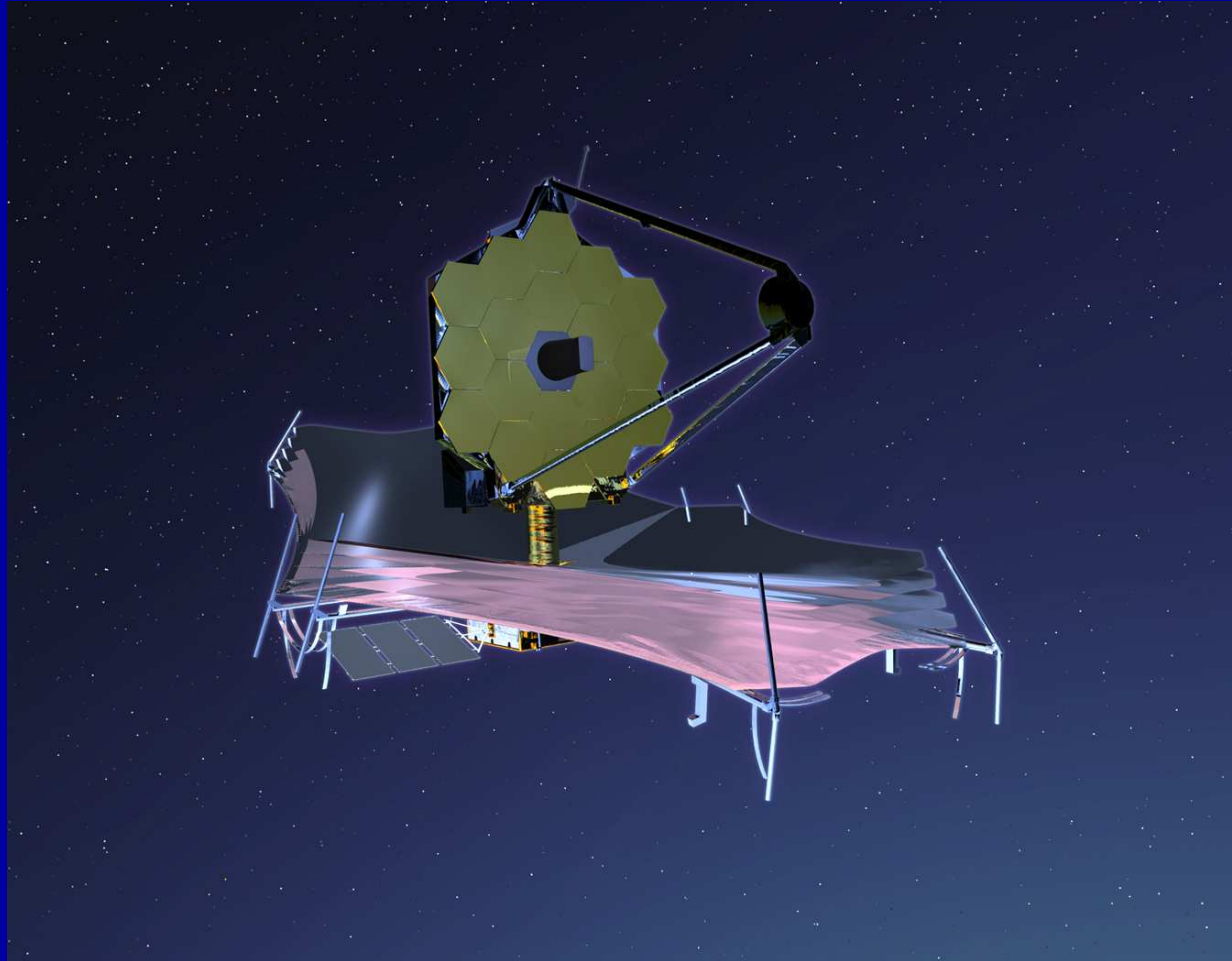


# Measuring First Light, Reionization, & Galaxy Assembly with the James Webb Space Telescope, and Penetrating the Dark Ages with a low-frequency Lunar Interferometer

---

Rogier Windhorst (Arizona State University)

*Collaborators: S. Cohen, R. Jansen, N. Hathi (ASU), C. Conselice & H. Yan (Caltech)*



*Colloquia at NAOC, BAO, and Tsinghua; Beijing, China, July 18 & 20, 2006*

# Outline

---

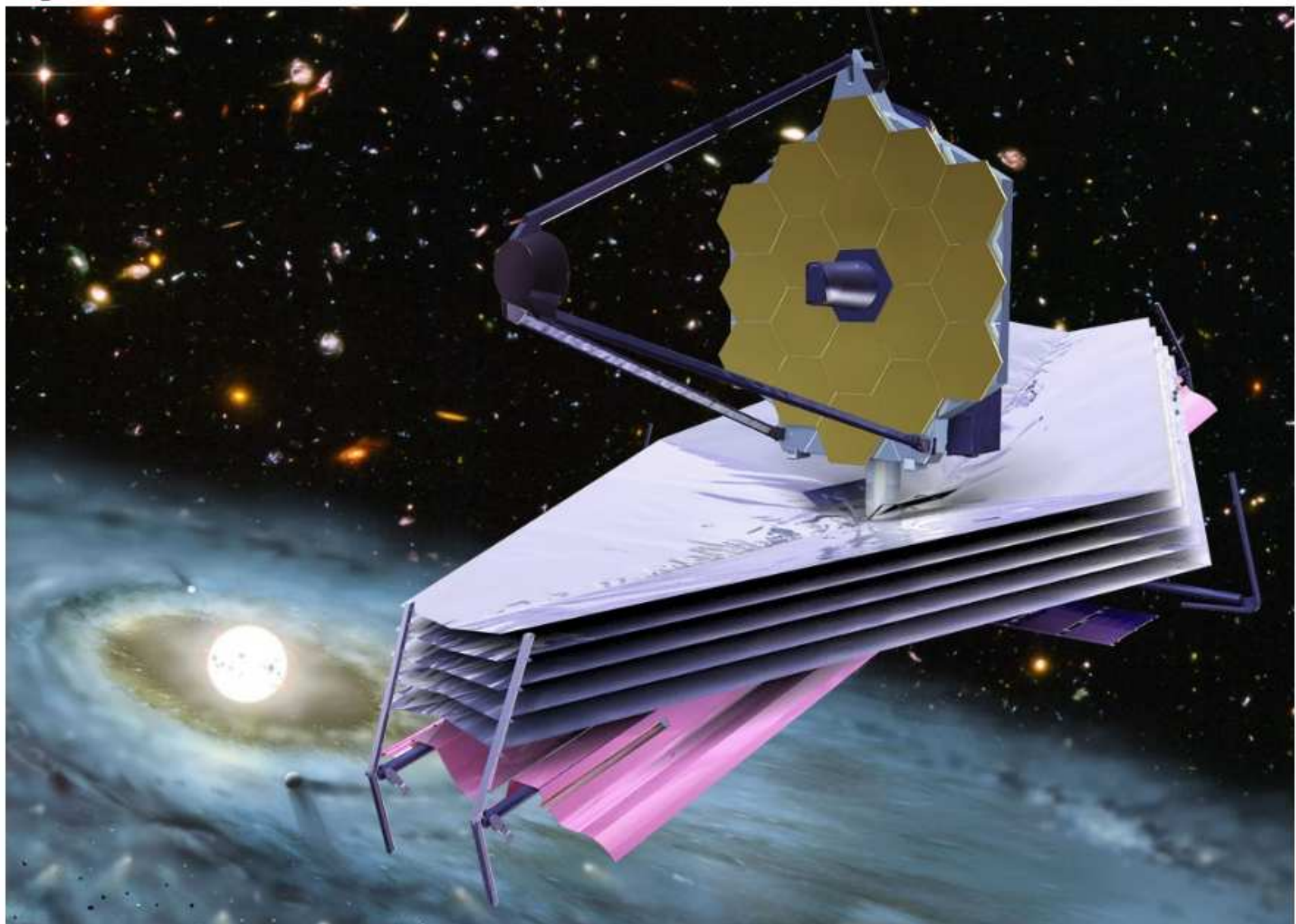
- (1) What is JWST and how will it be deployed?
- (2) What instruments and sensitivity will JWST have?
- (3) How JWST can measure First Light and Reionization
- (4) How JWST can measure Galaxy Assembly
- (5) Predicted Galaxy Appearance for JWST at  $z \simeq 1-15$
- (6) Penetrating the Dark Ages with a low-freq Lunar Interferometer
- (7) Summary and Conclusions

Sponsored by NASA/JWST





# James Webb Space Telescope





"Brilliantly done...breathtaking in its vision."

*The New York Times*

# JAMES WEBB

Author of *The Emperor's General*



A NOVEL

# SOMETHING TO DIE FOR

Need hard-working grad students & postdocs in  $\gtrsim 2013$  ... It'll be worth it!

- (1) What is the James Webb Space Telescope (JWST)?



- A fully deployable 6.5 meter ( $25 \text{ m}^2$ ) segmented IR telescope for imaging and spectroscopy from 0.6 to  $28 \mu\text{m}$ , to be launched by NASA  $\gtrsim 2013$ . It has a nested array of sun-shields to keep its ambient temperature at 35-45 K, allowing faint imaging ( $\text{AB} \lesssim 31.5$ ) and spectroscopy ( $\text{AB} \lesssim 29$  mag).



Life-sized model of JWST, used to test the deployment of its sun-shield.



Life-sized model of JWST, at NASA/GSFC Friday afternoon after 5 pm ...

- (1) How will JWST travel to its L2 orbit?

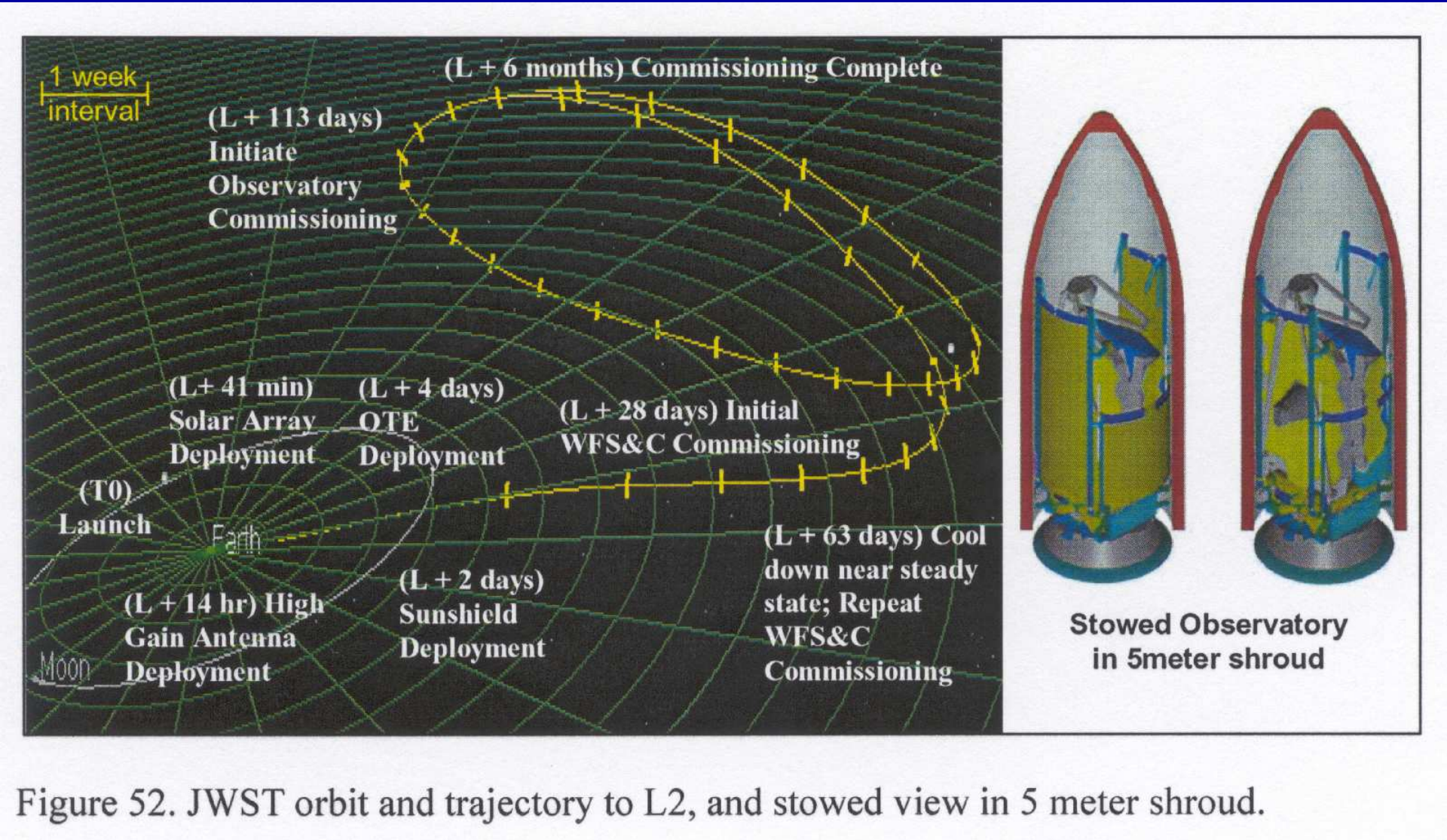


Figure 52. JWST orbit and trajectory to L2, and stowed view in 5 meter shroud.

After launch in  $\gtrsim$ 2013 with an Ariane V vehicle, JWST will orbit around the the Earth–Sun Lagrange point L2. From there, JWST can cover the whole sky in segments that move along in RA with the Earth, have an observing efficiency  $\gtrsim$ 70%, and send data back to Earth every day.

- (1) How will the JWST be automatically deployed?

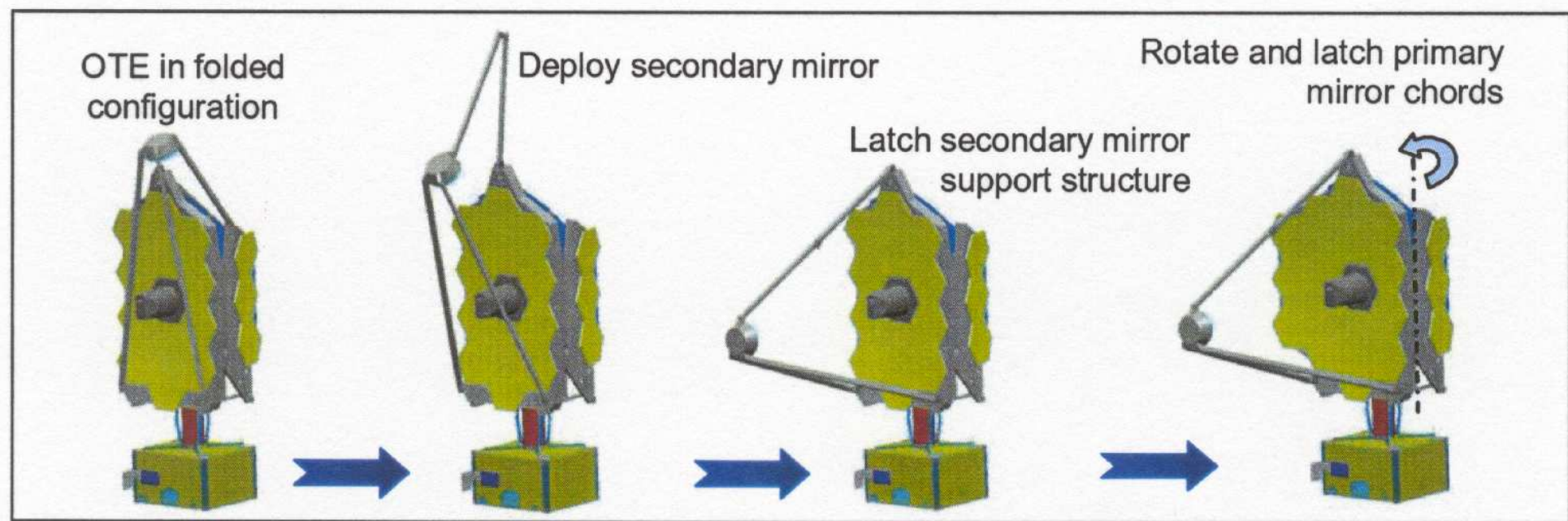
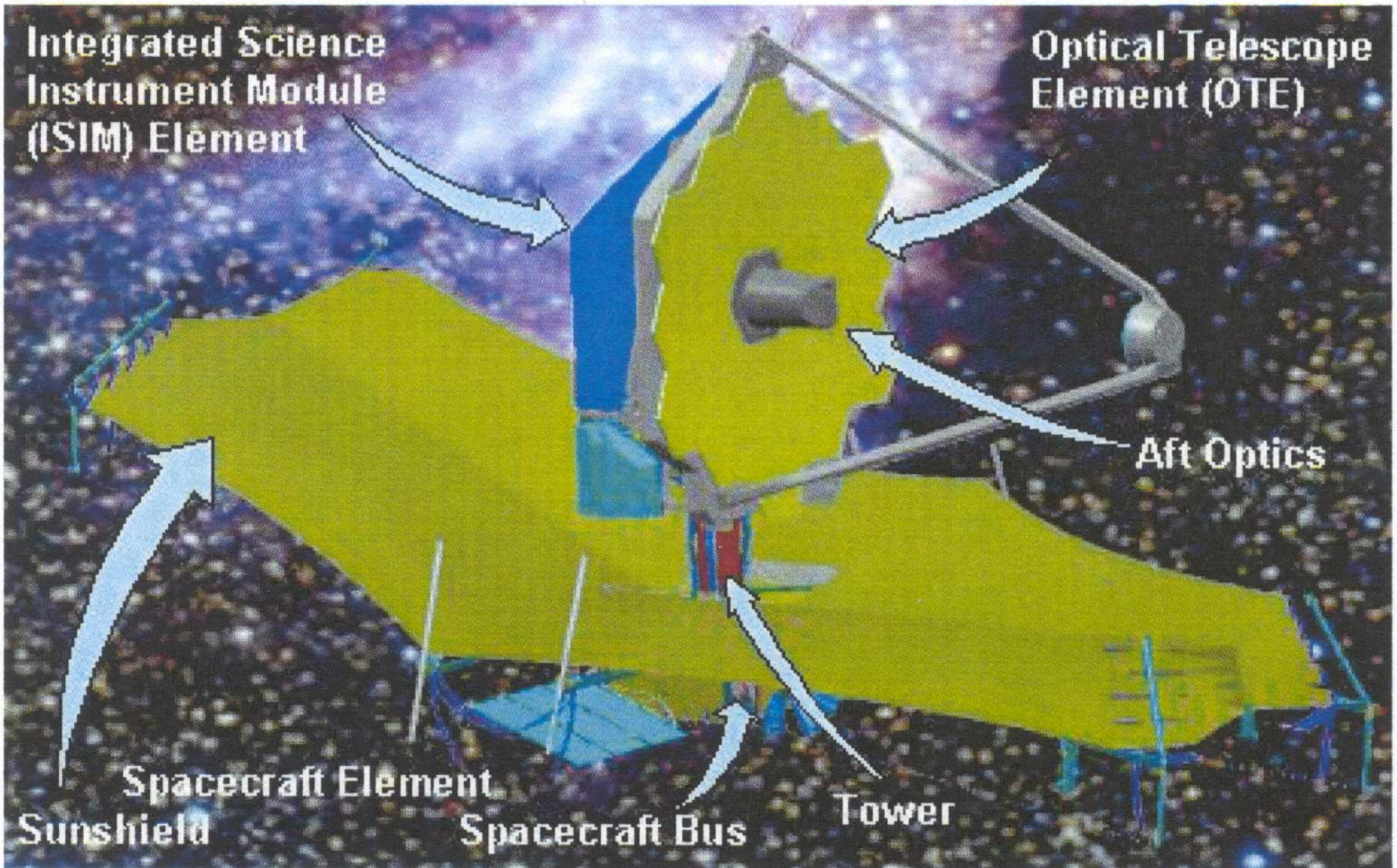


Figure 53. Telescope Deployment Sequence (Deployment steps 4 and 5)

During its several month journey to L2 (shown on a previous page), JWST will be automatically deployed in phases (as shown here), its instruments will be tested, and it will then be inserted into an L2 halo orbit.

From an orbit around the the Earth–Sun Lagrange point L2, JWST can cover the whole sky in segments, have an observing efficiency  $\gtrsim 70\%$ , and send data back to Earth every day.



JWST mission reviewed in Gardner, J. P., et al. 2006, Space Science Reviews, p. 1–80, in press; astro-ph/0606175)

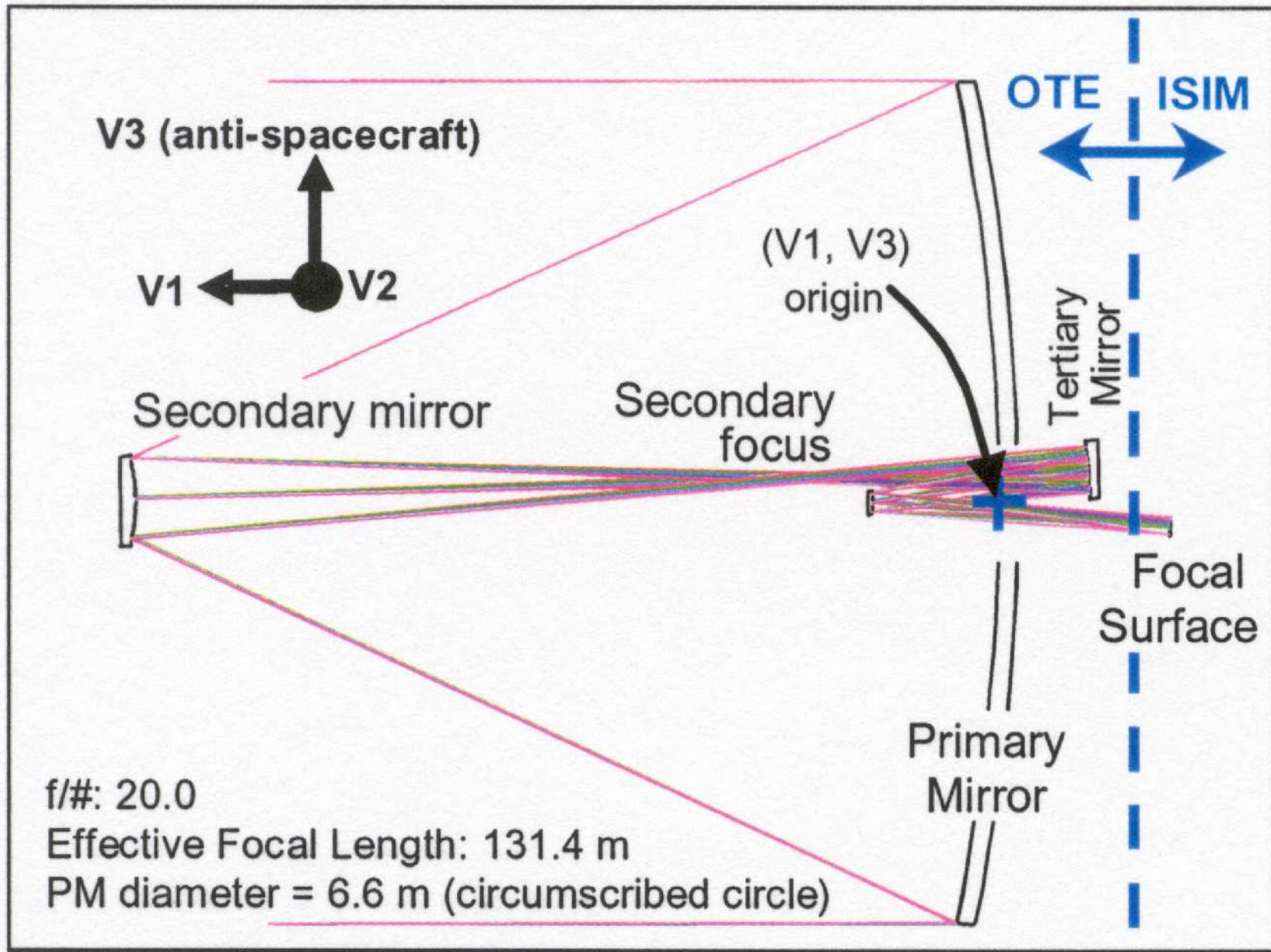
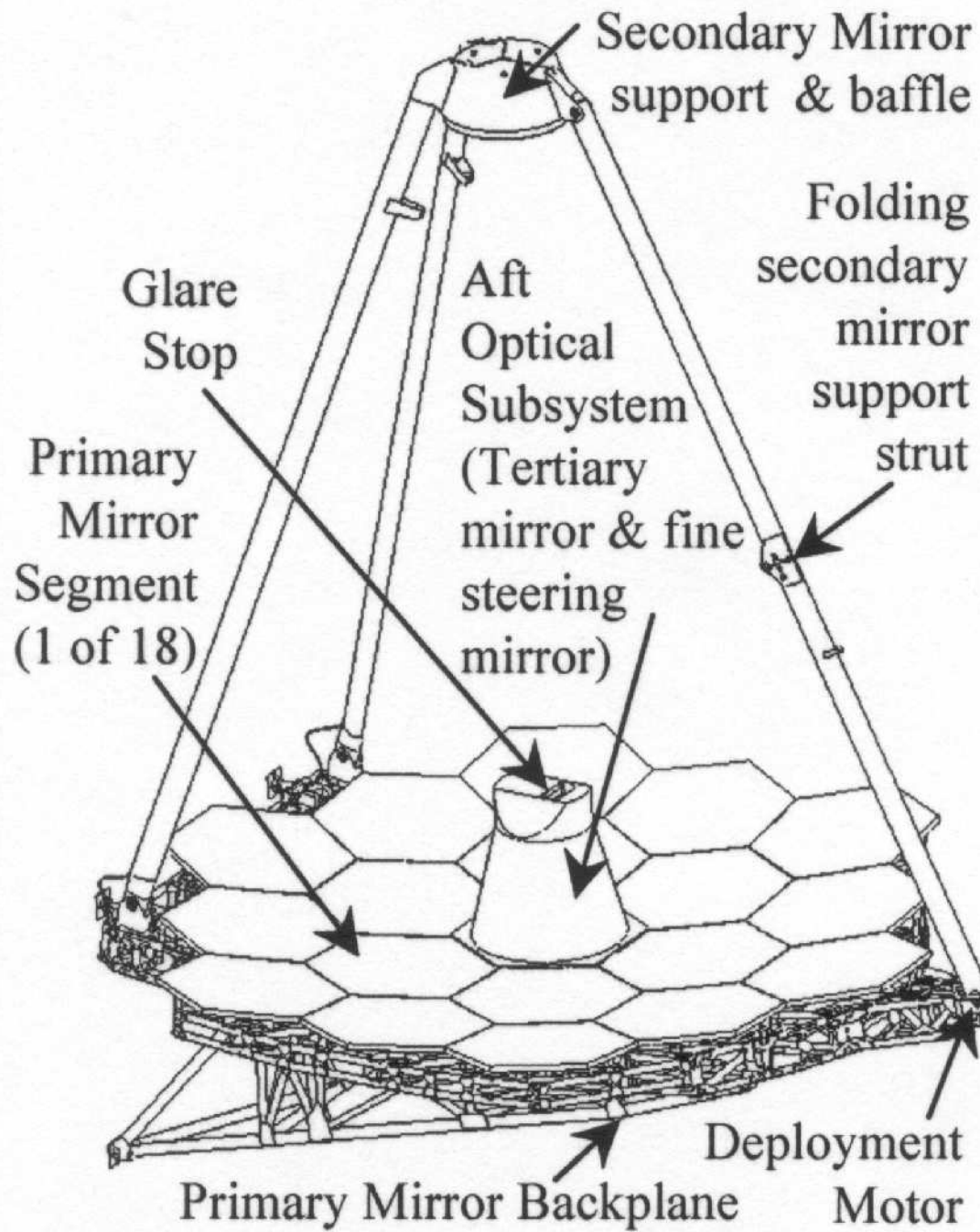


Figure 33. OTE optical layout



Actuators for 6 degrees of freedom rigid body motion

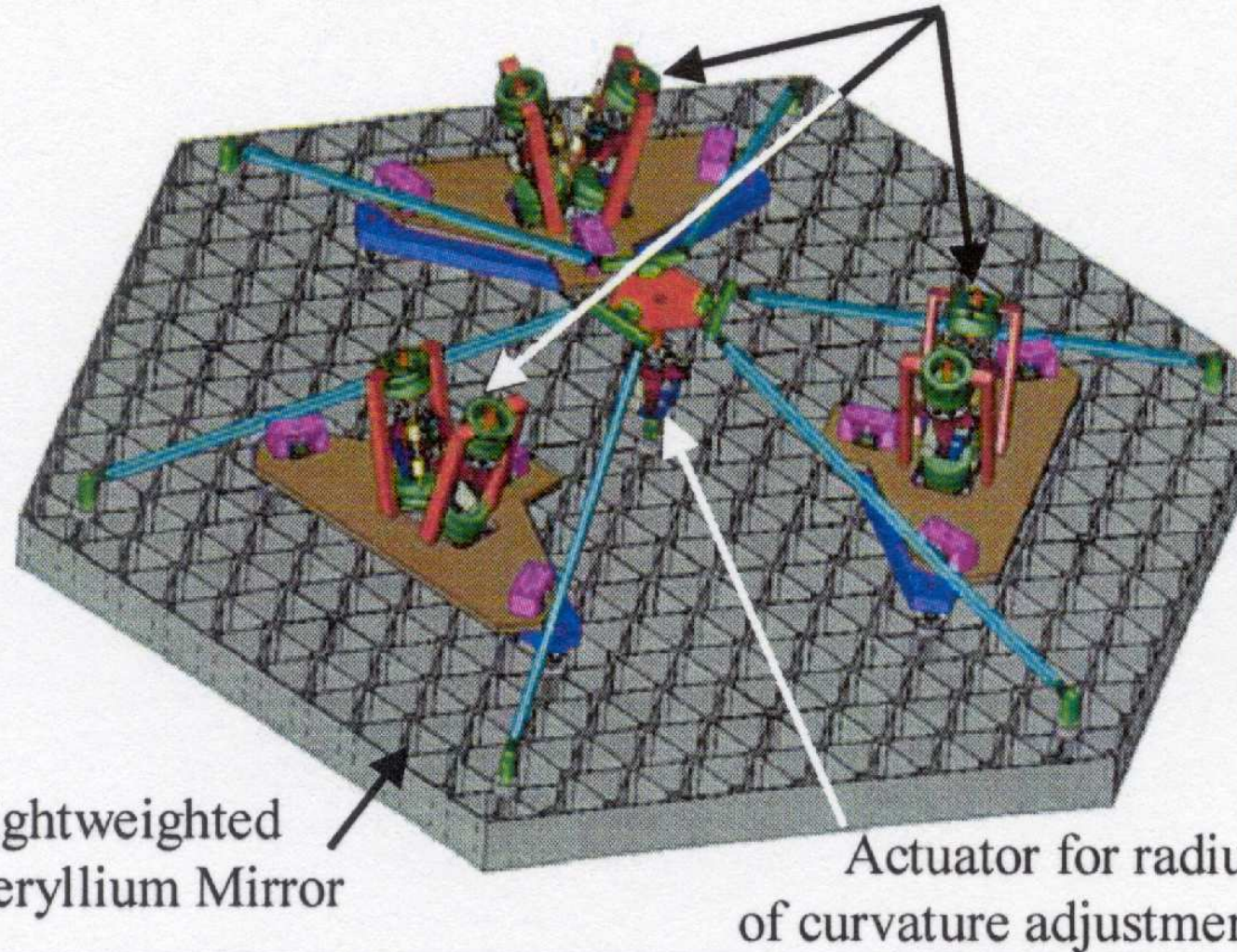
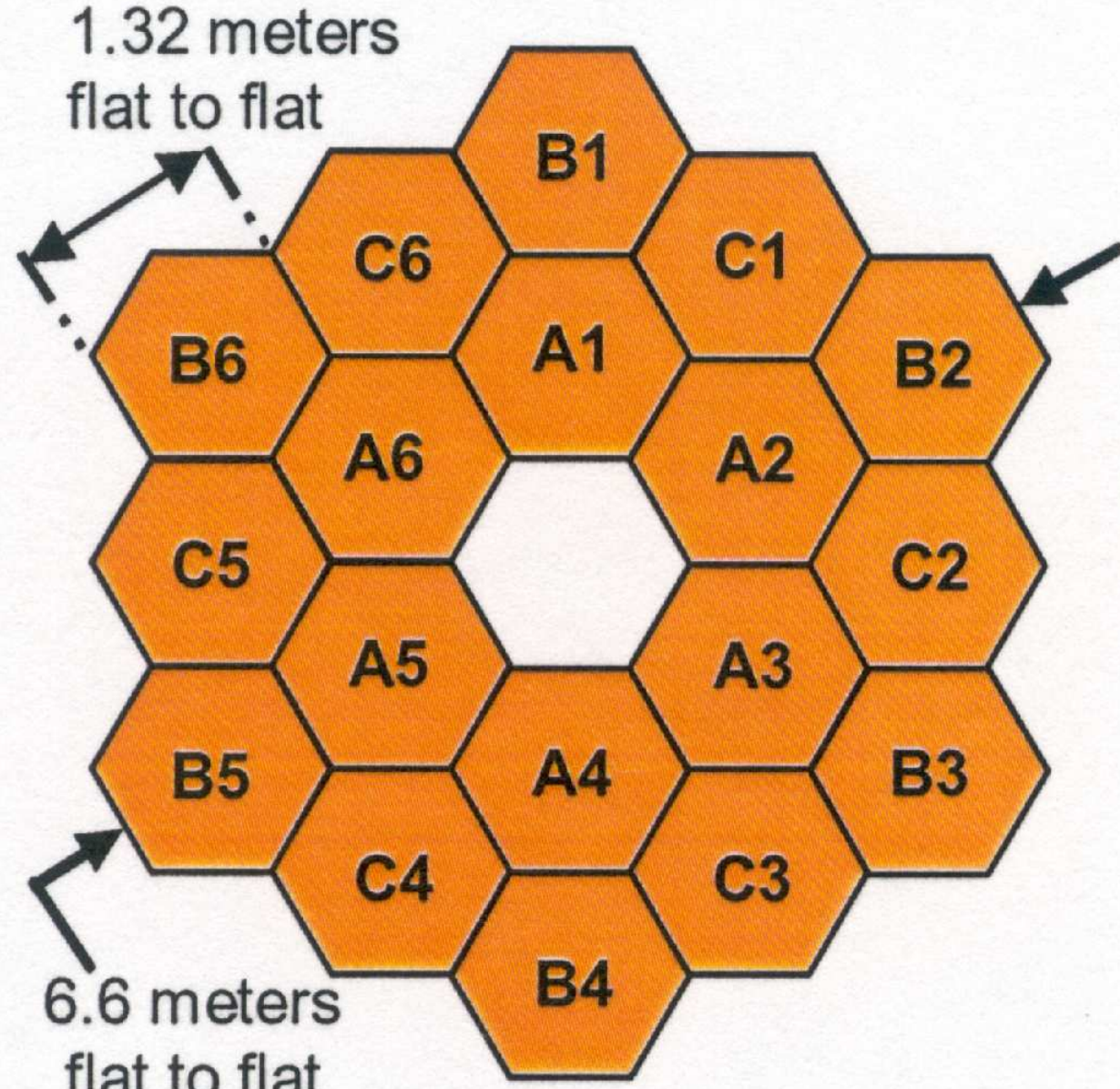


Figure 36. Rear view of a primary mirror segment.

Active mirror segment support through hexapods, like Keck whiffle-trees.



Edge-to-edge diameter is 6.60 m, but effective circular diameter is 5.85 m.  
Cannot cleanly descope aperture without doing major harm to PSF.

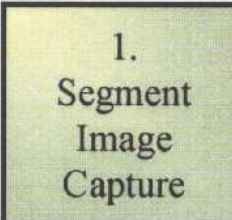
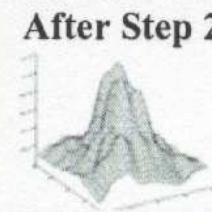
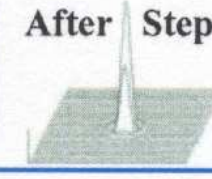
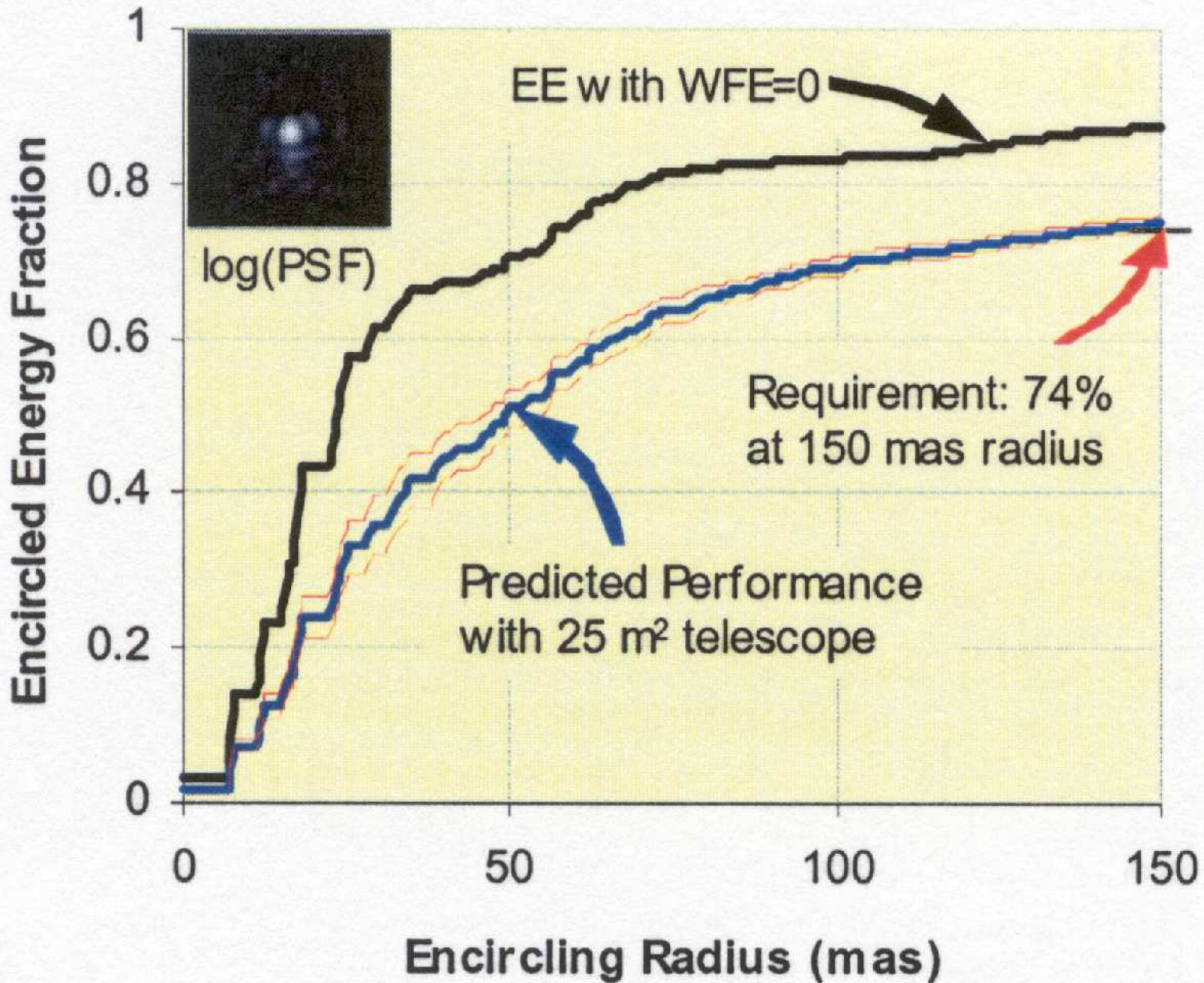
<i>First light NIRCam</i>	<i>After Step 1</i>	<i>Initial Capture</i>	<i>Final Condition</i>
	 1. Segment Image Capture	18 individual 1.6-m diameter aberrated sub-telescope images  PM segments: < 1 mm, < 2 arcmin tilt SM: < 3 mm, < 5 arcmin tilt	PM segments: < 100 $\mu\text{m}$ , < 2 arcsec tilt  SM: < 3 mm, < 5 arcmin tilt
<b>2. Coarse Alignment</b> Secondary mirror aligned Primary RoC adjusted	 <i>After Step 2</i>	Primary Mirror segments: < 1 mm, < 10 arcsec tilt  Secondary Mirror : < 3 mm, < 5 arcmin tilt	WFE < 200 mm (rms)
<b>3. Coarse Phasing - Fine Guiding (PMSA piston)</b>	 <i>After Step 3</i>	WFE: < 250 $\mu\text{m}$ rms	WFE < 1 $\mu\text{m}$ (rms)
<b>4. Fine Phasing</b>	 <i>After Step 4</i>	WFE: < 5 $\mu\text{m}$ (rms)	WFE < 110 nm (rms)
<b>5. Image-Based Wavefront Monitoring</b>	 <i>After Step 5</i>	WFE: < 150 nm (rms)	WFE < 110 nm (rms)

Figure 38. WFS&C commissioning and maintenance.

JWST's Wave Front Sensing and Control is similar to that at Keck and HET.



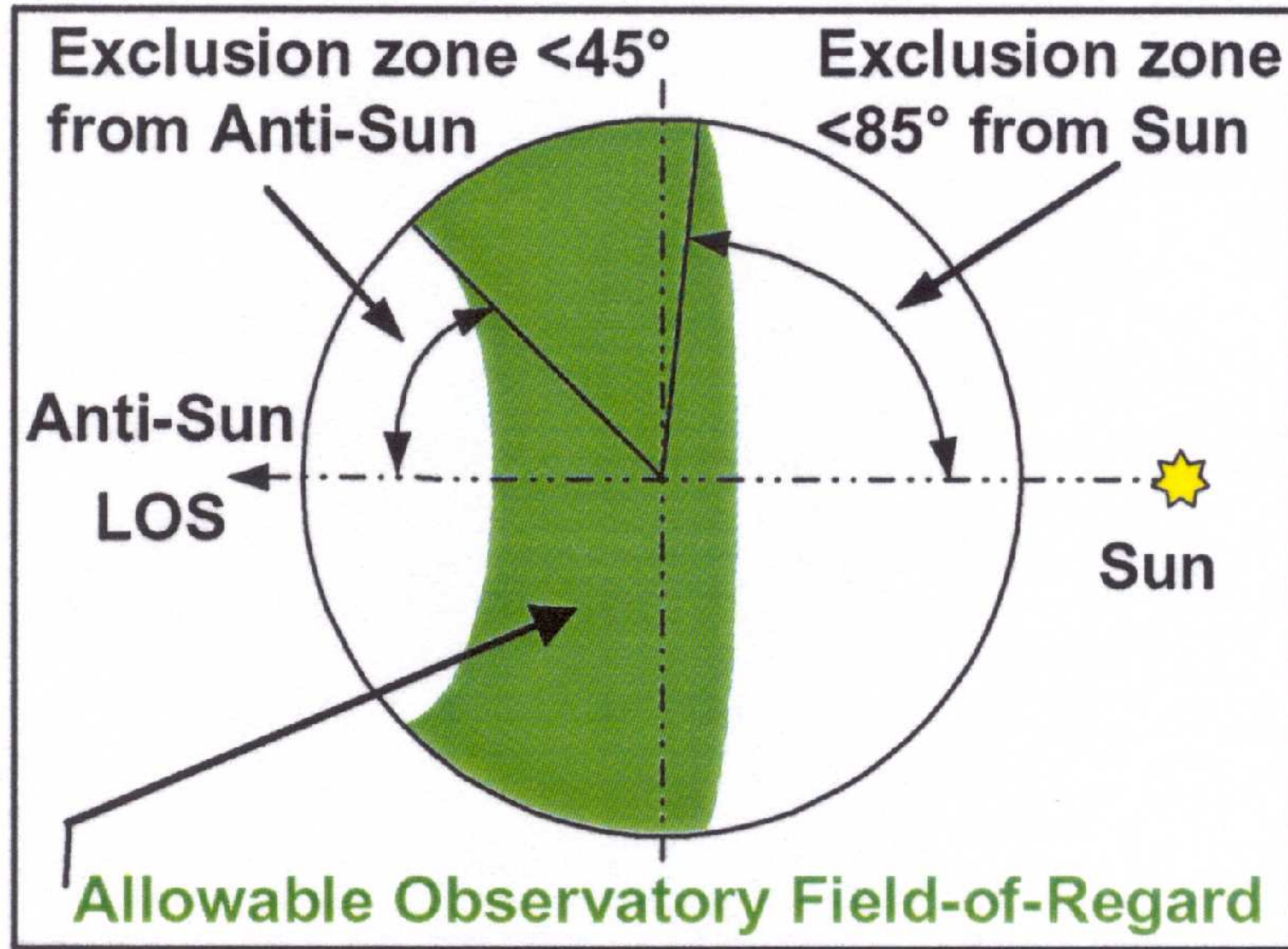
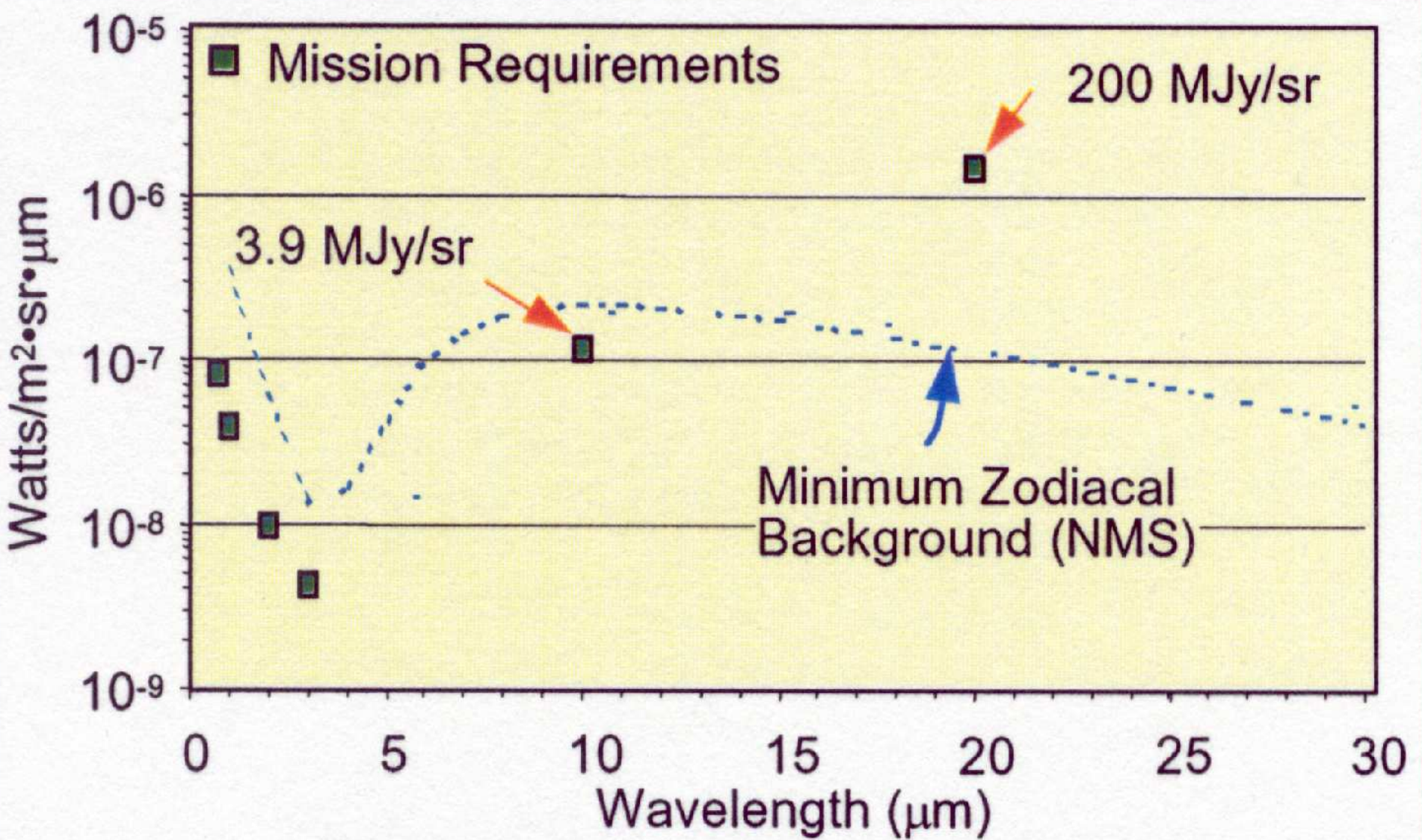


Figure 30. Observatory field of regard (FOR).

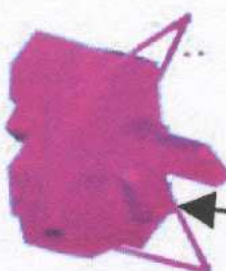
JWST can observe segments of sky that move around as it orbits the Sun.



JWST L2 sky minimizes  $\lambda \approx 3 \mu\text{m}$ :  $\gtrsim 10^4 \times$  fainter than ground-based sky!

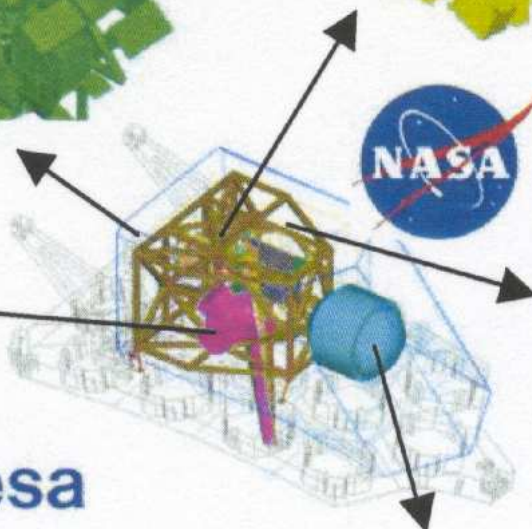
### Fine Guidance Sensor & Tunable Filter

- 0.6 to 5  $\mu\text{m}$  operation
- Guide star acquisition & tracking
- Tunable filter imager  
2 (2048x2048) 68mas pixels



### Mid Infrared Instrument (MIRI)

- 5 to 28  $\mu\text{m}$  operation
- Science Discovery Space
- Imaging  
1 (1024x1024) 110mas pixels
- Spectroscopy  
2 (1024x1024) 200-470mas pixels



### Near Infrared Camera (NIRCam)

- 0.6 to 5  $\mu\text{m}$  operation
- Coronagraph imaging capability
- Supports WFS&C
- 2 (4096x4096) 31mas pixels
- 2 (2048x2048) 62mas pixels



### Near Infrared Spectrometer (NIRSpec)

- 0.6 to 5  $\mu\text{m}$  operation
- Simultaneous Spectra of > 100 objects
- $\lambda/\Delta\lambda \sim 100$  to 1000
- 2 (2048x2048) 100mas pixels



### Solid Hydrogen Dewar

- Cools MIRI detectors to ~7K
- 5 year lifetime

Figure 37. ISIM element and its science instrumentation.

The JWST instrument complement: US (UofA), ESA, and CSA.

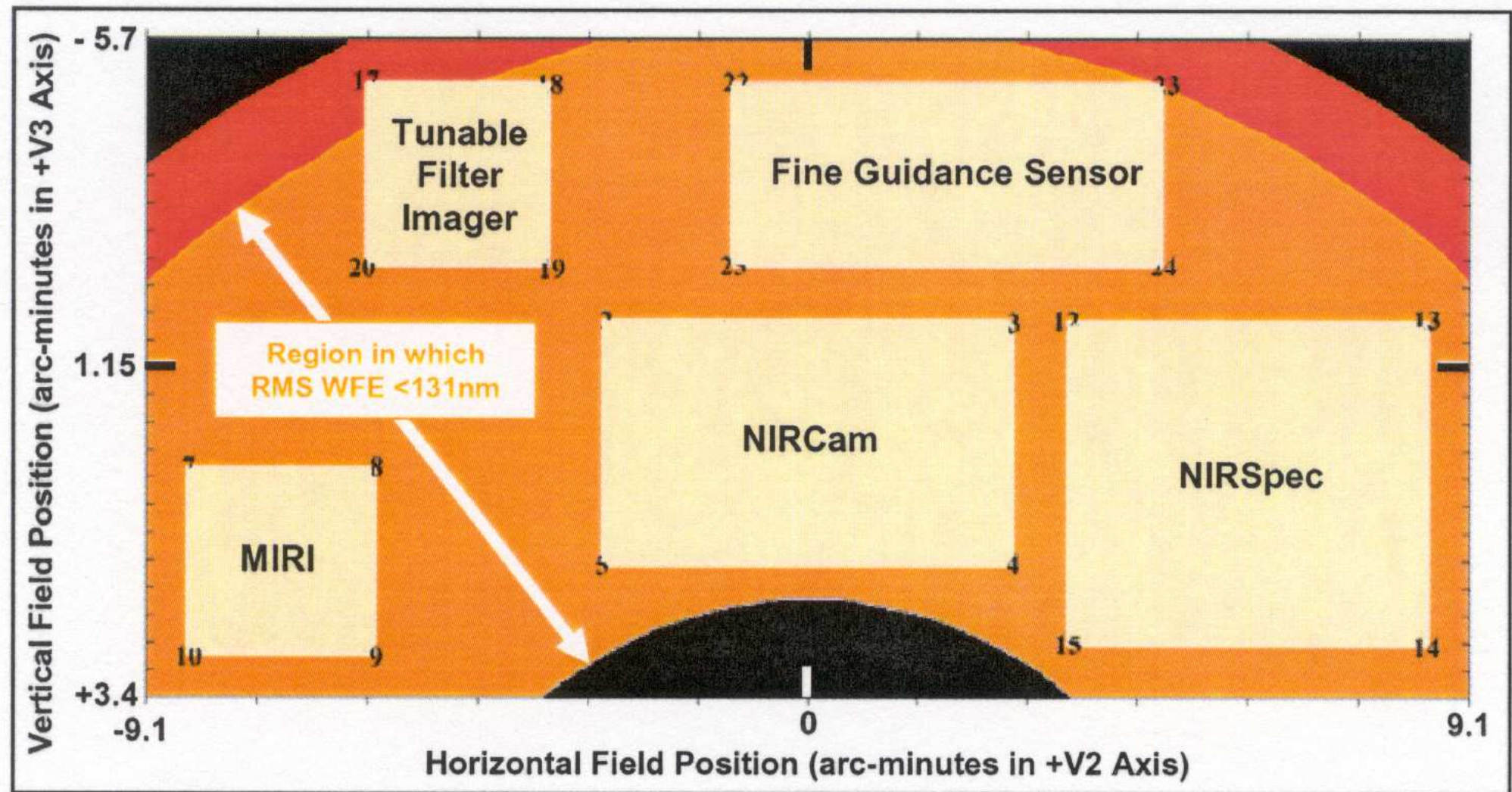


Figure 34. Placement of the ISIM instrument FPAs in the OTE field of view.

JWST instruments can in principle be used in parallel (not yet implemented).

Table 10. Predicted Performance of the JWST Observatory

Parameter	Capability
<b>Wavelength</b>	0.6 to 29 $\mu\text{m}$ . Reflective gold coatings
<b>Sensitivity</b>	SNR=10, integration time = $\tau_i$ , R= $\lambda/\Delta \lambda$ and Zodiacal of 1.2 times that at north ecliptic pole
NIRCam	12 nJy (1.1 $\mu\text{m}$ , $\tau_i=10,000\text{s}$ , and $\lambda/\Delta \lambda = 4$ )
NIRCam	10.4 nJy (2.0 $\mu\text{m}$ , $\tau_i=10,000\text{s}$ , and $\lambda/\Delta \lambda = 4$ )
TFI	368 nJy (3.5 $\mu\text{m}$ , $\tau_i=10,000\text{s}$ , and $\lambda/\Delta \lambda = 100$ )
NIRSpec	120 nJy (3.0 $\mu\text{m}$ , $\tau_i=10,000\text{s}$ , and $\lambda/\Delta \lambda = 100$ )
NIRSpec	560 nJy (10 $\mu\text{m}$ , $\tau_i=10,000\text{s}$ , and $\lambda/\Delta \lambda = 5$ )
MIRI	5000 nJy (21 $\mu\text{m}$ , $\tau_i=10,000\text{s}$ , and $\lambda/\Delta \lambda = 4.2$ )
NIRSpec Med	$5.2 \times 10^{-22} \text{ W m}^{-2}$ (2 $\mu\text{m}$ , $\tau_i=100,000\text{s}$ , R= 1000)
MIRI Spec	$3.4 \times 10^{-21} \text{ W m}^{-2}$ (9.2 $\mu\text{m}$ , $\tau_i=10,000\text{s}$ , R= 2400)
MIRI Spec	$3.1 \times 10^{-20} \text{ W m}^{-2}$ (22.5 $\mu\text{m}$ , $\tau_i=10,000\text{s}$ , R= 1200)
<b>Spatial Resolution &amp; Stability</b>	Encircled Energy of 75% at 1 $\mu\text{m}$ for 150mas radius Strehl ratio of $\sim 0.86$ at 2 $\mu\text{m}$ . PSF stability better than 1%

- (2) What instruments will JWST have?

The Near-Infrared Camera NIRCam made by an UofA + Lockheed + CSA consortium will do imaging from  $0.6\text{--}5.3 \mu\text{m}$  using a suite of broad-, medium-, and narrow-band filters. NIRCam uses two identical and independently operated imaging modules, with two wavelengths observable simultaneously via a dichroic that splits the beam around  $2.35 \mu\text{m}$ . Each of these two channels has an independently operated  $2!2 \times 4!6$  FOV. Both channels are Nyquist-sampled: the short-wavelength channel at  $2 \mu\text{m}$  with  $0!0317/\text{pixel}$ , and the long-wavelength at  $4 \mu\text{m}$  with  $0!0648/\text{pixel}$ . NIRCam's 10  $2\text{k} \times 2\text{k}$  HgCdTe arrays will be passively cooled.

The Near-Infrared Spectrograph NIRSpec made by an ESA + GSFC consortium will do spectroscopy with resolving powers of  $R \sim 100$  in prism mode, of  $R \sim 1000$  in multi-object mode using a micro-electromechanical array system (MEMS) of micro-shutters that can open slitlets on previously imaged known objects, and of  $R \sim 3000$  using long-slit spectroscopy. All NIRSpec spectroscopic modes have a  $\sim 3.4 \times 3.4'$  FOV.

- (2) What instruments will JWST have?

The Mid-Infra-Red Instrument MIRI made by an UofA + JPL + ESA consortium will do imaging and spectroscopy from 5–28  $\mu\text{m}$ . MIRI is actively cooled by a cryocooler, which will cool it without using consumable gas.

The Fine Guidance Sensor (FGS) is made by CSA and provide stable pointing at the milli-arcsecond level. The FGS will have sufficient sensitivity and a large enough FOV to find guide stars with  $\gtrsim 95\%$  probability at any point in the sky. The FGS will have three simultaneously imaged fields of view of  $2.3 \times 2.3'$ , one of which feeds a pure guider channel, one feeding a guider channel plus a long-wavelength  $R \sim 100$  tunable filter channel with light split by a dichroic, and another feeding the short wavelength tunable filter  $R \sim 100$  channel.

JWST has fully redundant imaging and spectroscopic modes. It will not be serviced at L2, and therefore will undergo an extensive series of ground-testing and thermal vacuum testing in 2008–2009, after its main construction in 2004–2008. The main NASA contractor is Northrop Grumman Space Technology (“NGST”) in Redondo Beach (CA).

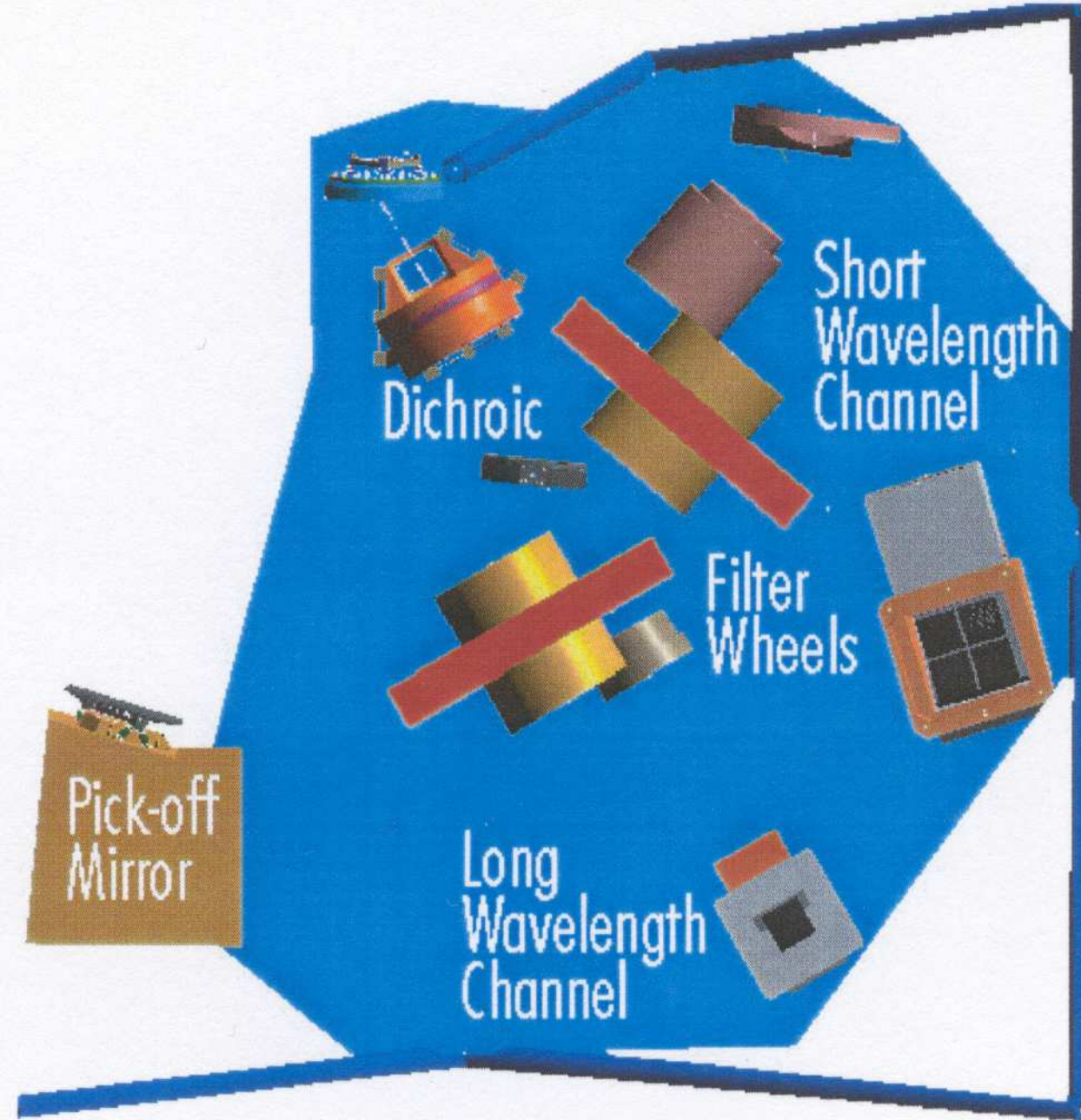


Figure 43. Optical layout of one of two NIRCam imaging modules.

- (2) What instruments will JWST have?

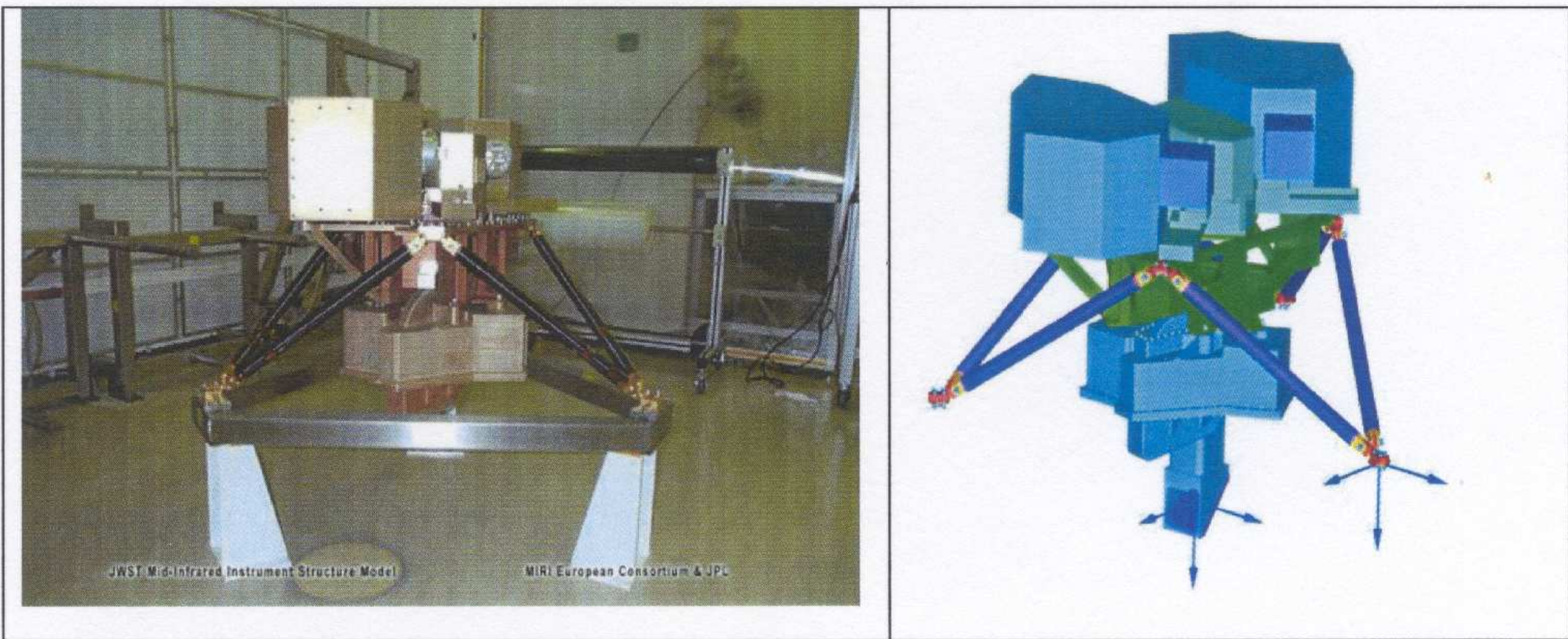


Figure 47. The MIRI structural and thermal model (left) compared to a computer design of the instrument (right).

The Mid-Infra-Red Instrument MIRI made by an UofA + JPL + ESA consortium will do imaging and spectroscopy from 5–28  $\mu\text{m}$ . MIRI is actively cooled by a cryocooler, so that its lifetime is not limited by consumables.

# MIRI IFUs fields of view

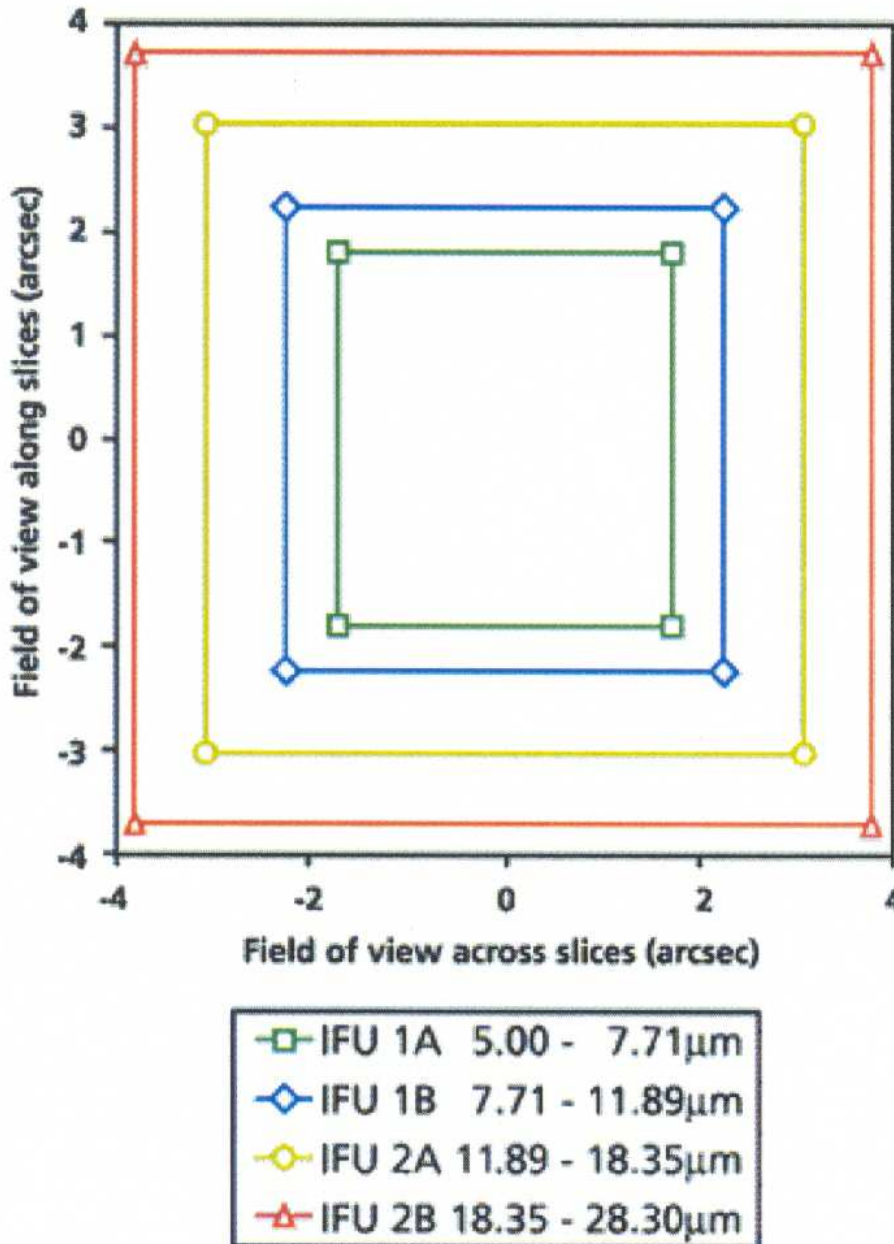


Figure 49. Fields of view of the MIRI IFU spectrograph.

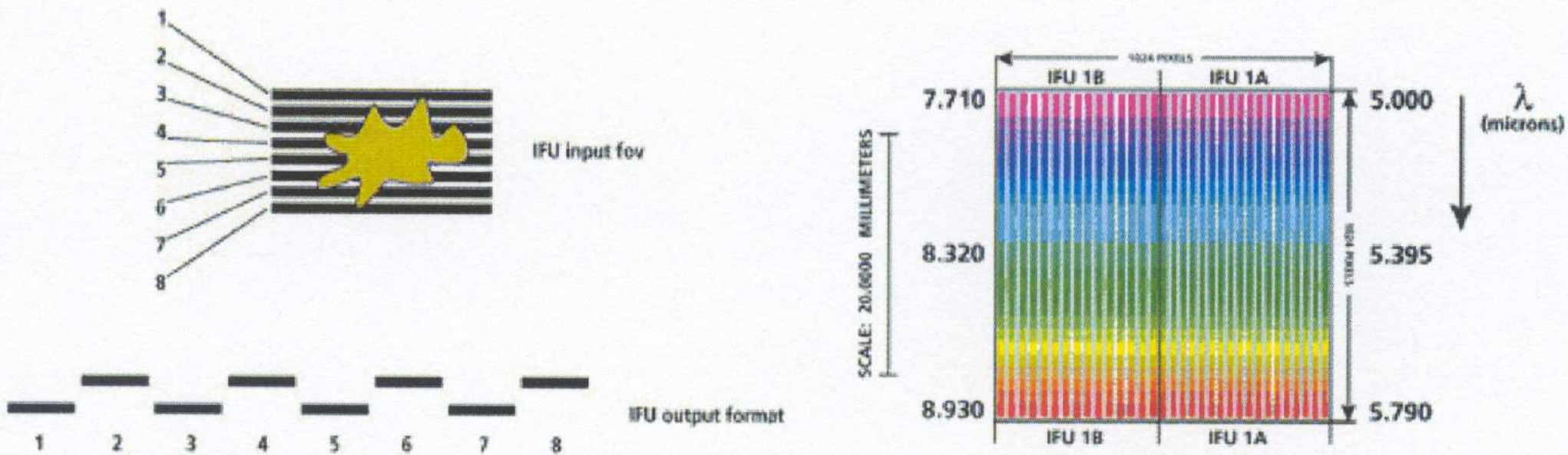


Figure 50. Schematic illustration of the MIRI IFU image slicer format (left) and dispersed spectra on detector (right)

The MIRI Integral Field Unit (IFU) has an image slicer that makes spatially resolved spectra at  $5 \mu\text{m} \lesssim \lambda \lesssim 9 \mu\text{m}$ .

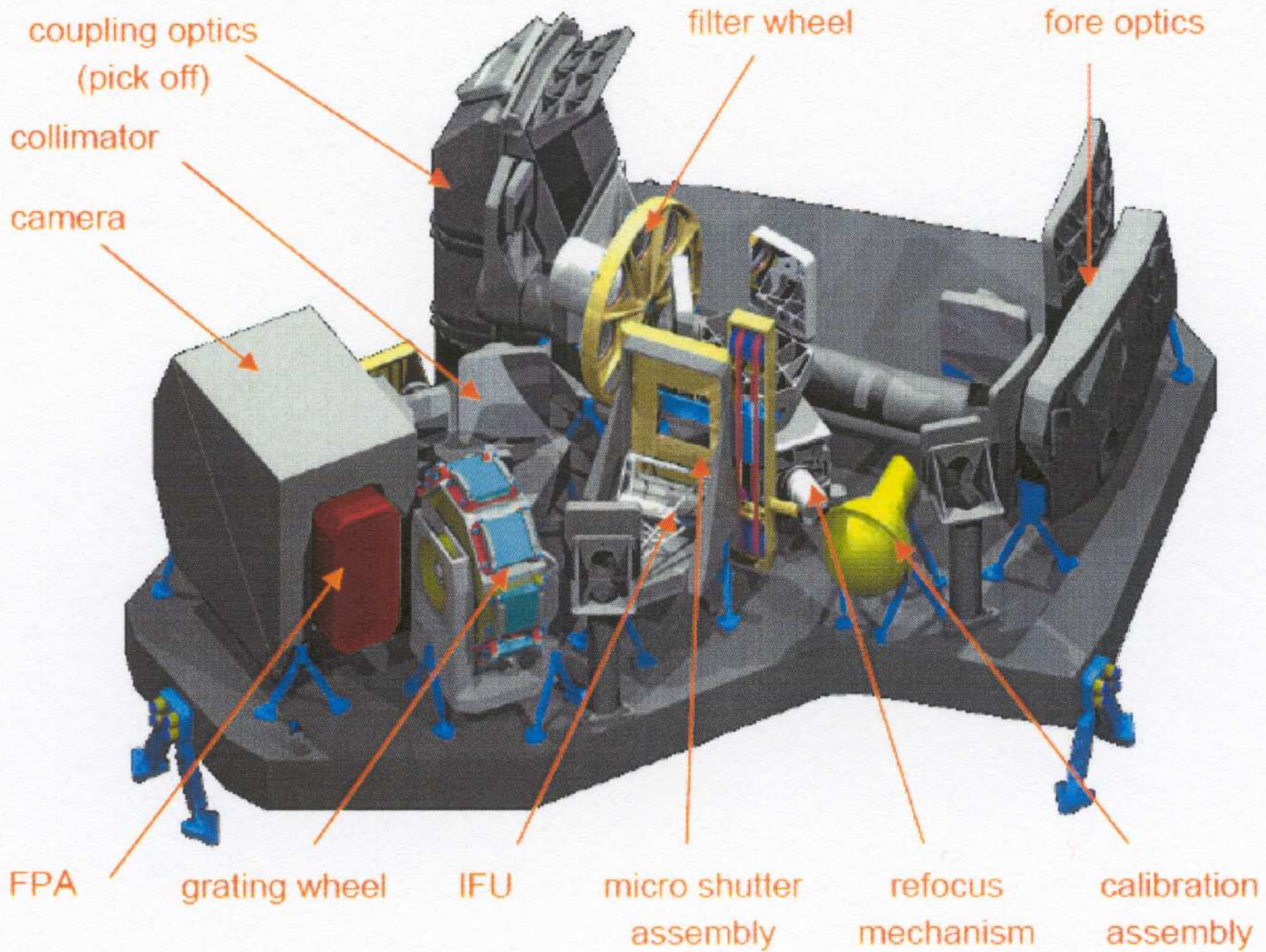


Figure 45. The NIRSpec instrument.

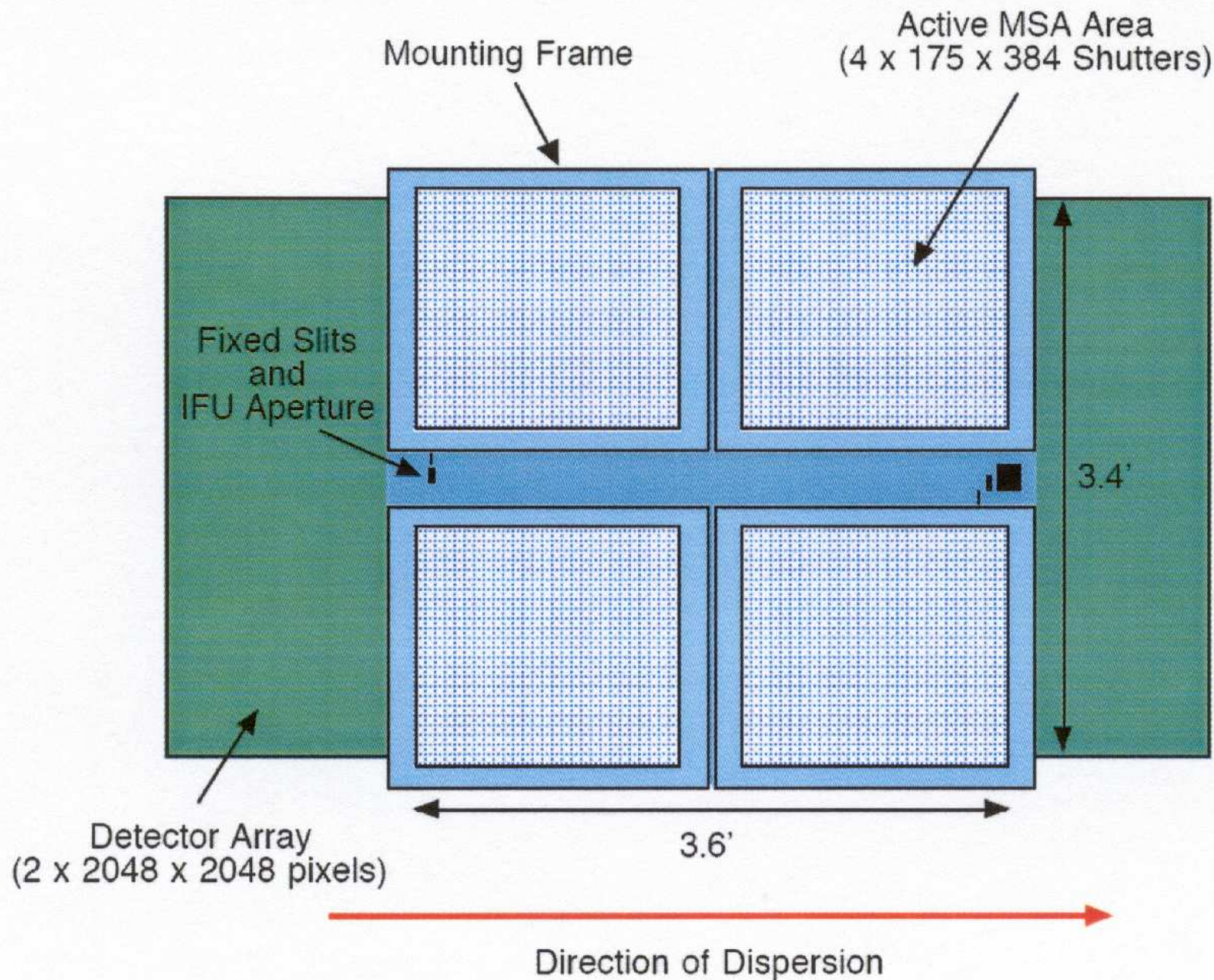
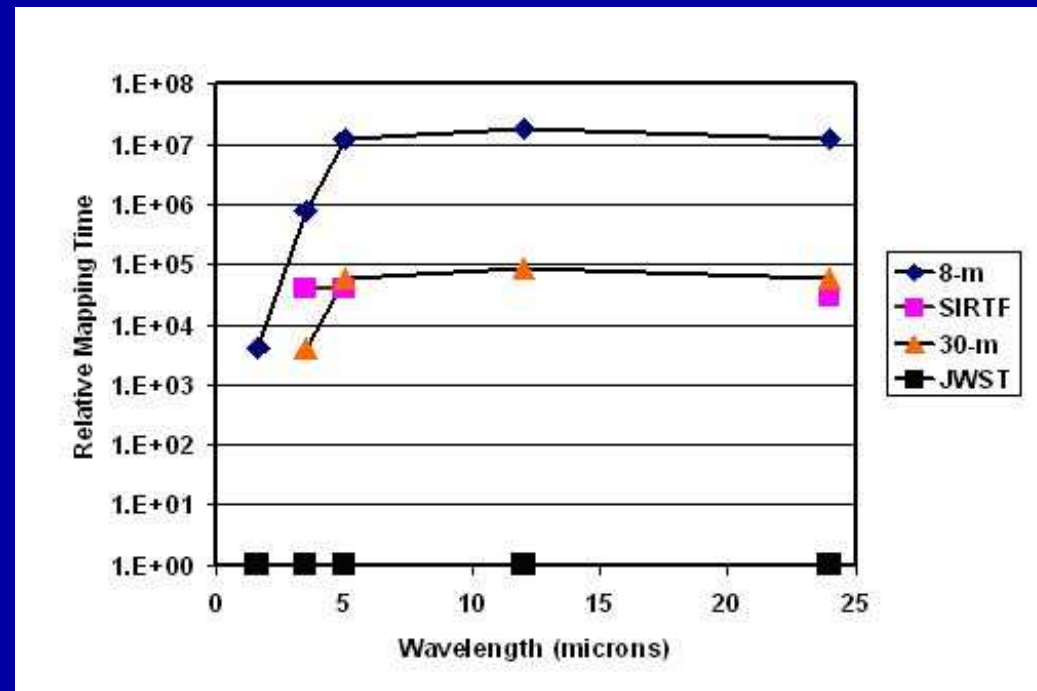
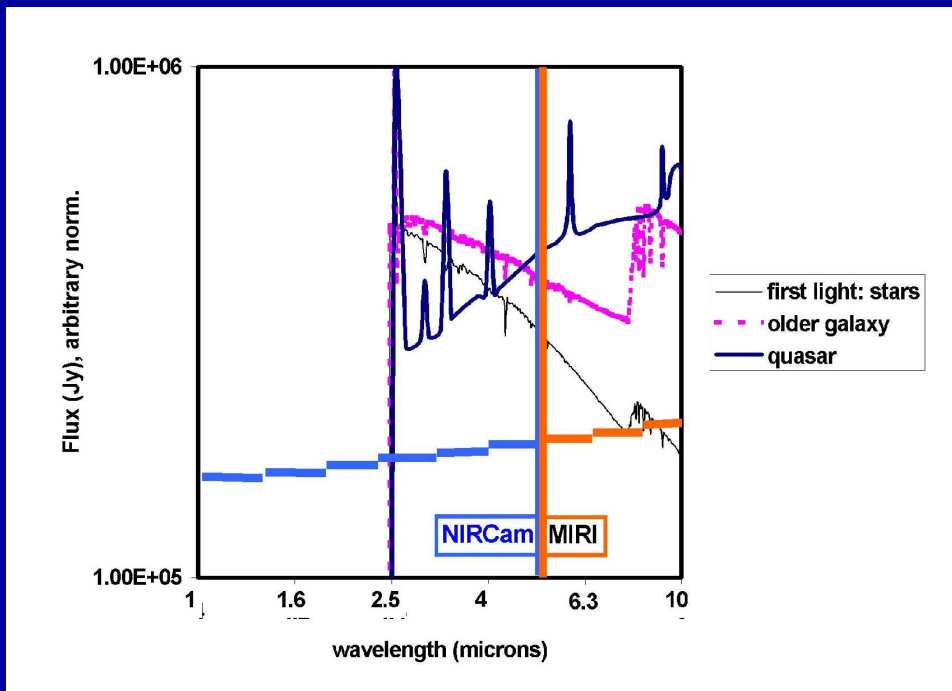


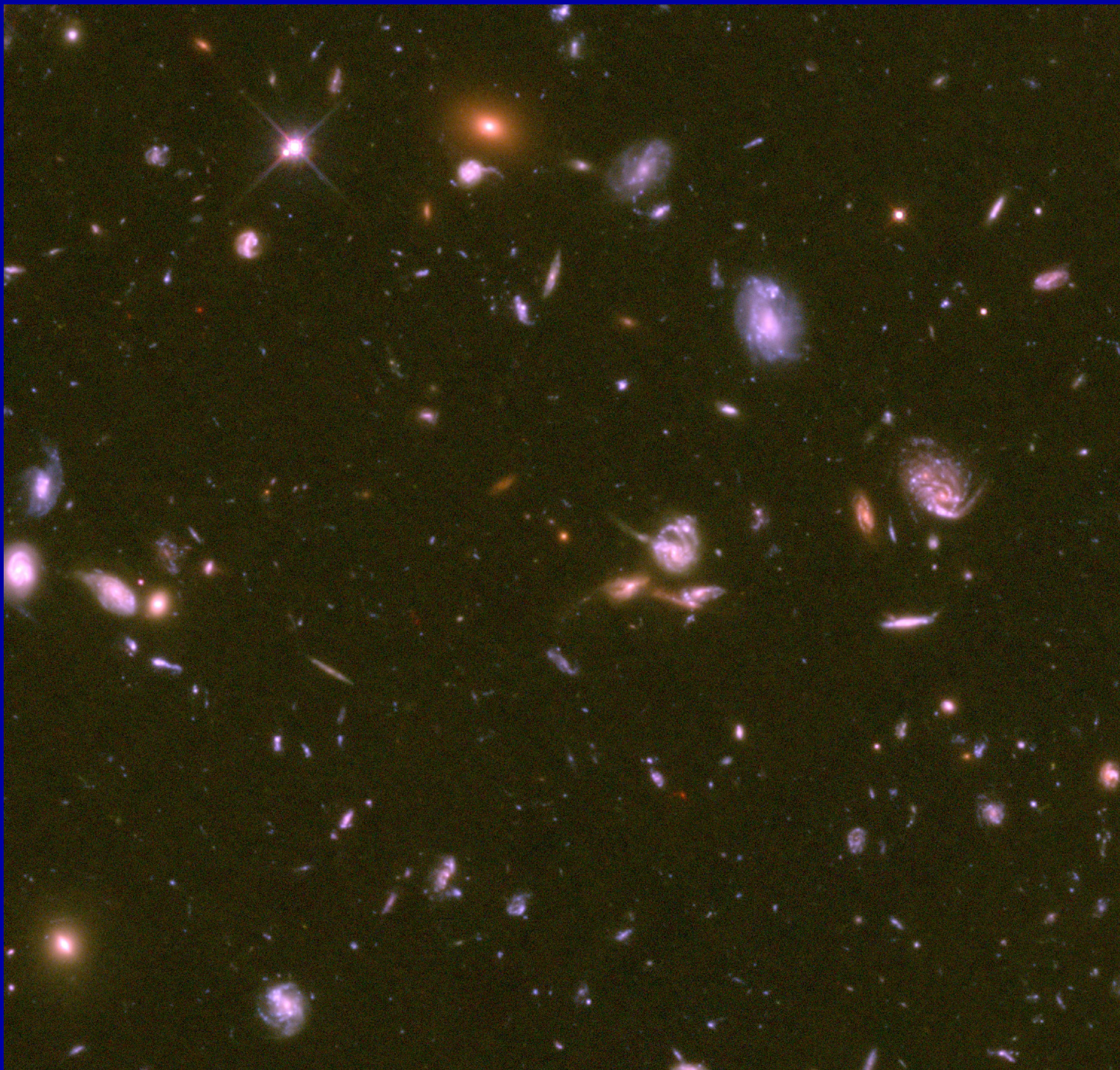
Figure 46. Schematic layout of the NIRSpec slit mask overlaid the detector array projected to the same angular scale.

- (2) What sensitivity will JWST have?



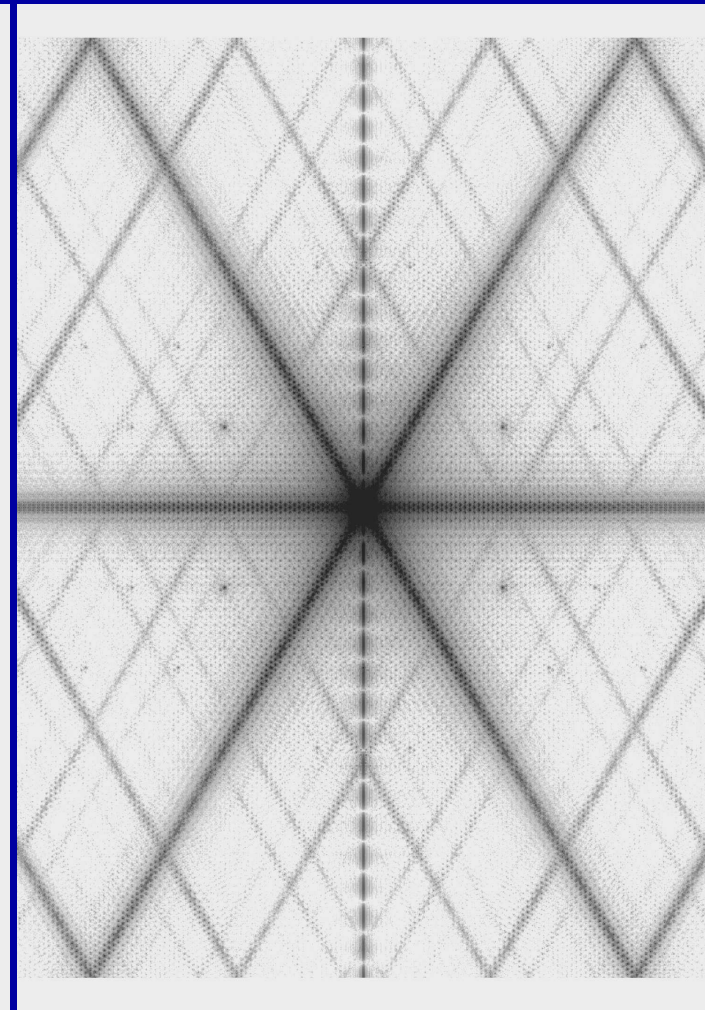
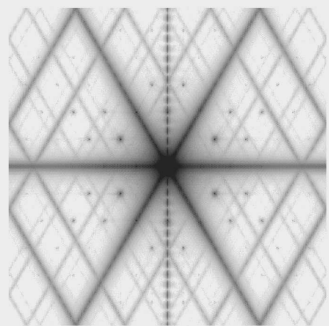
The NIRCam and MIRI sensitivity complement each other straddling  $5 \mu\text{m}$  in wavelength, and together allow objects to be found to redshifts  $z=15-20$  in  $\sim 10^5$  sec (28 hrs) integration times.

The left panel shows the NIRCam and MIRI broadband sensitivity to a Quasar, a “First Light” galaxy dominated by massive stars, and a 50 Myr “old” galaxy, all at  $z=20$ . The right panel shows the relative survey time versus wavelength that Spitzer, a ground-based IR-optimized 8-m (Gemini) and a 30-m telescope would need to match JWST.



240 hrs HST/ACS in  $Viz'$  in the Hubble UltraDeep Field (HUDF)

## 6.5m JWST PSF's models (Ball Aerospace and GSFC):



NIRCam 0.7  $\mu\text{m}$

1.0  $\mu\text{m}$  (<150 nm WFE)

2.0  $\mu\text{m}$  (diffr. limit)

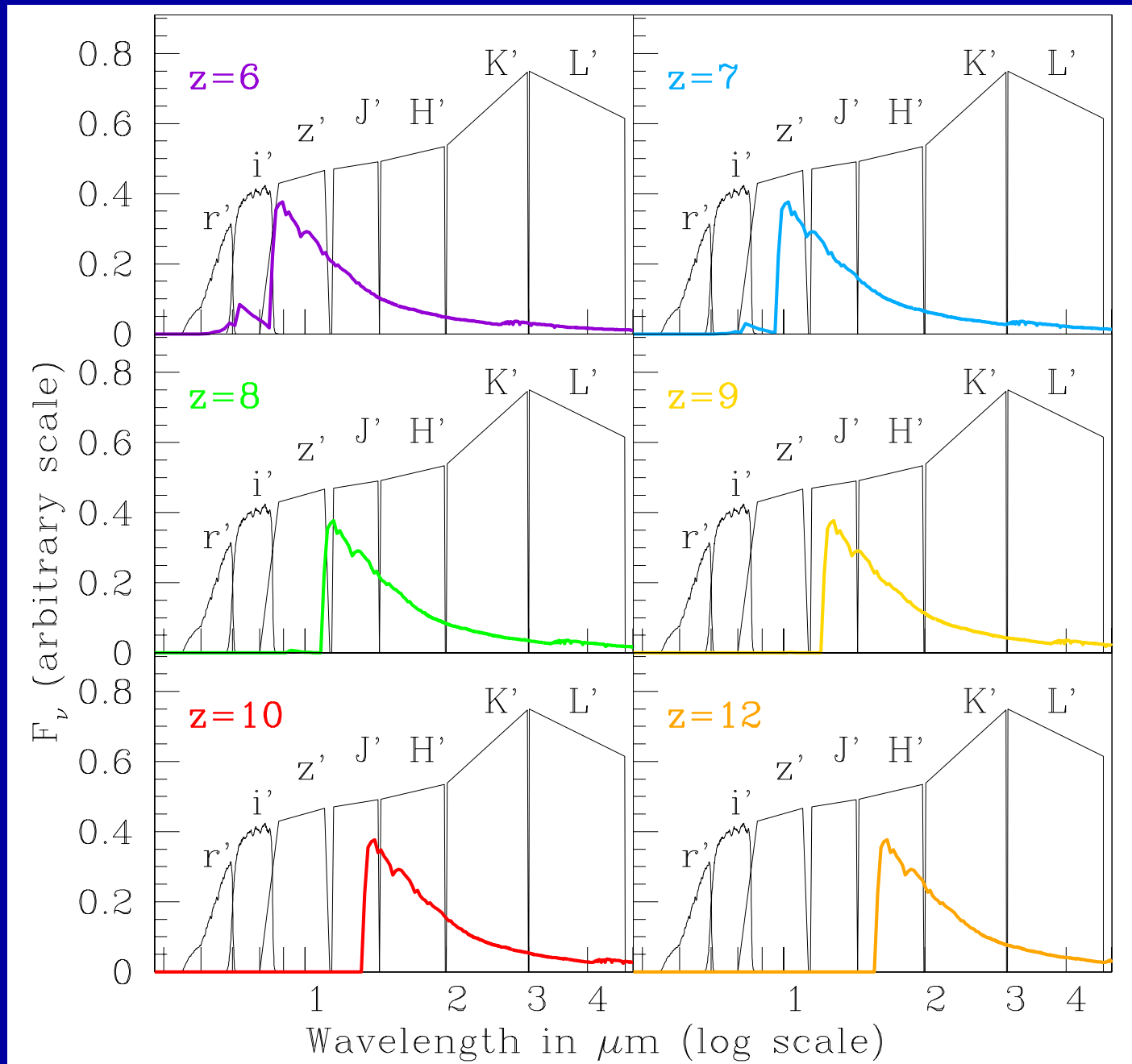
(PSF's are shown at logarithmic stretch — they still have  $\gtrsim 74\%$  EE for  $r \lesssim 0.15''$ ).



$\lesssim$ 20 hrs JWST NIRCam at 0.7, 0.9, 2.0  $\mu\text{m}$  in the HUDF

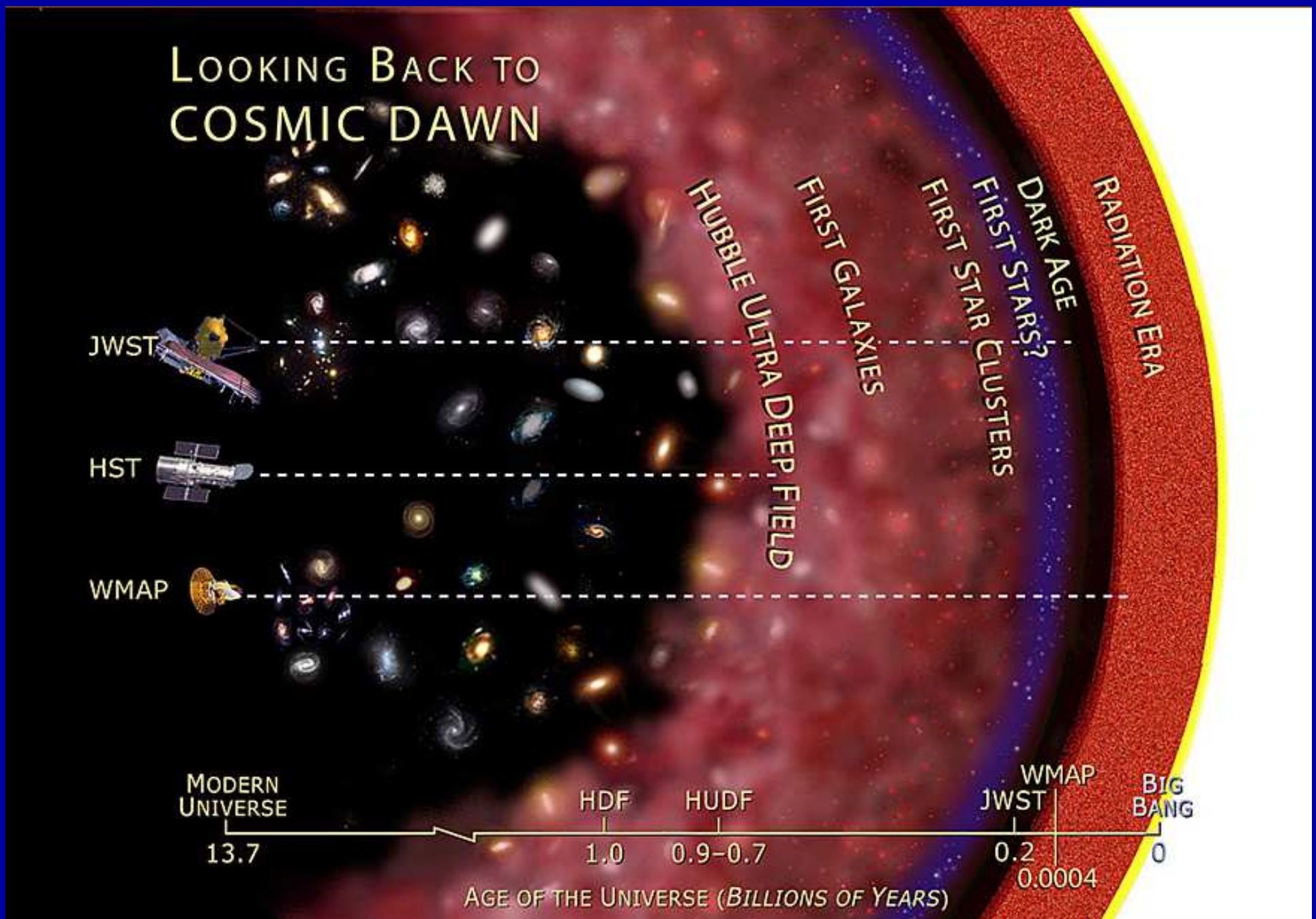


Truth $\equiv$ 240 hrs HUDF Vi'z'     $\lesssim$ 20 hrs JWST 0.7, 0.9, 2.0  $\mu$ m



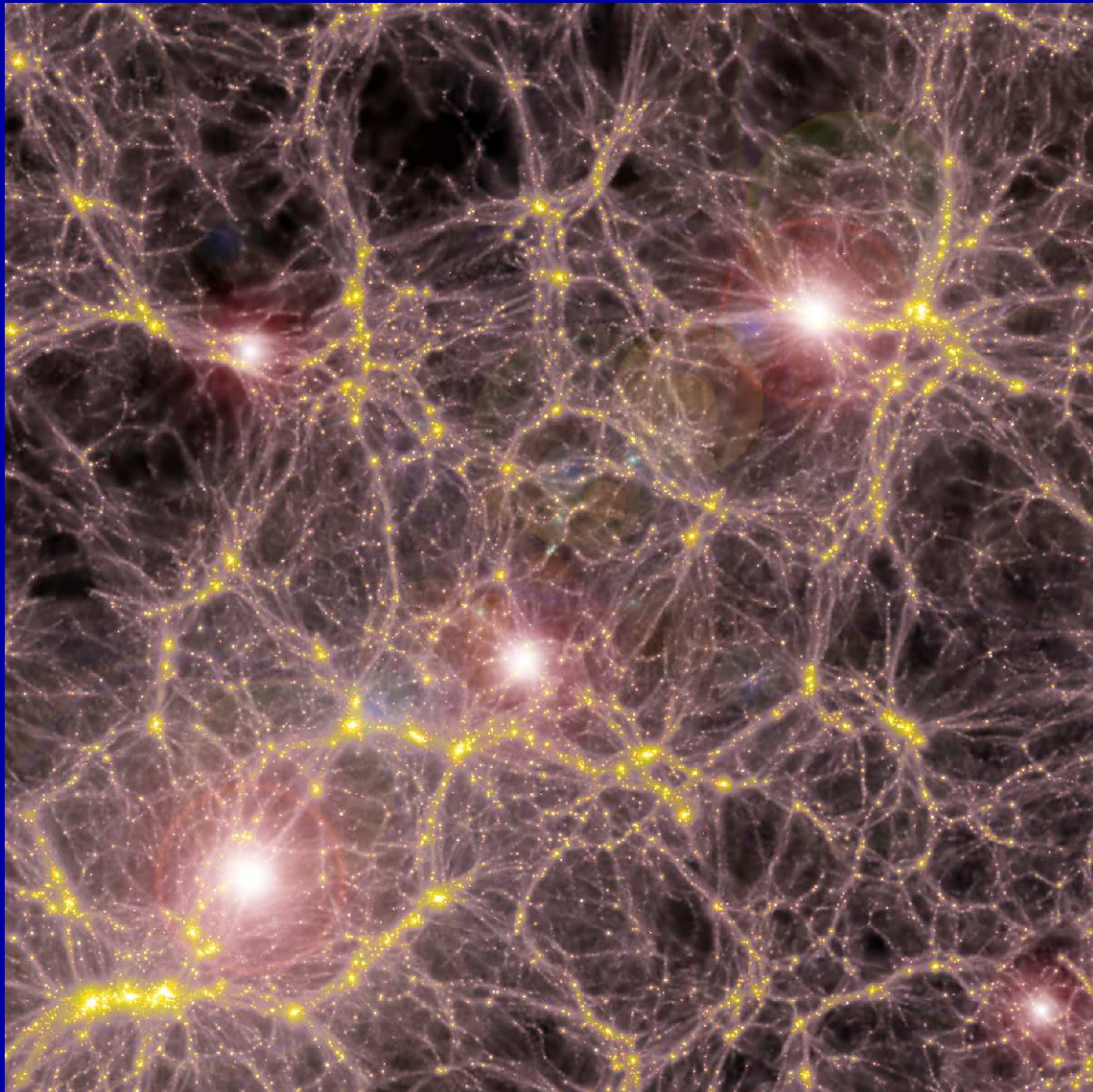
- Can't beat redshift: to see First Light, must observe near-mid IR.  
⇒ This is why JWST needs NIRCam at 0.8–5  $\mu\text{m}$  and MIRI at 5–28  $\mu\text{m}$ .

### (3a) What is First Light, Reionization, and Galaxy Assembly?



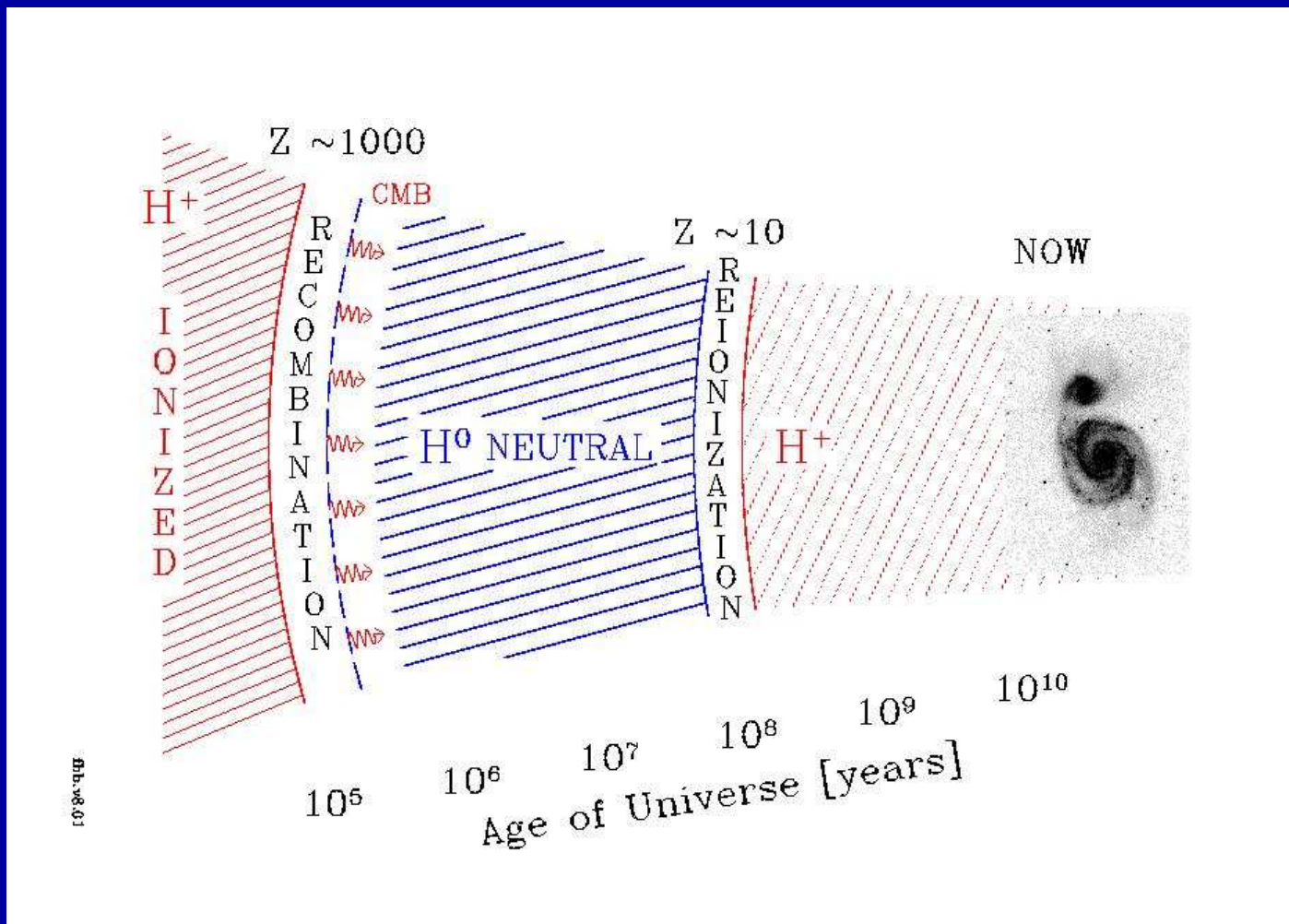
NASA telescopes penetrating Cosmic Dawn, First Light, & Recombination

- (3a) What is First Light and Reionization?



- Detailed Hydrodynamical models (V. Bromm) show that formation of Pop III stars reionized universe for the first time at  $z \lesssim 10-30$  (First Light).
- At this should be visible to JWST as the first Pop III star clusters, and perhaps their extremely luminous supernovae at  $z \simeq 10 \rightarrow 30$ .

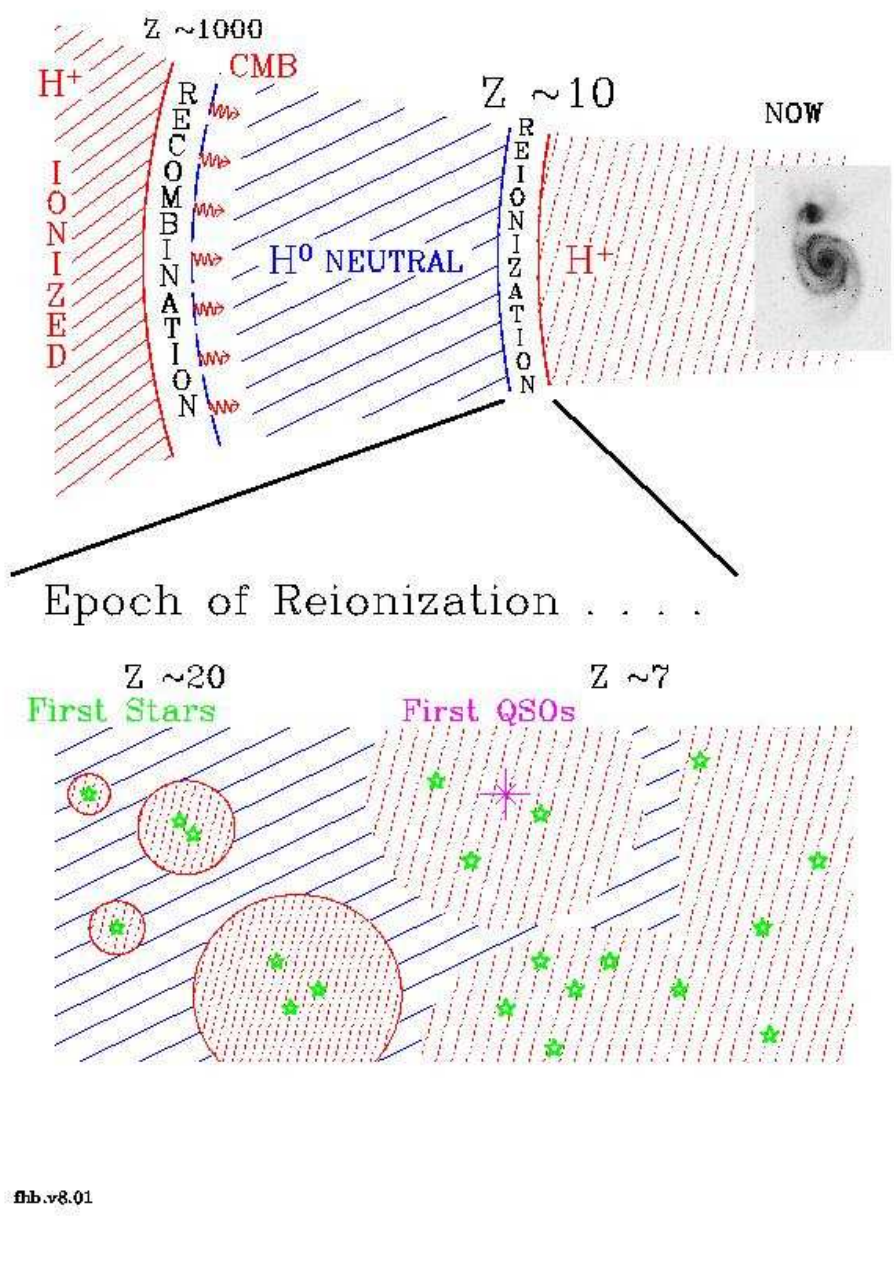
### ● (3a) What is First Light and Reionization?



WMAP: First light may have happened in two epochs (Cen 2003):

- (1) Population III stars with  $200\text{--}1000 M_{\odot}$  at  $z \simeq 11\text{--}20$  (First Light).
  - (2) First Population II stars (halo stars) form in dwarf galaxies of mass =  $10^6$  to  $10^9 M_{\odot}$  at  $z \simeq 6\text{--}9$ , which complete reionization (*cf.* F. Briggs 2002).
- ⇒ JWST needs NIRCam at 0.8–5  $\mu\text{m}$  and MIRI at 5–28  $\mu\text{m}$ .

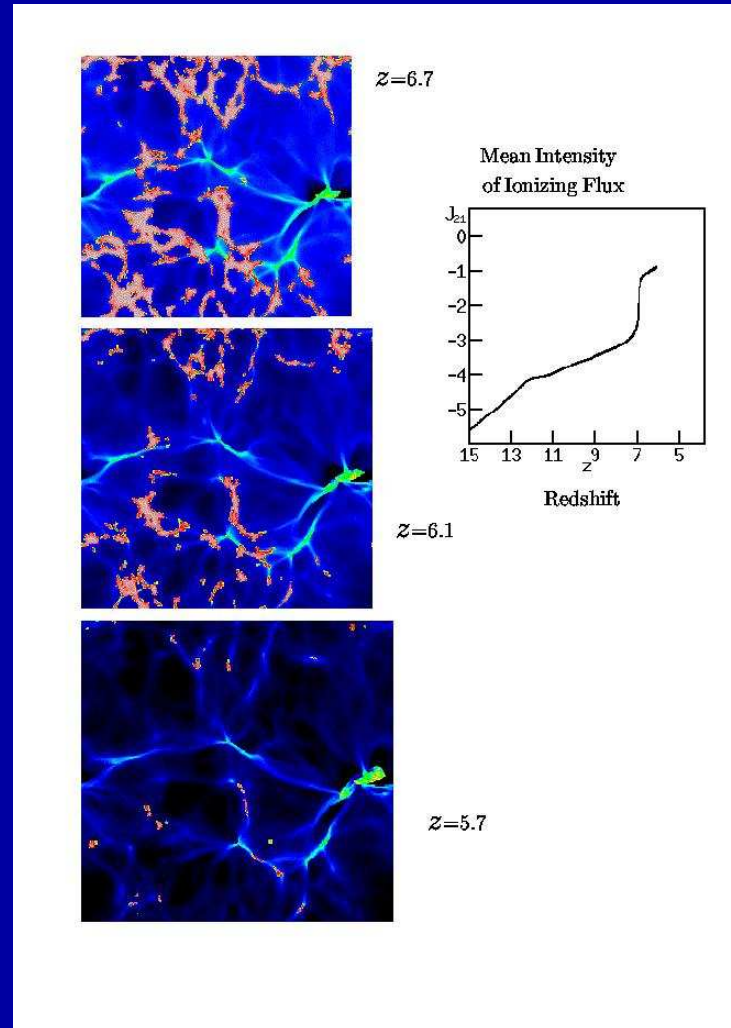
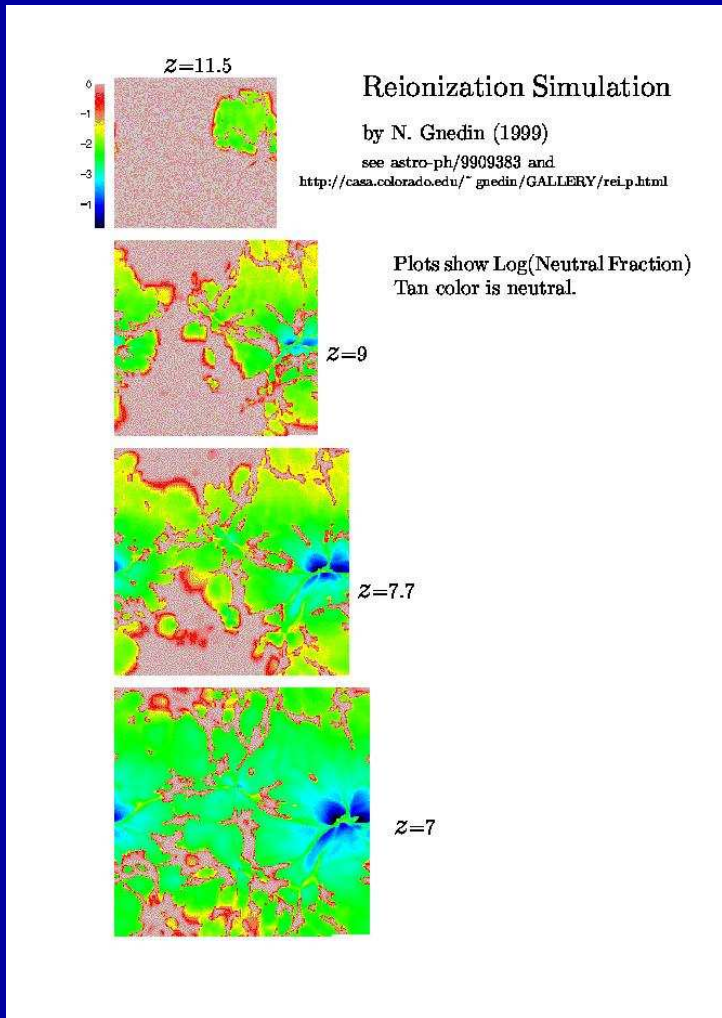
## End of 'The Dark Age'



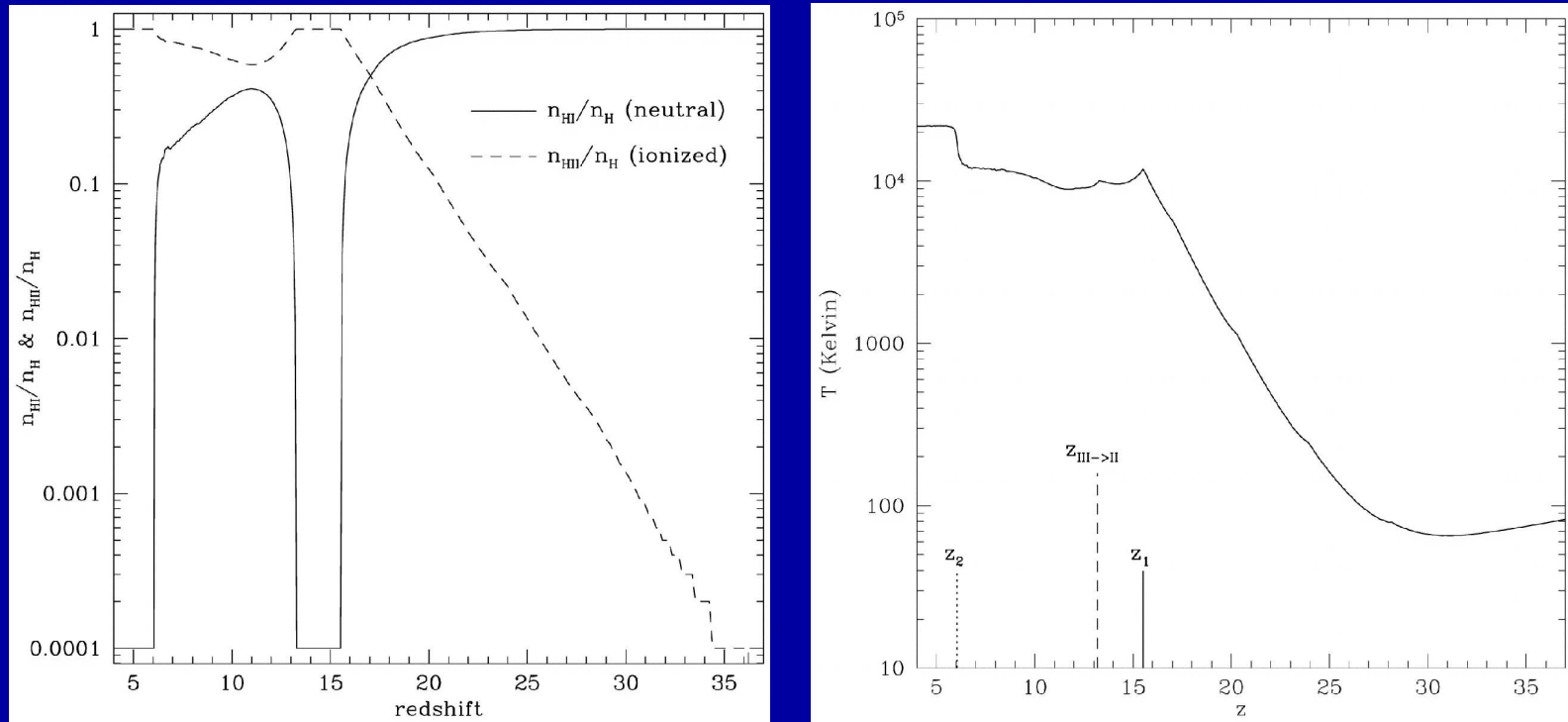
WMAP: First Light may have happened as following:

- (0) First Dark Ages since recombination ( $z=1089$ ) until first light objects started shining ( $z=11-20$ )
- (1) First Light when Population III stars start shining with mass= $200-1000 M_\odot$  at  $z\simeq 11-20$
- (2) Second Dark Ages since Pop III supernovae heated gas which could not cool and form normal Pop II halo stars until  $z\simeq 9-11$ .
- (3) This is followed by Pop II stars forming in dwarf galaxies (mass $\simeq 10^7-10^9 M_\odot$ ) at  $z\simeq 6-9$ , ending the epoch of reionization.

(Fig. courtesy of Dr. F. Briggs)



- Hydrodynamical models (Gnedin 2000) show that percolation of H-II regions due to Pop II stars started at  $z \simeq 9$  and ended in fully overlapping H-II regions at  $z \simeq 6$  (reionization completed, now seen in  $z \simeq 6$  QSO spectra).



WMAP and detailed Hydrodynamical models (Cen 2003) suggest that:

- (1) Population III stars caused epoch of First Light at  $z \simeq 11\text{--}20$ .
- (2) Pop III supernovae may have caused the Second Dark Ages at  $z = 9\text{--}11$ , since they heated the IGM, which could not cool until:
- (3) The first Pop II stars started forming in dwarf galaxies with  $10^7\text{--}10^9 M_\odot$  at  $z \simeq 6\text{--}9$ .

⇒ This will be visible to JWST in the luminosity function (LF) of the first star-forming objects at  $z \simeq 20 \rightarrow 6$ .



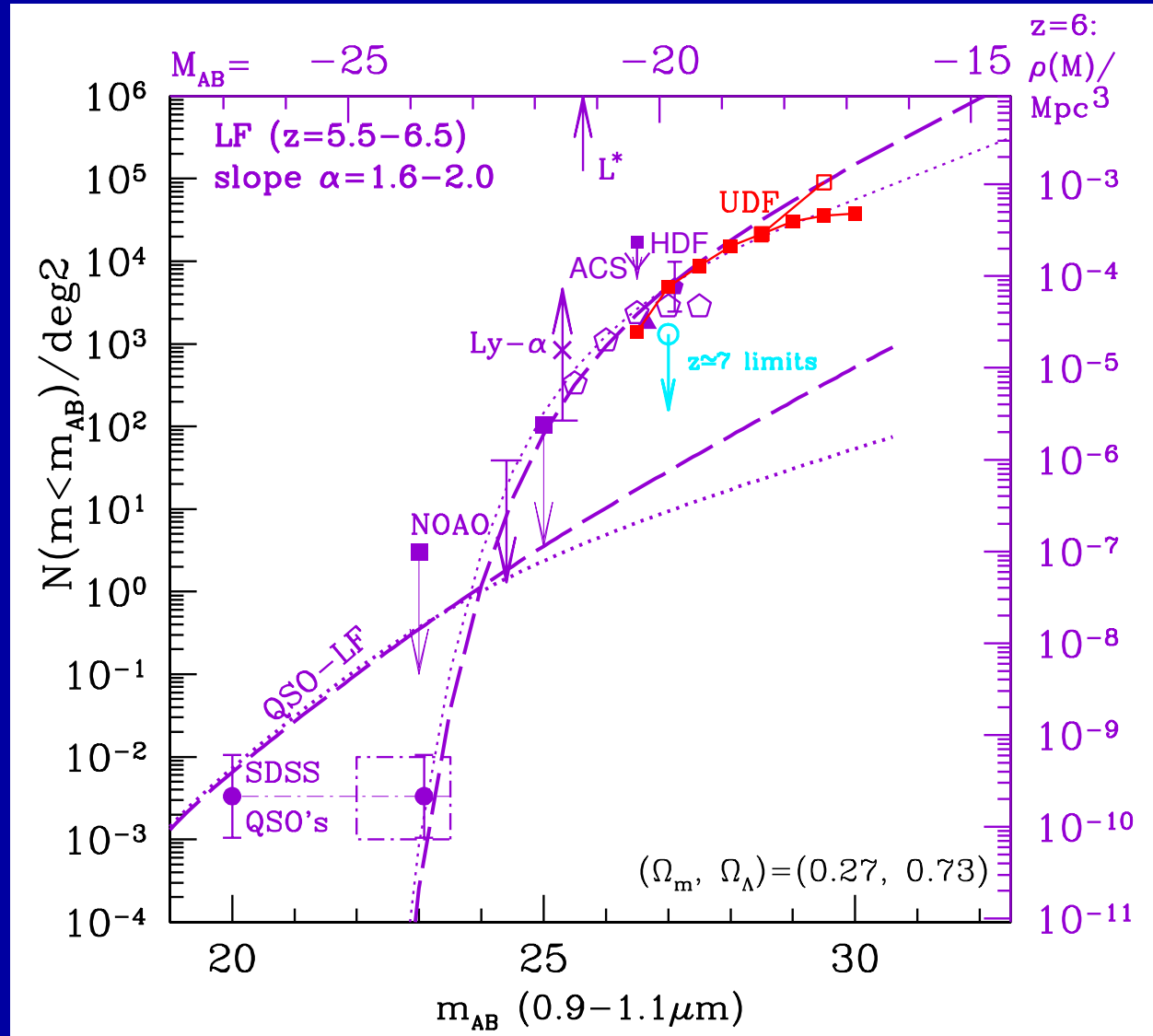
**Distant Galaxies in the Hubble Ultra Deep Field**  
Hubble Space Telescope • Advanced Camera for Surveys

NASA, ESA, R. Windhorst (Arizona State University) and H. Yan (Spitzer Science Center, Caltech)

STScI-PRC04-28

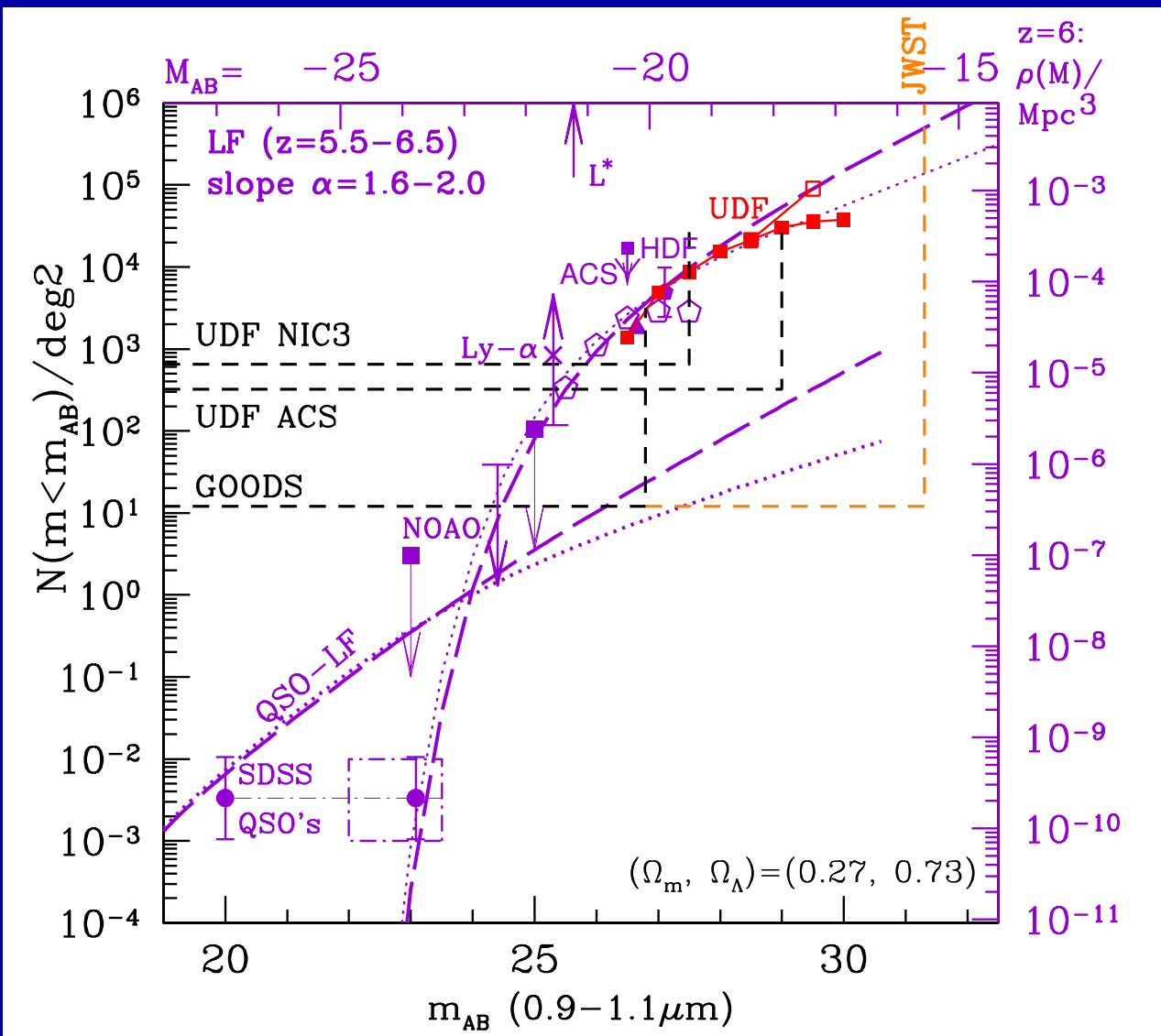
i-band drops in the HUDF: Most confirmed at  $z \approx 6$  (Malhotra et al. 2005)

- (3b) How JWST can measure First Light and Reionization

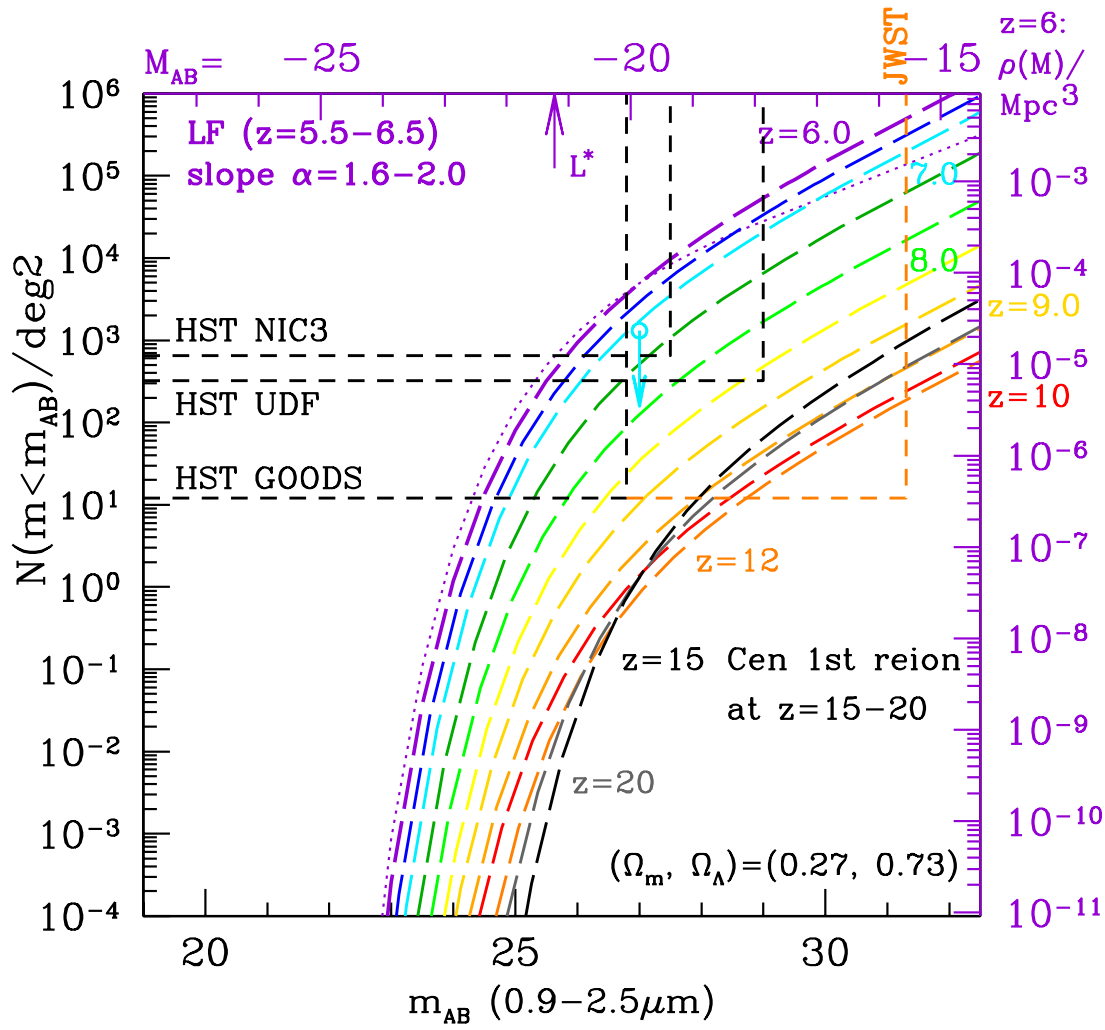


HUDF shows that luminosity function of  $z \simeq 6$  objects (Yan & Windhorst 2004a, b) may be very steep: faint-end Schechter slope  $|\alpha| \simeq 1.6-2.0$ .

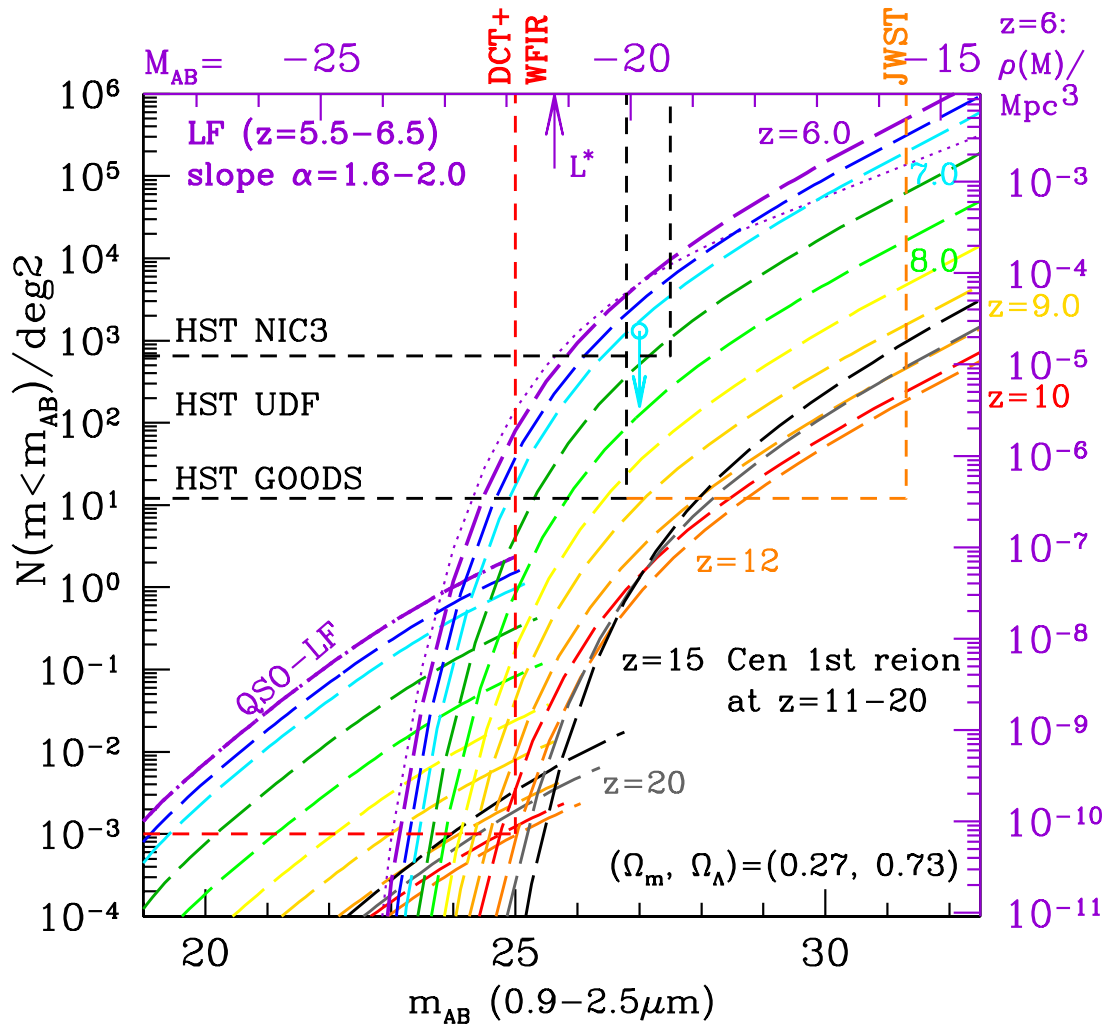
⇒ Dwarf galaxies and not quasars likely completed the reionization epoch at  $z \simeq 6$ . This is what JWST will observe in detail to  $z \gtrsim 20$ .



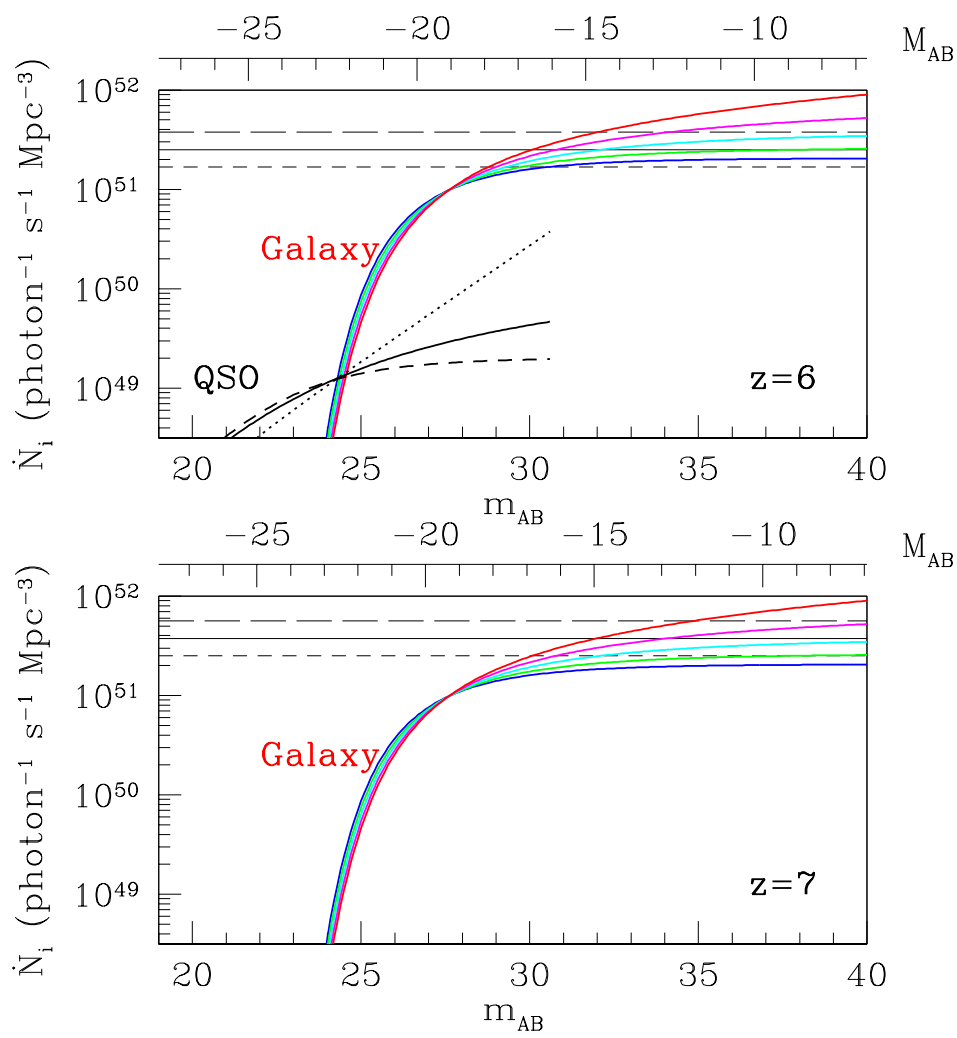
- HST/ACS has made significant progress at  $z \approx 6$ , surveying very large areas (GOODS, GEMS, COSMOS), or using very long integrations (HDF). ACS can detect objects at  $z \lesssim 6.5$ , but its discovery space  $A \cdot \Omega \cdot \Delta \log(\lambda)$  cannot map the entire reionization epoch. NICMOS similarly is limited to  $z \lesssim 8-10$ . JWST will be able to trace the entire reionization epoch.



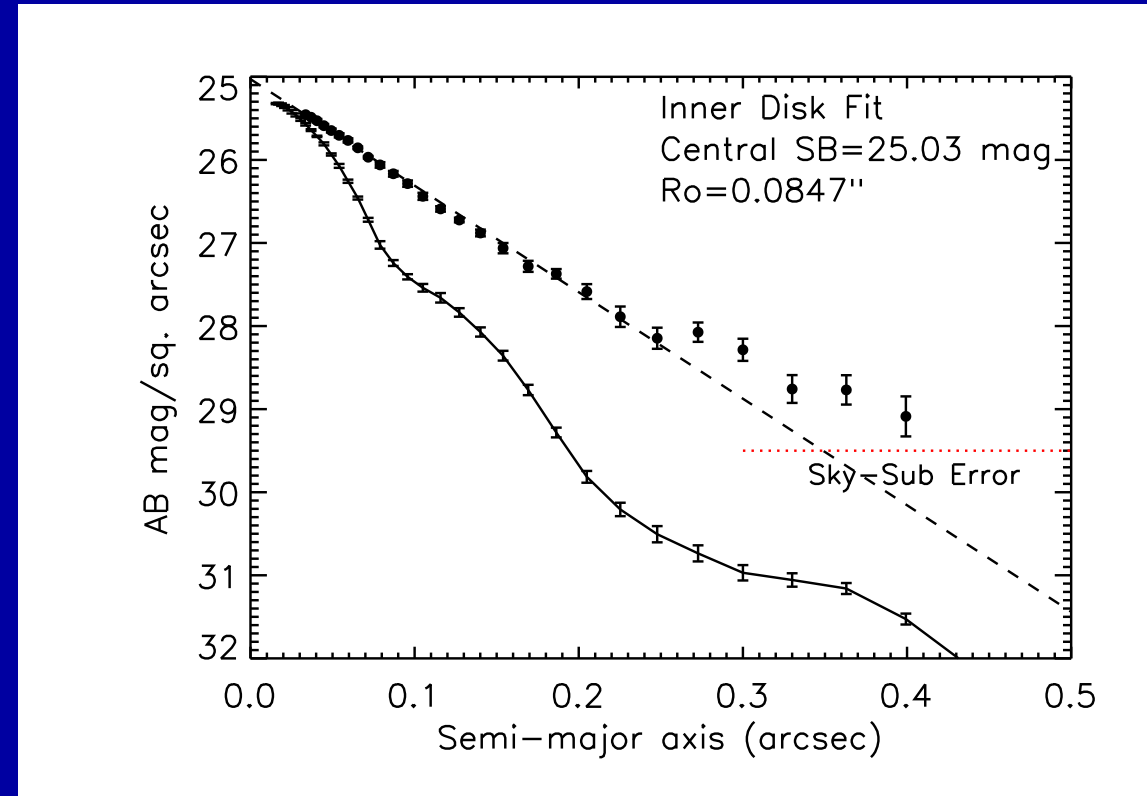
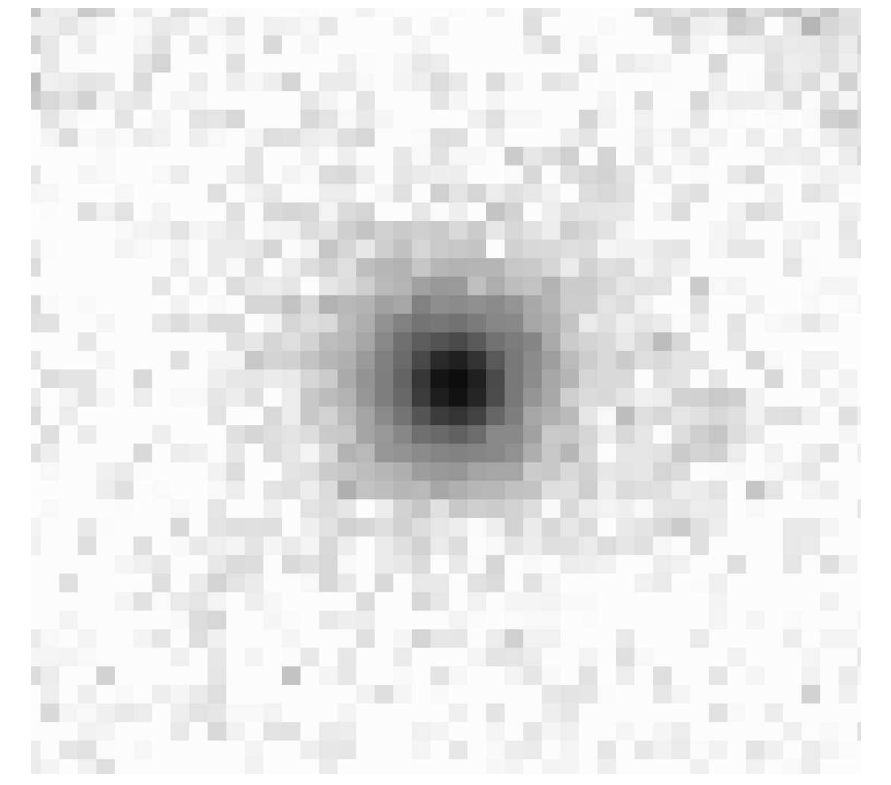
- With proper survey strategy (area AND depth), JWST can trace the entire reionization epoch and detect the first star-forming objects.
- Objects at  $z \gtrsim 9$  are rare, since volume element is small and JWST samples brighter part of LF. JWST needs the quoted sensitivity/aperture (A), field-of-view (FOV=Ω), and wavelength range (0.7-28 μm).



- Red boundaries indicate part of the galaxy and QSO LF that Discovery Channel Telescope with WF IRCam can explore to  $z=10$  and  $AB \lesssim 25$  mag.
- A ground-based wide-field near-IR survey to  $AB \lesssim 25$  mag  $z \lesssim 10$  is an essential complement to the JWST First Light studies:  
Co-evolution of supermassive black-holes and proto-bulges for  $z \lesssim 10$ .



- A steep LF of  $z \simeq 6$  objects (Yan & Windhorst 2004a, ApJL, 600, L1) could provide enough UV-photons to complete the reionization epoch at  $z \simeq 6$ .
- Pop II dwarf galaxies may not have started shining *pervasively* much before  $z \simeq 7\text{--}8$ , or no H-I would be seen in the foreground of  $z \gtrsim 6$  quasars.
- JWST will measure this numerous population of dwarf galaxies from the end of the reionization epoch at  $z \simeq 6$  into the epoch of First Light (Pop III stars) at  $z \gtrsim 10$ .

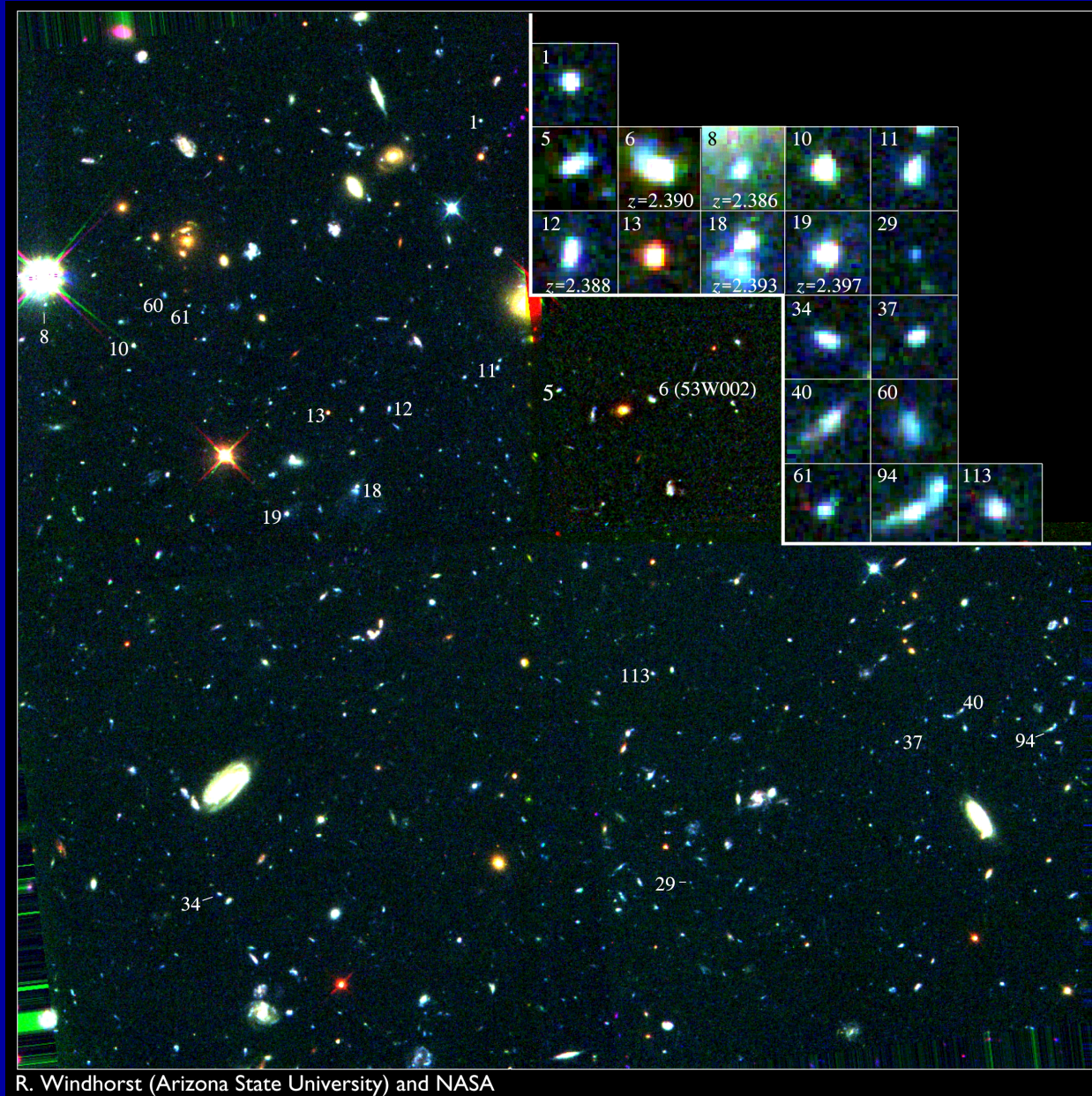


Sum of 49 isolated i-drops:  
=5000 hrs HUDF z-band.  
[ $\simeq 330$  hrs JWST 1  $\mu\text{m}$ ]

ACS light-profile, PSF and sky-error:  
Deviates from exp. disk at  $r_e \gtrsim 0\farcs25$   
 $\Rightarrow$  Dyn. age ( $z \simeq 6$ )  $\simeq 100$ -200 Myr  
(cf. N. Hathi et al. 2006)

HST/ACS cannot accurately measure individual light-profiles at  $z \simeq 6$ .  
JWST can do this well for  $z \gtrsim 6$  in very long integrations.  
Dynamical timescale  $\simeq$  SED timescale  $\Rightarrow$  Bulk of SF at  $z_{form} \simeq 7.0 \pm 0.5??$

- (4) How JWST can measure Galaxy Assembly

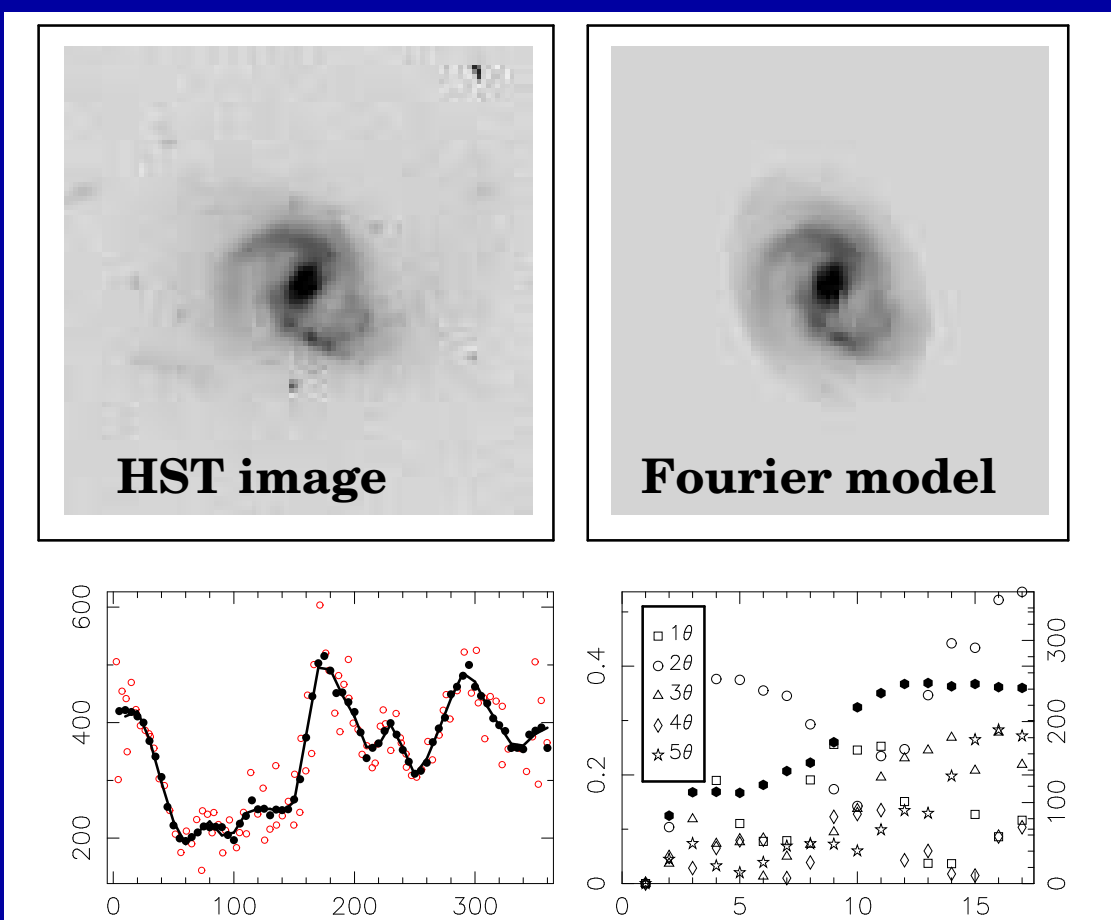


One of the remarkable discoveries of HST was how numerous and small faint galaxies are — the building blocks of the giant galaxies seen today.

# THE HUBBLE DEEP FIELD CORE SAMPLE ( $I < 26.0$ )



- (4) How JWST can measure Galaxy Assembly
- Galaxies of Hubble types formed over a wide range of cosmic time, but with a notable phase transition around  $z \simeq 0.5\text{--}1.0$ :
  - (1) Subgalactic units rapidly merge from  $z \simeq 7 \rightarrow 1$  to grow bigger units.
  - (2) Merger products start to settle as galaxies with giant bulges or large disks around  $z \simeq 1$ . These evolved mostly passively since then, resulting in the giant galaxies that we see today.
- JWST can measure how galaxies of all types formed over a wide range of cosmic time, by accurately measuring their distribution over rest-frame structure and type as a function of redshift or cosmic epoch.

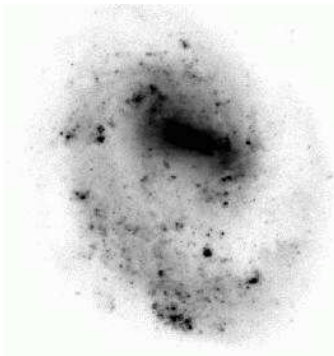


Fourier Decomposition is a robust way to measure galaxy morphology and structure in a quantitative way (Odewahn et al. 2002):

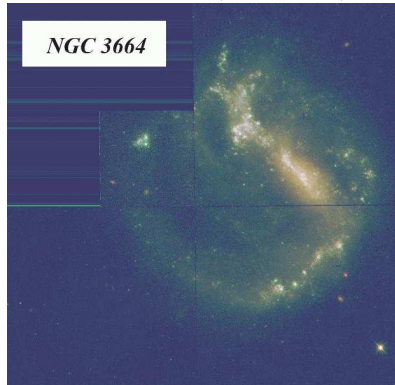
- (1) Fourier series are made in successive concentric annuli.
- (2) Even Fourier components indicate symmetric parts (arms, rings)
- (3) Odd Fourier components indicate asymmetric parts (bars etc).
- (4) JWST can measure the evolution of each feature directly.

## Massive Star Formation: Near and Far

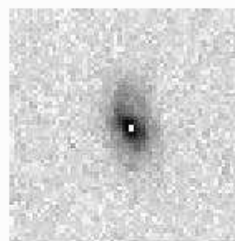
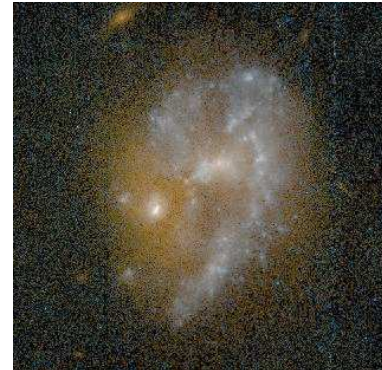
NGC 4618 (VATT, B)



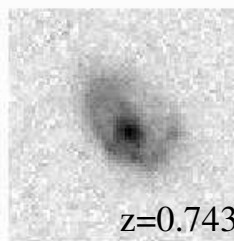
NGC 3664 (WFPC2)



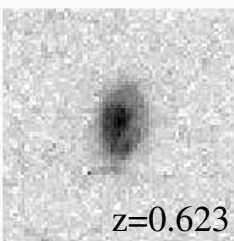
UGC 5028 (HST,Cyc9)



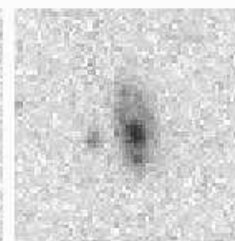
$z=0.743$



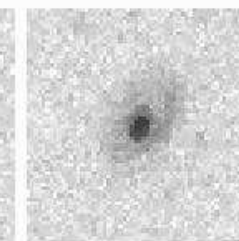
$z=0.623$



$z=0.6-0.7$



$z=0.6-0.7$

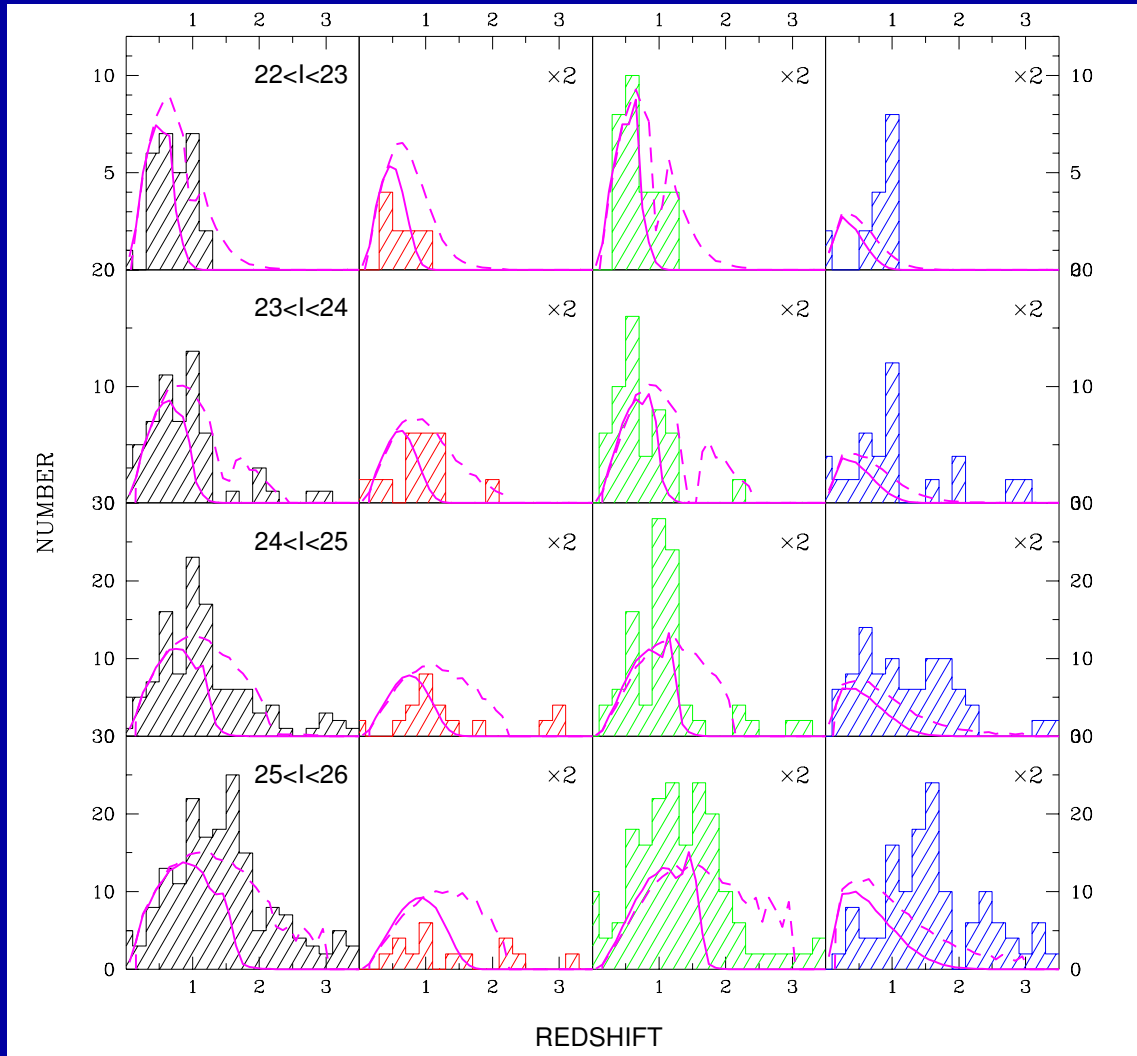


BBP

53W02  
HDFS

Fourier Decomposition of nearby and distant galaxies in JWST images will directly trace the evolution of bars, rings, spiral arms, and other structural features. This measures the detailed history of galaxy assembly in the epoch  $z \simeq 1-3$  when most of today's giant galaxies were made.

# Total Ell/S0 Sabc Irr/Mergers



- JWST can measure how galaxies of all Hubble types formed over a wide range of cosmic time, by measuring their redshift distribution as a function of rest-frame type.
- For this, the types must be well imaged for large samples from deep, uniform and high quality multi-wavelength images, which JWST can do.

NGC 3310



ESO0418-008



UGC06471-2



## Ultraviolet Galaxies

NASA and R. Windhorst (Arizona State University) • STScI-PRC01-04

HST • WFPC2

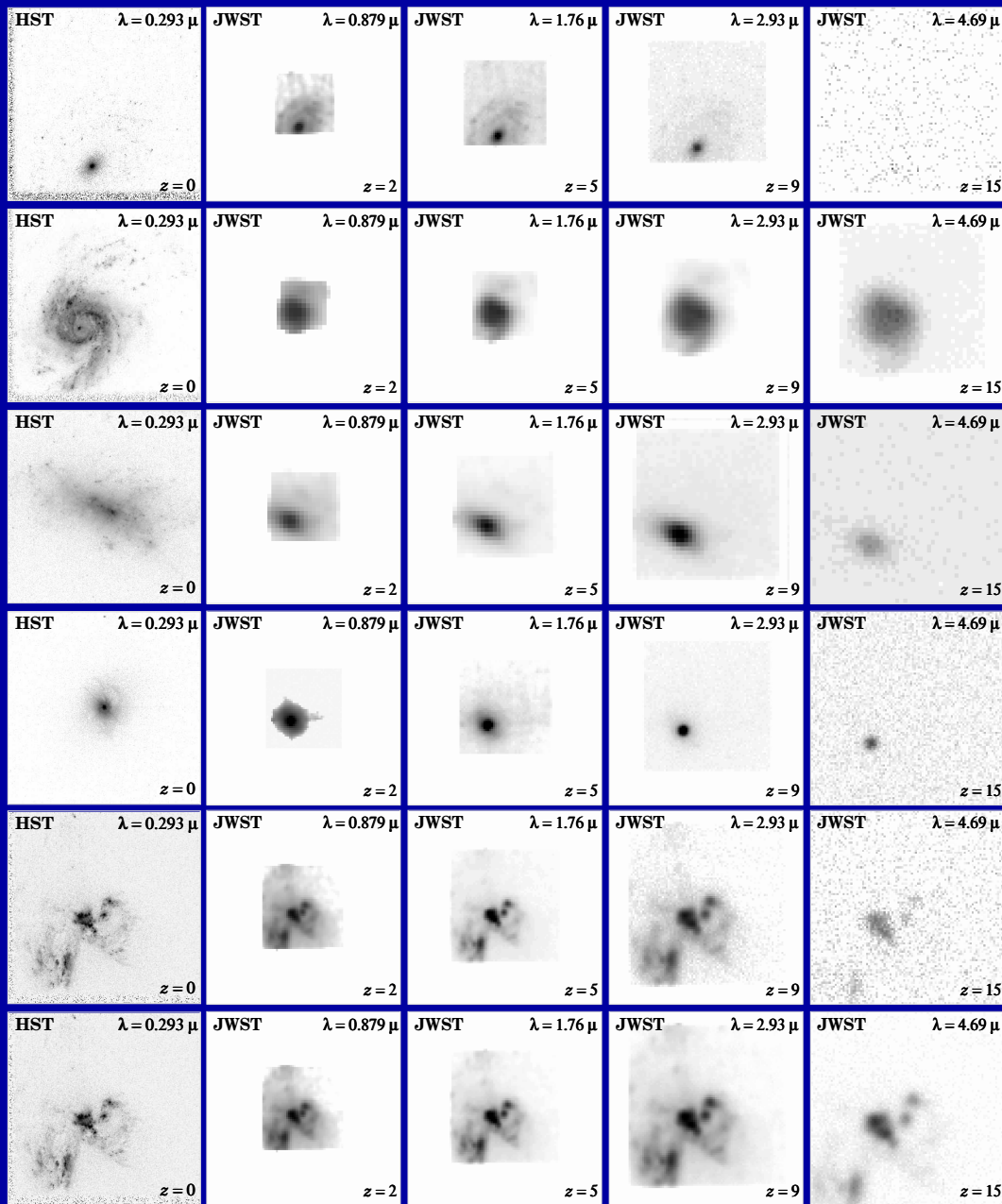
- The uncertain rest-frame UV-morphology of galaxies is dominated by young and hot stars, with often copious amounts of dust superimposed.
- This makes comparison with very high redshift galaxies seen by JWST complicated, although with good images a quantitative analysis of the restframe-wavelength dependent morphology and structure can be made.



Hubble UV image of galaxy NGC 6782: spectacular star-forming rings

## (5) Predicted Galaxy Appearance for JWST at $z \simeq 1-15$

HST  $z=0$    JWST  $z=2$        $z=5$        $z=9$        $z=15$



With proper restframe-UV training, JWST can quantitatively measure the evolution of galaxy morphology and structure over a wide range of cosmic time:

- (1) Most disks will SB-dim away at high  $z$ , but most formed at  $z \lesssim z_{form} \simeq 1-2$ .
- (2) High SB structures are visible to very high  $z$ .
- (3) Point sources (AGN) are visible to very high  $z$ .
- (4) High SB-parts of mergers/train-wrecks are visible to very high  $z$ .

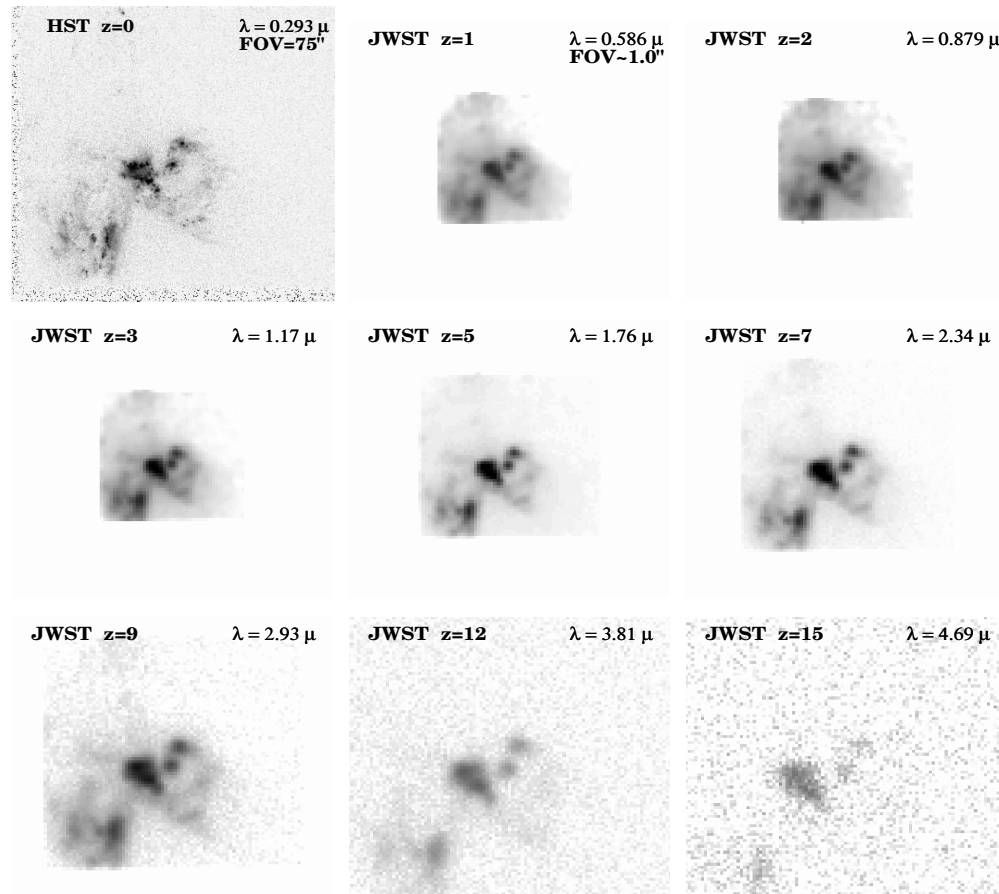


**Fig. 4.06.a.** JWST simulations based on HST/WFPC2 F300W images of the merger UGC06471-2 ( $z=0.0104$ ). Note that the two unresolved star-bursting knots in the center remain visible until  $z\sim 12$ , beyond which the SB-dimming also kills their flux. This is the NOMINAL JWST [= (GOALS+REQUIREMENTS)/2].

ASSUMPTIONS: COSMOLOGY:  $H_0=71 \text{ km/s/Mpc}$ ,  $\Omega_m=0.27$ , and  $\Omega_\Lambda=0.73$ .

INSTRUMENT: 6.0 m effective aperture, JWST/NIRCam,  $0.034''/\text{pix}$ ,  $RN=5.0 \text{ e}^-$ ,  $\text{Dark}=0.020 \text{ e}^-/\text{sec}$ , NEP  $H\text{-band Sky}=21.7 \text{ mag/arcsec}^2$  in L2, Zodiacal spectrum,  $t_{exp}=1.0 \text{ hrs}$ , read-out every 900 sec ("NOMINAL").

**Row 1:**  $z=0.0$  (HST  $\lambda=0.293\mu\text{m}$ , FWHM= $0.04''$ ),  $z=1.0$  (JWST  $\lambda=0.586\mu\text{m}$ , FWHM= $0.084''$ ), and  $z=2.0$  (JWST  $\lambda=0.879\mu\text{m}$ , FWHM= $0.084''$ ). **Row 2:**  $z=3.0$  (JWST  $\lambda=1.17\mu\text{m}$ , FWHM= $0.084''$ ),  $z=5.0$  (JWST  $\lambda=1.76\mu\text{m}$ , FWHM= $0.084''$ ), and  $z=7.0$  (JWST  $\lambda=2.34\mu\text{m}$ , FWHM= $0.098''$ ). **Row 3:**  $z=9.0$  (JWST  $\lambda=2.93\mu\text{m}$ , FWHM= $0.122''$ ),  $z=12.0$  (JWST  $\lambda=3.81\mu\text{m}$ , FWHM= $0.160''$ ), and  $z=15.0$  (JWST  $\lambda=4.69\mu\text{m}$ , FWHM= $0.197''$ )

The galaxy merger UGC06471-2 ( $z=0.0104$ ) is a major and very dusty collision of two massive disk galaxies.

It shows two bright unresolved star-bursting knots to the upper-right of the center, which remain visible until  $z\simeq 12$ , beyond which the cosmic SB-dimming kills their flux. These are more typical for the small star-forming objects expected at  $z\simeq 10-15$ .

This is the NOMINAL JWST = (GOALS+REQUIREMENTS)/2.

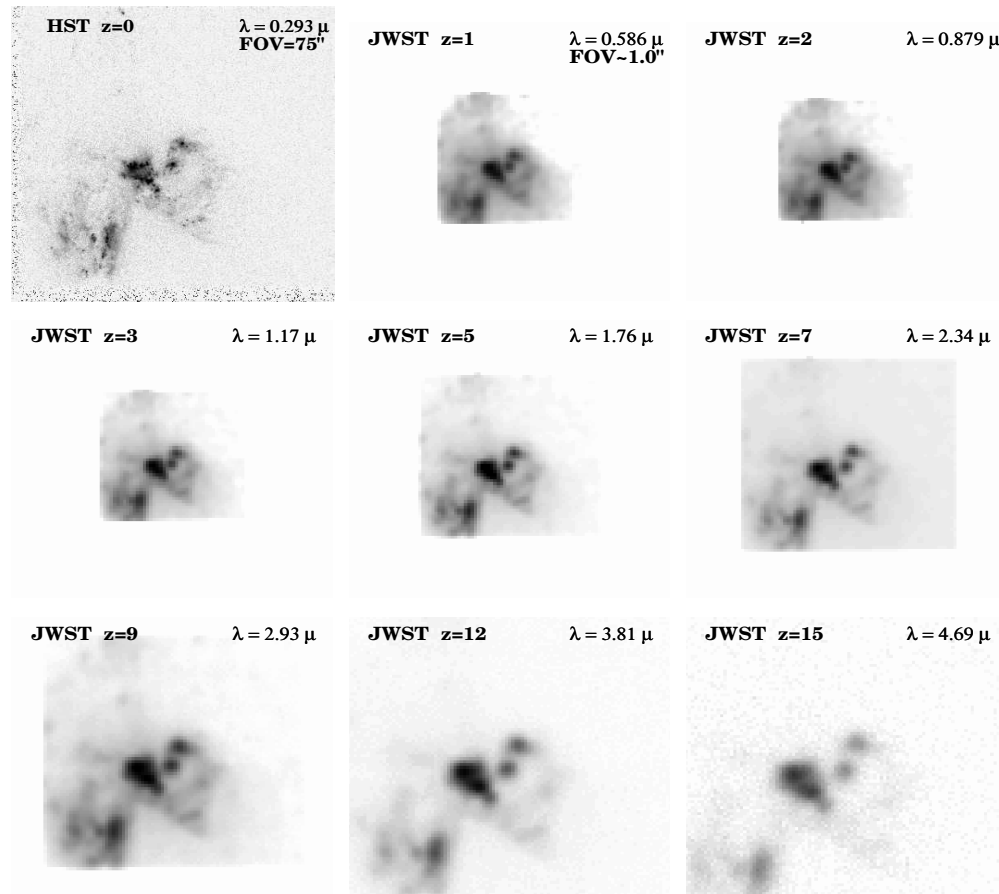


**Fig. 4.06.c.** JWST simulations based on HST/WFPC2 F300W images of the merger UGC06471-2 ( $z=0.0104$ ). This is the BEST CASE JWST [meeting all GOALS, and  $t_{exp}=100$  hrs]. The object is recognizable to  $z\simeq 15$ .

ASSUMPTIONS: COSMOLOGY:  $H_0=71$  km/s/Mpc,  $\Omega_m=0.27$ , and  $\Omega_\Lambda=0.73$ .

INSTRUMENT: 6.0 m effective aperture, JWST/NIR camera,  $0.034''/\text{pix}$ ,  $RN=3.0\text{ e}^-$ ,  $\text{Dark}=0.010\text{ e}^-/\text{sec}$ , NEP H-band Sky=21.7 mag/arcsec<sup>2</sup> in L2, Zodi spectrum,  $t_{exp}=100.0$  hrs, read-out every 900 sec ("GOALS").

**Row 1:**  $z=0.0$  (HST  $\lambda=0.293\mu\text{m}$ , FWHM= $0.04''$ ),  $z=1.0$  (JWST  $\lambda=0.586\mu\text{m}$ , FWHM= $0.084''$ ), and  $z=2.0$  (JWST  $\lambda=0.879\mu\text{m}$ , FWHM= $0.084''$ ). **Row 2:**  $z=3.0$  (JWST  $\lambda=1.17\mu\text{m}$ , FWHM= $0.084''$ ),  $z=5.0$  (JWST  $\lambda=1.76\mu\text{m}$ , FWHM= $0.084''$ ), and  $z=7.0$  (JWST  $\lambda=2.34\mu\text{m}$ , FWHM= $0.098''$ ). **Row 3:**  $z=9.0$  (JWST  $\lambda=2.93\mu\text{m}$ , FWHM= $0.122''$ ),  $z=12.0$  (JWST  $\lambda=3.81\mu\text{m}$ , FWHM= $0.160''$ ), and  $z=15.0$  (JWST  $\lambda=4.69\mu\text{m}$ , FWHM= $0.197''$ )

## The galaxy merger UGC06471-2 ( $z=0.0104$ ).

This is the BEST CASE JWST. It assumes that all GOALS are met, and that  $t_{exp}=100$  hrs. The whole object (including the two star-forming knots) is recognizable to  $z\simeq 15$ .

This does not imply that observing galaxies at  $z=15$  with JWST will be easy. On the contrary, since galaxies formed through hierarchical merging, many objects at  $z\simeq 10-15$  will be  $10^1-10^4\times$  less luminous, requiring to push JWST to its limits.

## (6) Penetrating the Dark Ages with a low-frequency Lunar Interferometer



- Very Large Array (VLA, NM): 27 radio dishes (25-m) movable on railroad tracks over 1–27 km baselines  $\Rightarrow$  1–30" resolution at  $\nu \simeq$ GHz.

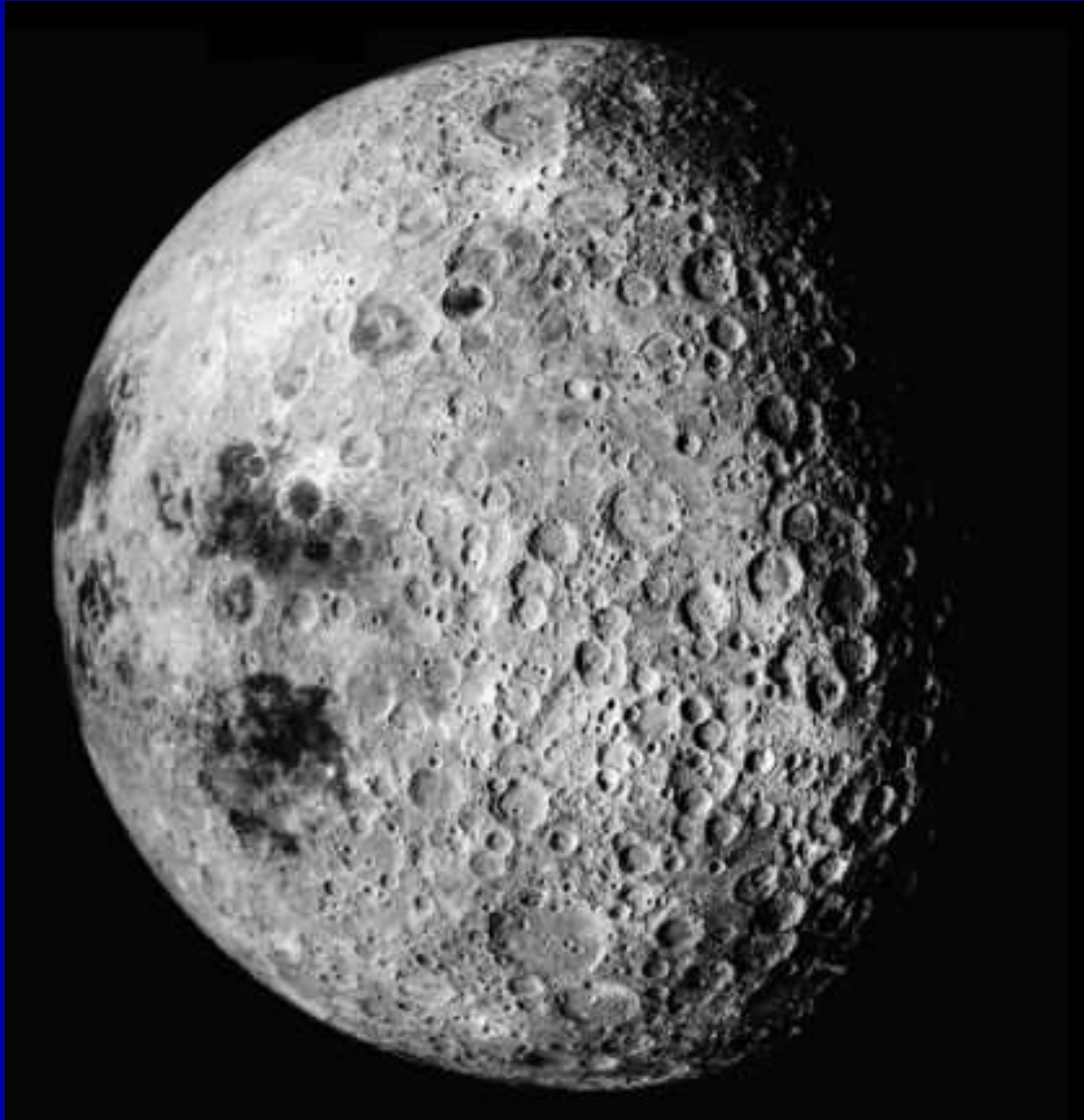
- (6) Radio Telescopes — Transcontinental Interferometers



- Very Long Baseline Array (VLBA): 10 fixed 25-m radio dishes across the US with 5000 km maximum baselines  $\Rightarrow \lesssim 0.01''$  resolution at  $\nu \simeq \text{GHz}$ .

- (6) A Low-frequency Interferometer on the Moon's far-side

Only place free of: (a) human ULF interference; (b) ionospheric absorption



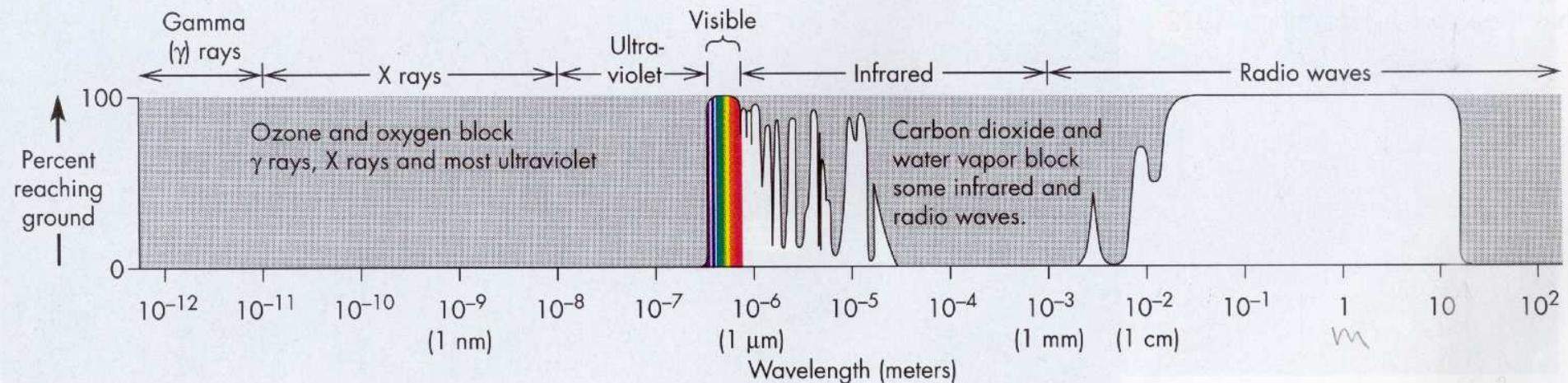
- Moon's far-side has enough flat craters for interferometers of  $\lesssim 3000$  km baselines and hectare-collecting area  $\Rightarrow \text{FWHM} \lesssim 1''$  at  $\nu \lesssim 30$  MHz.

- (6) Far-side of the Moon — only place to find H-I at redshifts  $z \gtrsim 45$ :

**FIGURE 6.28**

**The Transmission of Earth's Atmosphere**

The percentage of radiation that reaches the ground varies greatly with wavelength. Only in the visible, infrared, and radio wavelengths are there spectral regions in which the atmosphere is transparent.



- Far-side of Moon only place free of human-made ULF interference and ionospheric absorption.
- $\Rightarrow$  H-I studies at  $\nu \lesssim 30$  MHz  $\Leftrightarrow$  can see  $\nu$ (H-I=1421 MHz) at  $z \gtrsim 45$  !
- $\Rightarrow$  Moon's far-side needed to penetrate first 55 Myr of the Universe's history: the Cosmic Dark Ages.

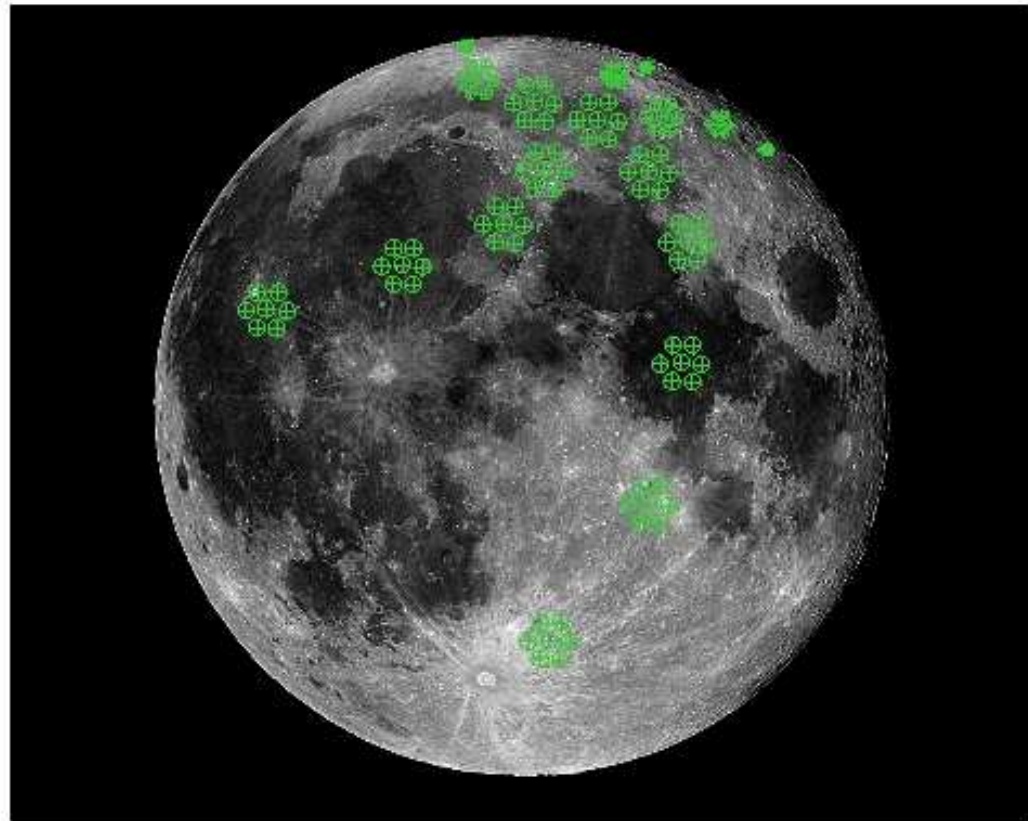
## ● (6) Lunar Dark-Ages Array — How to build it?

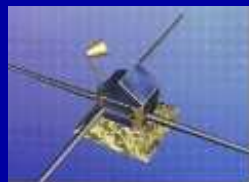


- Use long-duration science rovers to lay down a fractal grid of foil and dipoles. Foil backs up as solar panels. The EU LOFAR is a proto-type.
- Exact geometry is not important. Surface accuracy may be  $\lesssim 50$  cm!
- Use Ka-band to correlate data, Lunar TDRSS to send to Earth (Tb/day).
- Weeks–months to build. Then use rovers to explore interesting areas.

# Lunar LOFAR: *Distributed array of radio sensors*

- Number N of antennas: growing from 4 to 100 to 10000
- Collecting area  $A_{\text{eff}}$ :  
 $N \times \lambda^2$  ( $10 \text{ MHz} \sim \lambda 30 \text{ m}$ )  
 $A_{\text{eff}} \sim 0.09 \text{ km}^2, 9 \text{ km}^2$   
( $N=10^2, N=10^4, =10 \text{ MHz}$ )  
 $A_{\text{eff}} \sim 9 \text{ km}^2, 90 \text{ km}^2$   
( $N=10^2, N=10^4, =1 \text{ MHz}$ )
- Baselines  $D \sim 100-1000 \text{ km}$   
⇒ Resolution ( $\lambda/D$ ):  
~6'' ( $D/1000 \text{ km}$ ) @ 10 MHz  
~1' ( $D/1000 \text{ km}$ ) @ 1 MHz
- Grouping in 100 stations with 100 antennas (alternative: 30×30)?
  - Minimum diameter of station ~3.3 km (densely packed for 1 MHz)
  - Average separation of dipoles ~ 300 Meter

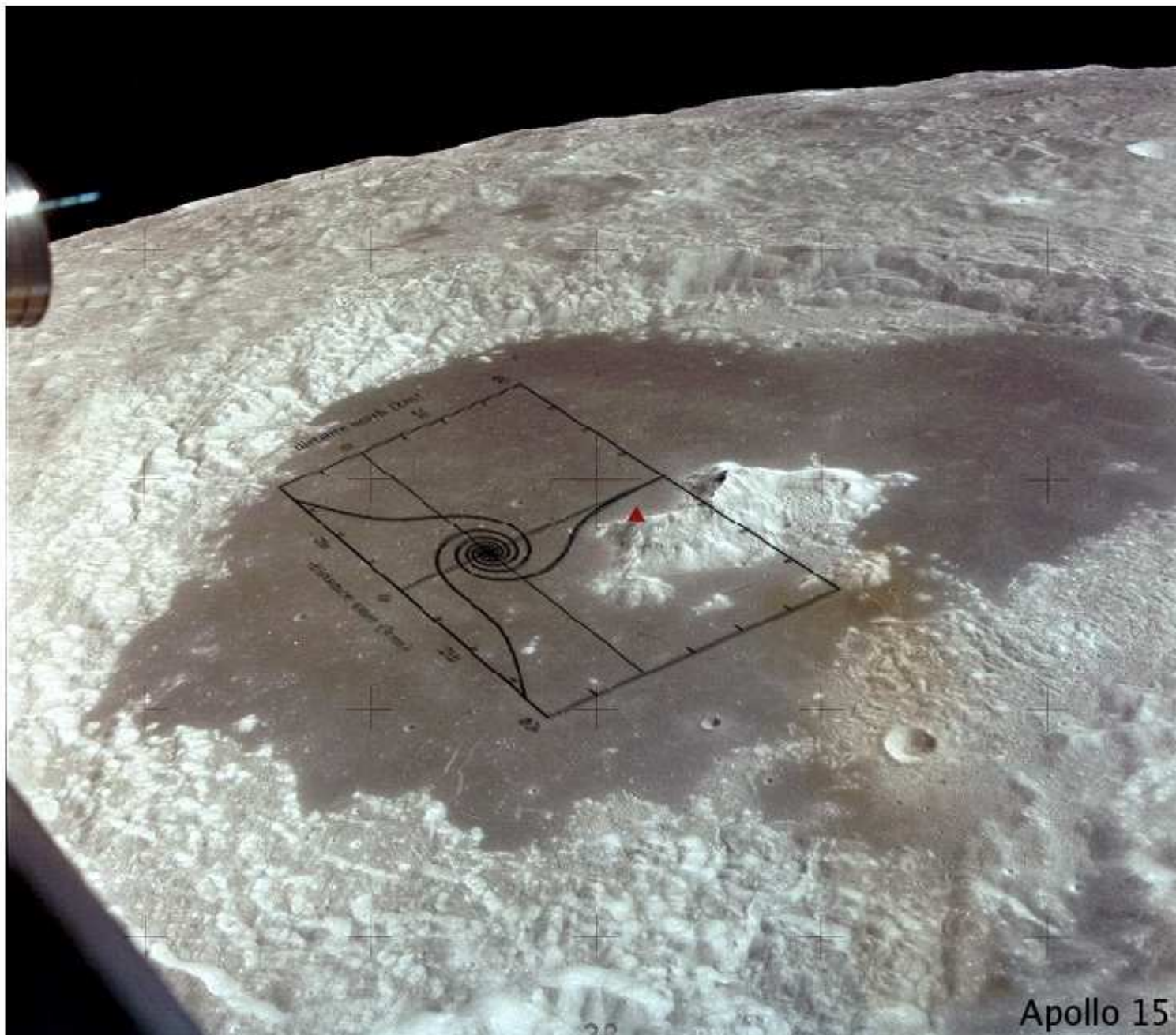
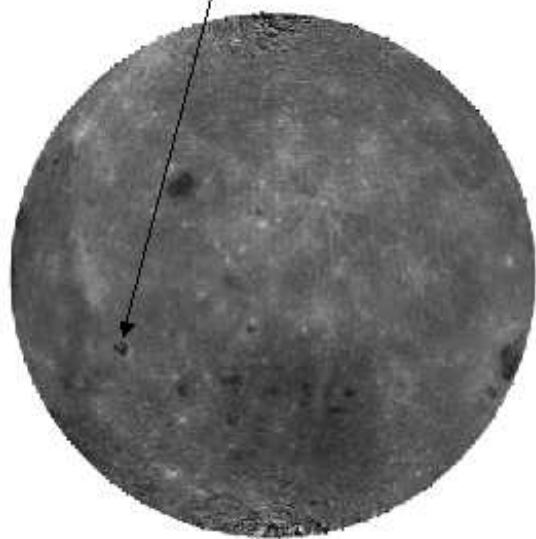




# proposed site: Tsiolkovsky crater

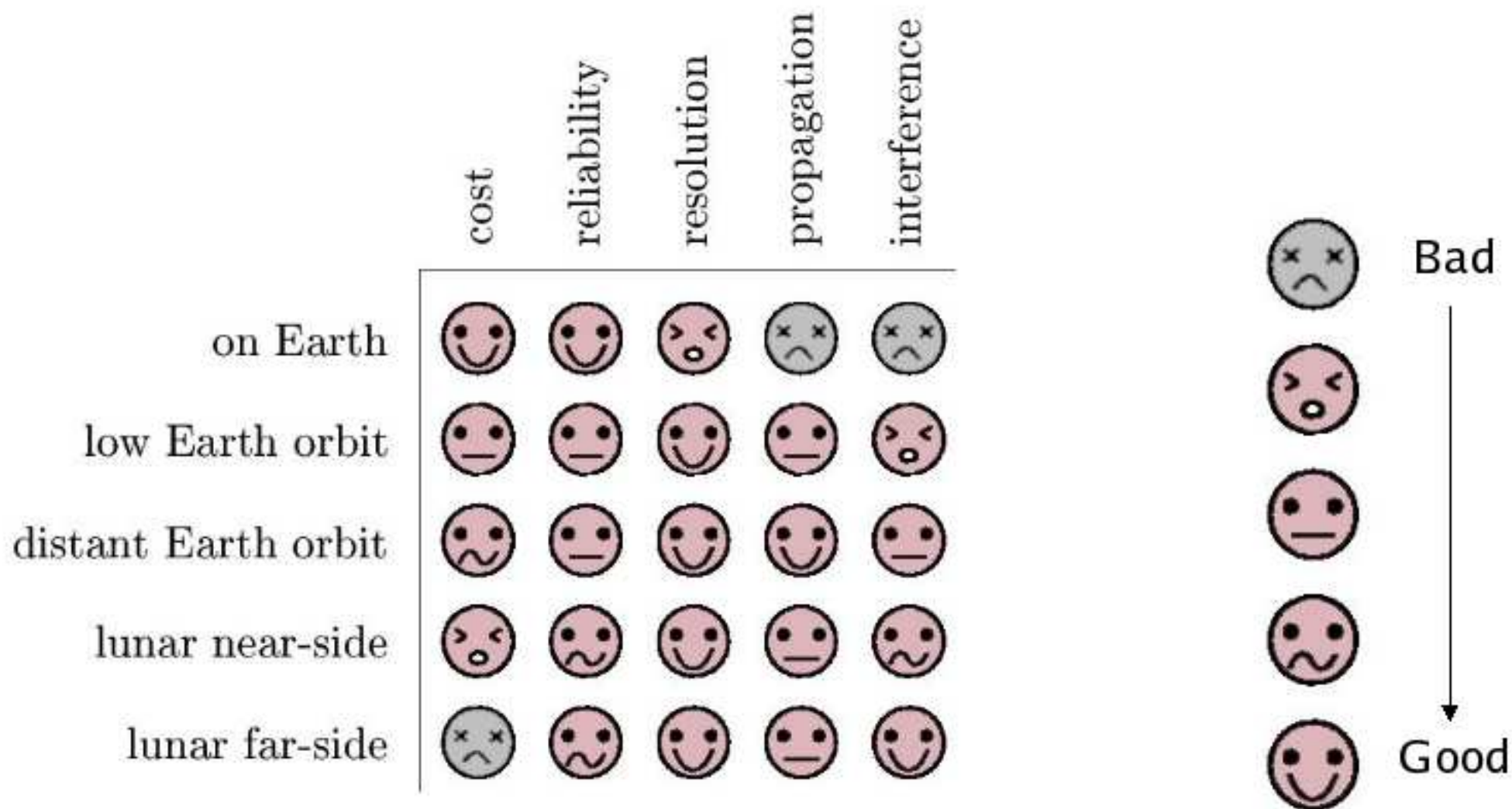
Tsiolkovsky crater  
(100 km diameter)

20°S 129°E

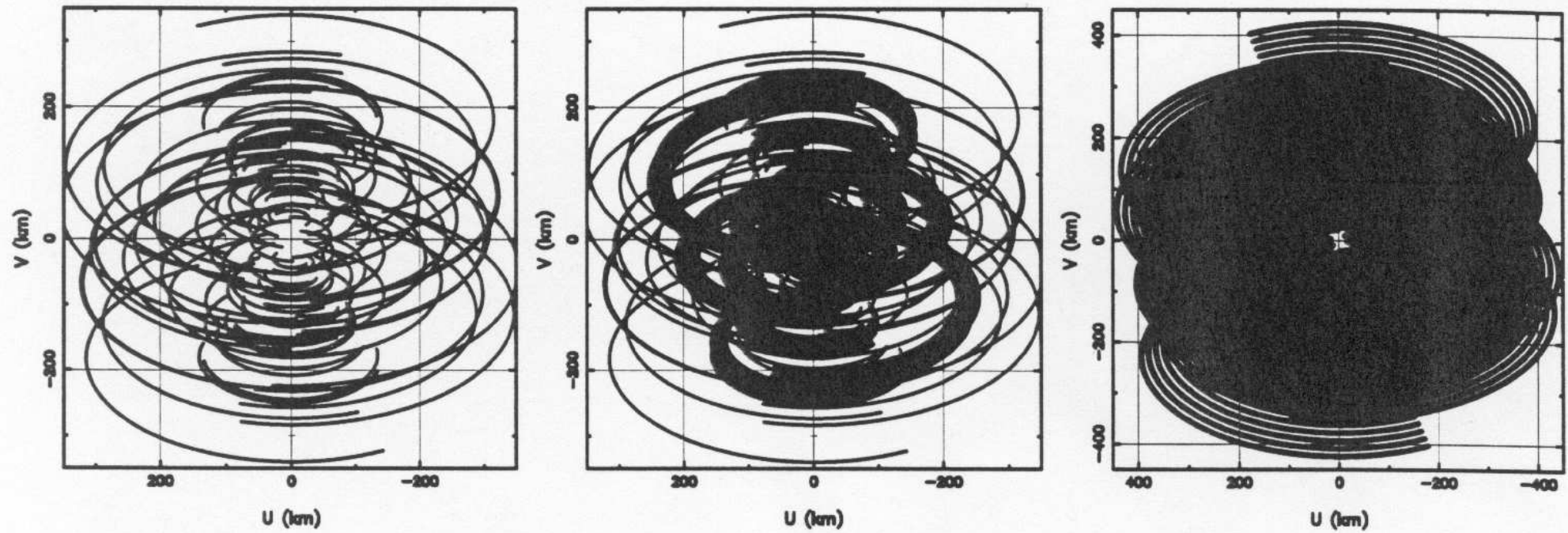


European Lunar Low-Frequency Array (G. Woan, U. Glasgow & ESA)

# environments compared



- (6) LUnar Dark-ages ARray (LUDAR) — How does it work?



- Use Lunar rotation to get 14-day integrations on large patches of sky.
- Fourier UV-tracks for 10 stations fill aperture fairly well (left).
- Multi-frequency UV-tracks will provide better aperture coverage (right).
- FFT of UV-coverage yields PSF, and FFT of (Ampl,  $\phi$ ) yields image.
- (Cannot do free floater, since need baselines  $\gtrsim$  few 100 km, and must rotate aperture to optimally fill UV-plane. Only Moon provides both).

## (7) Conclusions

---

(1) Need large telescopes beyond Earth because of rapid cosmic expansion!

- Golden age of space (& ground)-based telescopes is still ahead.
- JWST will have major impact on First Light and Reionization.

(2) Need Large Radio Interferometer to penetrate the Dark Ages.

- A Radio Interferometer on Moon's far-side will work best.
- This is complex enough to require a large international collaboration.

## (7) Lessons to be learned from new NASA Vision

---

- In the New NASA Vision: Moon/Mars/Beyond, we must keep in mind:

Earth/Moon/Mars/Beyond  $\simeq 10^{51}/10^{49}/10^{50}/10^{80}$  baryons.

(and 96% of the Universe's energy density is not listed here!)

Funding doesn't have to be proportional to these numbers! : )

But, for this new Vision to succeed, we must not forget to:

- (1) Build a balanced program that covers all relevant areas.
- (2) Build strong interdisciplinary ties between fields.
- (3) Use L2 and the Moon to deploy the next generation of telescopes.
- (4) Use the Moon for projects that are too large to do from (Low-Earth or Solar) orbit, and that cannot be done from Earth.
- (5) Build strong international collaborations to establish Lunar projects.

# SPARE CHARTS

---

- References and other sources of material shown:

<http://www.jwst.nasa.gov/>

<http://www.stsci.edu/jwst/>

<http://www.jwst.nasa.gov/ISIM/index.html>

<http://ircamera.as.arizona.edu/nircam/>

<http://ircamera.as.arizona.edu/MIRI/>

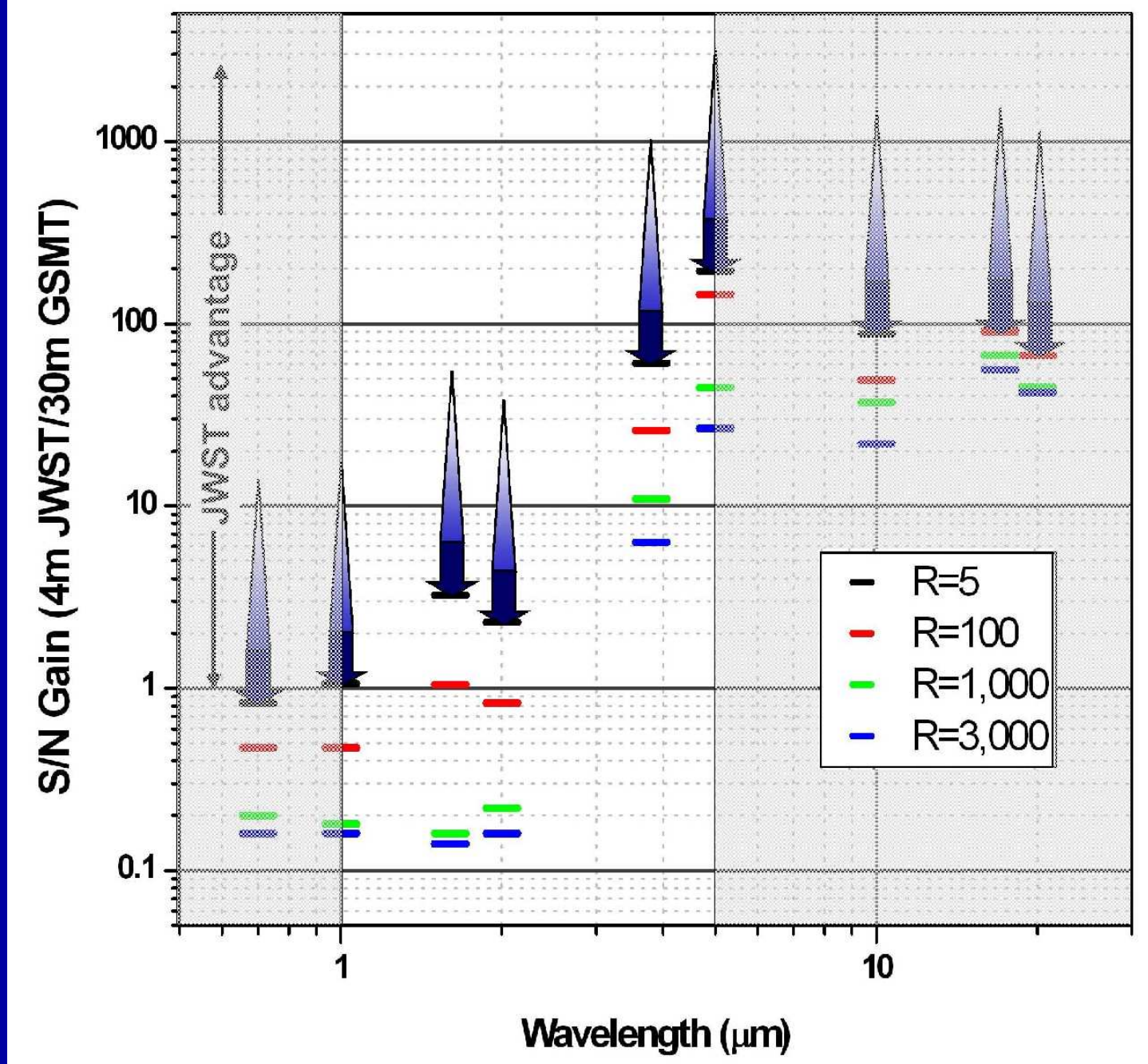
<http://www.stsci.edu/jwst/instruments/nirspec/>

<http://www.stsci.edu/jwst/instruments/nirspec/mems.html>

<http://www.stsci.edu/jwst/instruments/guider/>

Gardner, J., Mather, J., Clampin, M., Greenhouse, M., Hammel, H., Hutchings, J., Jakobsen, P., Lilly, S., Lunine, J., McCaughean, M., Mountain, M., Rieke, G., Rieke, M., Smith, E., Stiavelli, M., Stockman, H., Windhorst, R., & Wright, G. (“the JWST Flight Science Working Group”) 2004, Proc. SPIE, Vol. 4014, p. 001–012, in press “The Science Requirements of the James Webb Space Telescope” (and references therein).

Mather, J., Stockman, H. 2000, Proc. SPIE Vol. 4013, p. 2-16, in “UV, Optical, and IR Space Telescopes and Instruments”, Eds. J. B. Breckinridge & P. Jakobsen (Berlin: Springer)



Conclusion: JWST must not be descoped to a 4 meter Arrows indicate:  
 Top: 6m JWST/Keck; Middle: 6m JWST/30m gb; Bottom: 4m JWST/30m gb



Table 11. Science Instrument Characteristics

Instrument	Wavelength ( $\mu\text{m}$ )	Optical Elements	FPA	Plate Scale (milliarcsec/ pixel)	Field of View
NIRCam (Short Wavelength)	0.6 - 2.3	fixed filters (R~4, R~10, R~100), coronagraphic spots	Two 2×2 mosaics of 2048×2048 arrays	32	2.2×4.4 arcmin
NIRCam (Long Wavelength) <sup>1</sup>	2.4 - 5.0	fixed filters (R~4, R~10, R~100), coronagraphic spots	Two 2048×2048 arrays	65	2.2×4.4 arcmin
NIRSpec (prism, R=100)	0.6 - 5.0	Transmissive slit mask: four 384×175 micro-shutter array, 250 (spectral) by 500 (spatial) milliarcsec; fixed slits 200 or 300 mas wide by 4 arcsec long	Two 2048×2048 arrays	100	3.4×3.1 arcmin
NIRSpec (grating, R=1000)	1.0-5.0				
NIRSpec (IFU, R=3000)	1.0-5.0	Integral field unit	1024×1024	110	3.0×3.0 arcmin
MIRI (imaging)	5 - 27	Broad-band filters, coronagraphic spots & phase masks			
MIRI (prism spectroscopy)	5 - 10	R ~ 100	Two 1024×1024 arrays	200 to 470	1.4×1.9 arcmin (26×26 arcsec coronographic)
MIRI (spectroscopy)	5 - 27	Integral field spectrograph (R~3000) in 4 bands			
TFI (Short-wavelength)	1.2 - 2.4	Order-blocking filters+etalon (R~100)	2048×2048	68	2.3×2.3 arcmin
TFI (Long-wavelength) <sup>2</sup>	2.5 - 4.8	Order-blocking filters+etalon (R~100)	2048×2048	68	2.3×2.3 arcmin

NOTE: <sup>1</sup>Use of a dichroic renders the NIRCam long-wavelength field of view co-spatial with the short wavelength channel, and the two channels acquire data simultaneously.

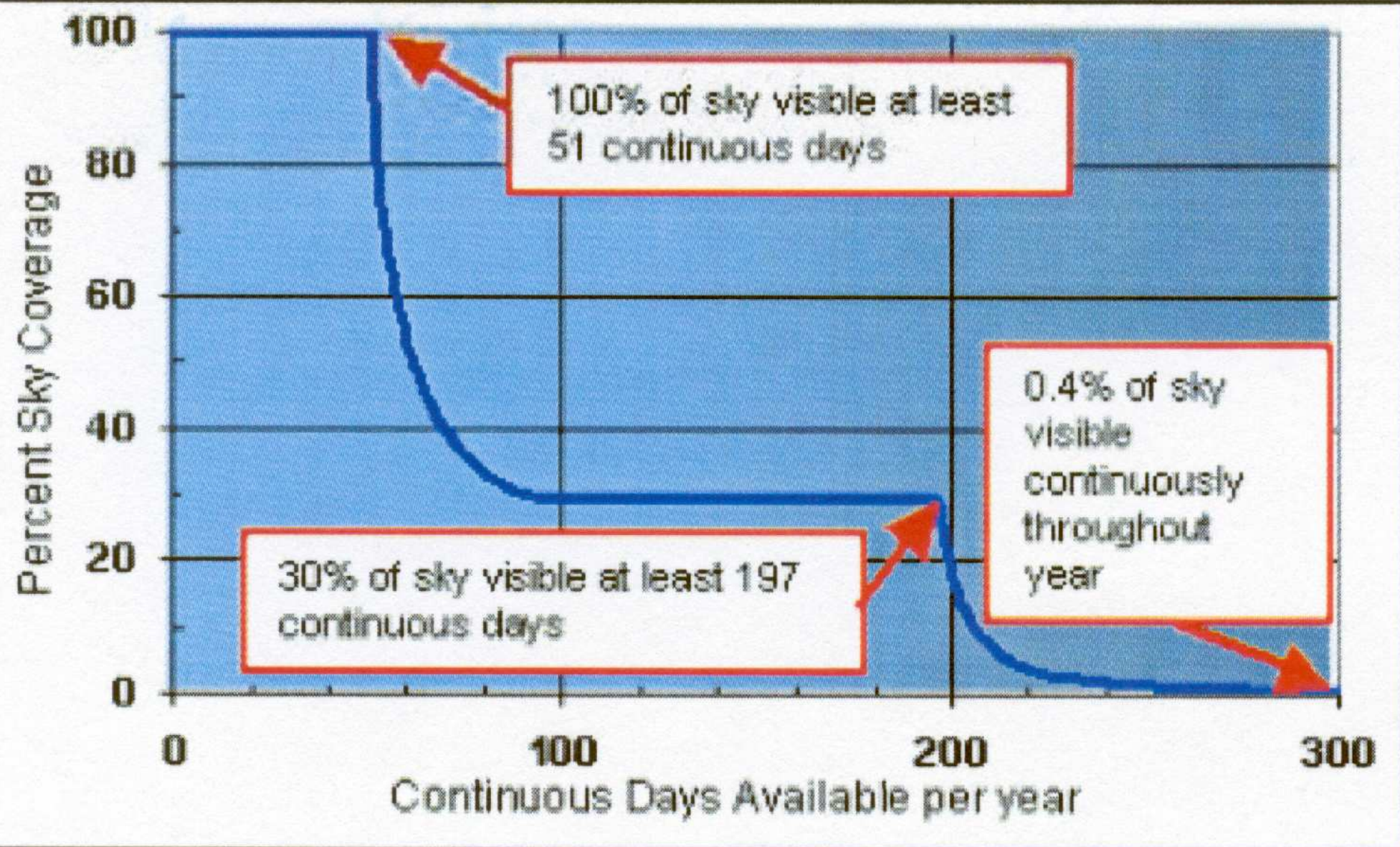


Figure 29. Sky coverage and continuous visibility.

<b>Telescope FOV</b>	~ 166 square arcminutes FOV. ISIM instruments share FOV with common aperture
<b>Orbit</b>	Lissajous orbit about L2
<b>Celestial Sphere Coverage</b>	<p>100% annually</p> <p>39.7% at any given time</p> <p>100% of sphere has at least 51 contiguous days visibility</p> <p>30% for &gt; 197 days</p> <p>Continuous within 5 degrees of ecliptic poles</p>
<b>Overall Observing Efficiency</b>	Observatory ~ 80.7%
<b>Mission Life</b>	<p>5-year minimum lifetime</p> <p>11 years for fuel</p> <p>Commissioning in less than 6 months</p>
<b>Schedule</b>	August 2011 launch

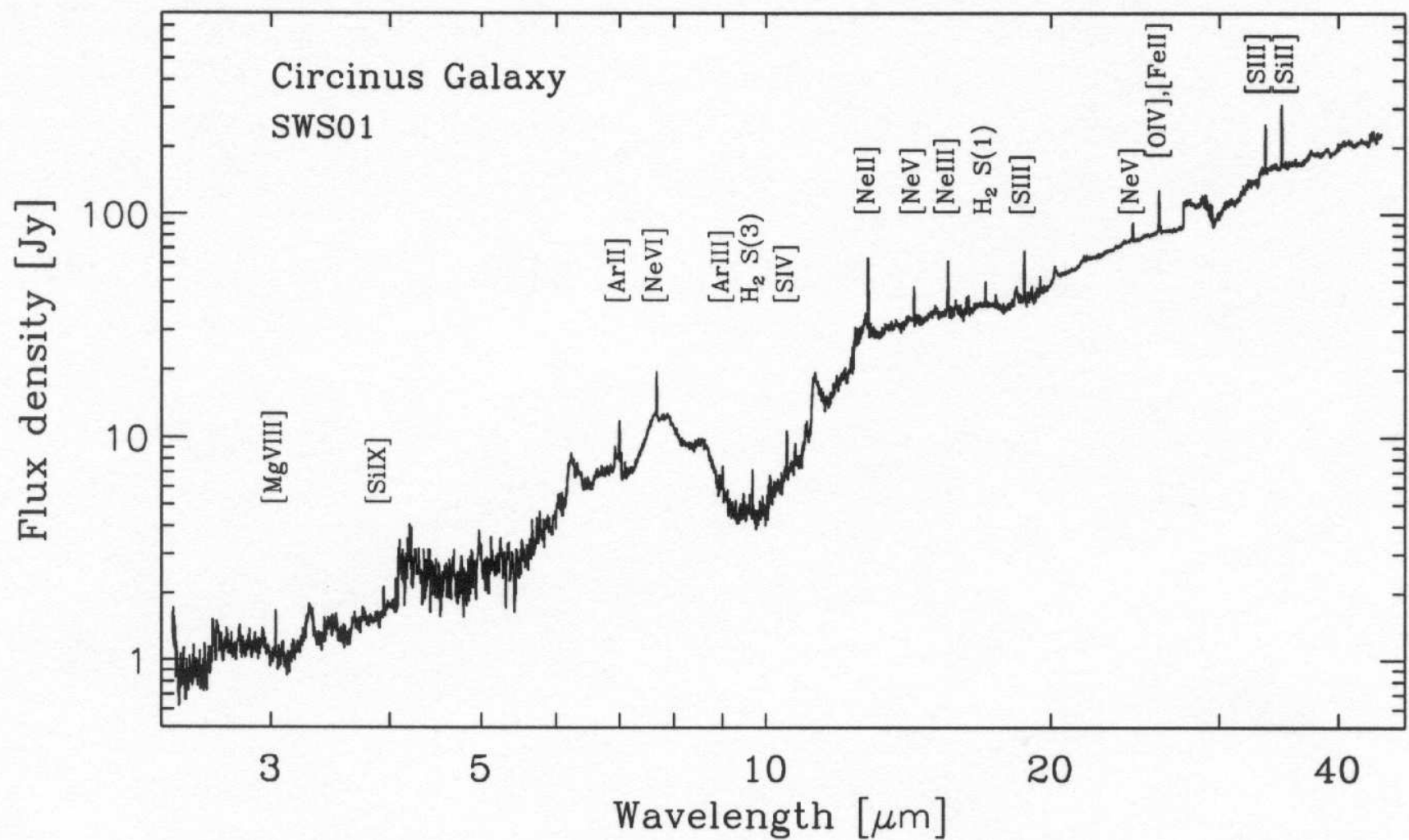


Figure 9. ISO Circinus Spectrum. Mid-infrared spectrum of the Circinus galaxy taken with ISO shows an abundance of emission lines useful for diagnosing the energy sources which power ULIRGs (From Moorwood et al. 1996).

Table 6. Required Sensitivity Values

Wave-length ( $\mu\text{m}$ )	Instrument / Mode	Sensitivity	Equivalents
1.1	NIRCam	$1.21 \times 10^{-34} \text{ Wm}^{-2}\text{Hz}^{-1}$ SN=10 in 10,000 s or less and R=4 bandwidth	12.1 nJy, AB=28.7
2	NIRCam	$1.04 \times 10^{-34} \text{ Wm}^{-2}\text{Hz}^{-1}$ SN=10 in 10,000 s or less and R=4 bandwidth	10.4 nJy, AB=28.9
3.5	TFI	$3.68 \times 10^{-33} \text{ Wm}^{-2}\text{Hz}^{-1}$ SN=10 in 10,000 s or less and R=100 bandwidth	368 nJy, AB=25.0
3.0	NIRSpec/ Low Res	$1.2 \times 10^{-33} \text{ Wm}^{-2}\text{Hz}^{-1}$ SN=10 in 10,000 s or less and R=100 bandwidth	120 nJy, AB=26.2
2.0	NIRspec/ Med Res	$5.2 \times 10^{-22} \text{ Wm}^{-2}$ SN=10 in 100,000 s or less and R=1000 bandwidth	$5.2 \times 10^{-19} \text{ erg s}^{-1} \text{ cm}^{-2}$
10	MIRI/ Broad-Band	$7.0 \times 10^{-33} \text{ Wm}^{-2}\text{Hz}^{-1}$ SN=10 in 10,000 s or less and R=5 bandwidth	700 nJy, AB=24.3
21	MIRI/ Broad-Band	$7.3 \times 10^{-32} \text{ Wm}^{-2}\text{Hz}^{-1}$ SN=10 in 10,000 s or less and R=4.2 bandwidth	7.3 $\mu\text{Jy}$ , AB=21.7
9.2	MIRI/ Spect.	$1.0 \times 10^{-20} \text{ Wm}^{-2}$ SN=10 in 10,000 s or less and R=2400 bandwidth	$1.0 \times 10^{-17} \text{ erg s}^{-1} \text{ cm}^{-2}$
22.5	MIRI/ Spect.	$5.6 \times 10^{-20} \text{ Wm}^{-2}$ SN=10 in 10,000 s or less and R=1200 bandwidth	$5.6 \times 10^{-17} \text{ erg s}^{-1} \text{ cm}^{-2}$

Note: "Sensitivity" is defined to be the brightness of a point source detected with the signal-to-noise ratio and integration time specified. Targets at the North Ecliptic Pole are assumed.

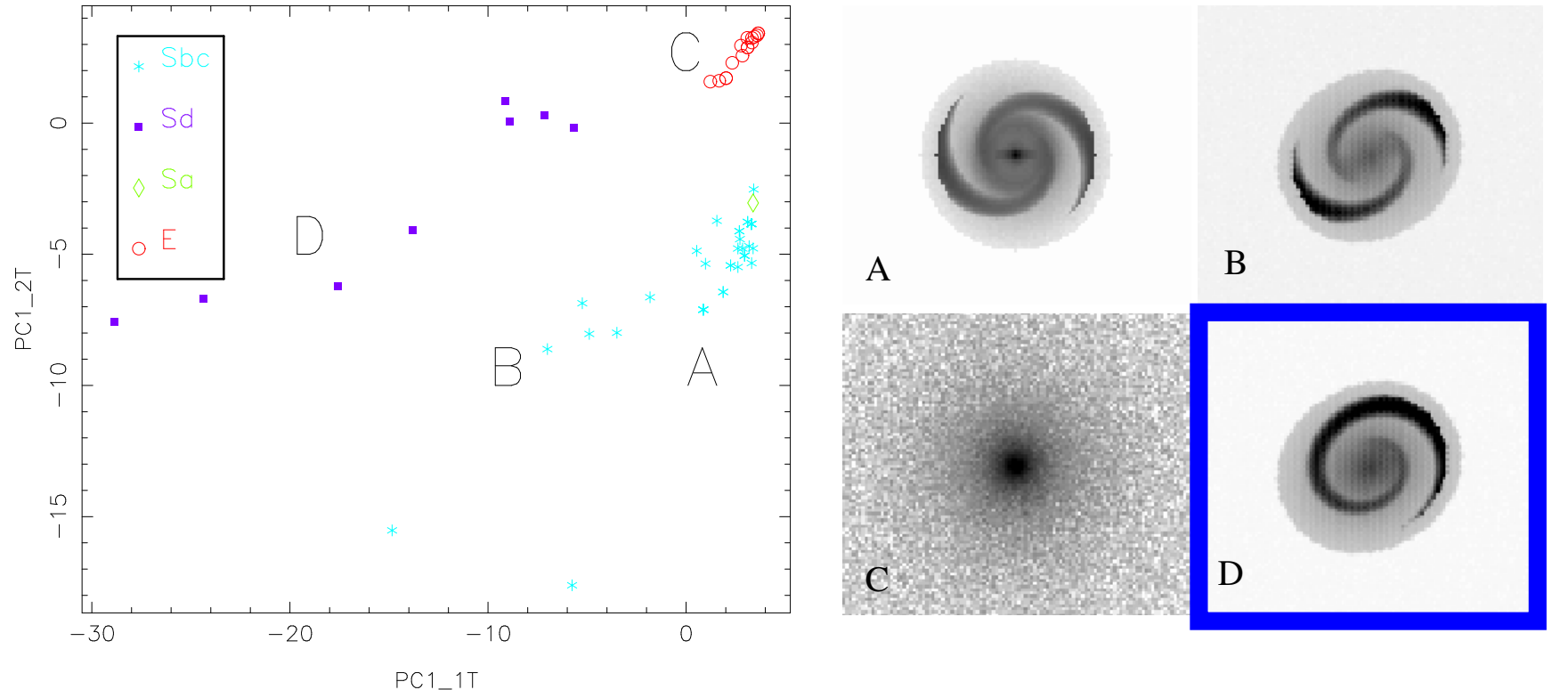
Table 1. JWST Measurements for the End of the Dark Ages Theme

Observation	Primary Instrument	Magnitude or flux	Target Density
Ultra-deep survey, SNe	NIRCam	AB = 31 mag	1 arcmin <sup>-2</sup>
In-depth study	NIRSpec	AB = 28 mag, R~100	1 arcmin <sup>-2</sup>
	MIRI	AB = 28 mag	1 arcmin <sup>-2</sup>
Ly $\alpha$ forest diagnostics	NIRSpec	$2 \times 10^{-19}$ erg cm <sup>-2</sup> s <sup>-1</sup> , R~1000	Individual
Transition in Ly $\alpha$ properties	TFI	$2 \times 10^{-19}$ erg cm <sup>-2</sup> s <sup>-1</sup> , R~1000	1 arcmin <sup>-2</sup>
Transition in Ly $\alpha$ /Balmer	NIRSpec	$2 \times 10^{-19}$ erg cm <sup>-2</sup> s <sup>-1</sup> , R~1000	1 arcmin <sup>-2</sup>
Measure ionizing continuum	NIRSpec	$2 \times 10^{-19}$ erg cm <sup>-2</sup> s <sup>-1</sup> , R~1000	1 arcmin <sup>-2</sup>
Ionization source nature	NIRSpec		
	MIRI		
LF of dwarf galaxies	NIRCam	AB = 31 mag	

Table 2. JWST Measurements for the Assembly of Galaxies Theme

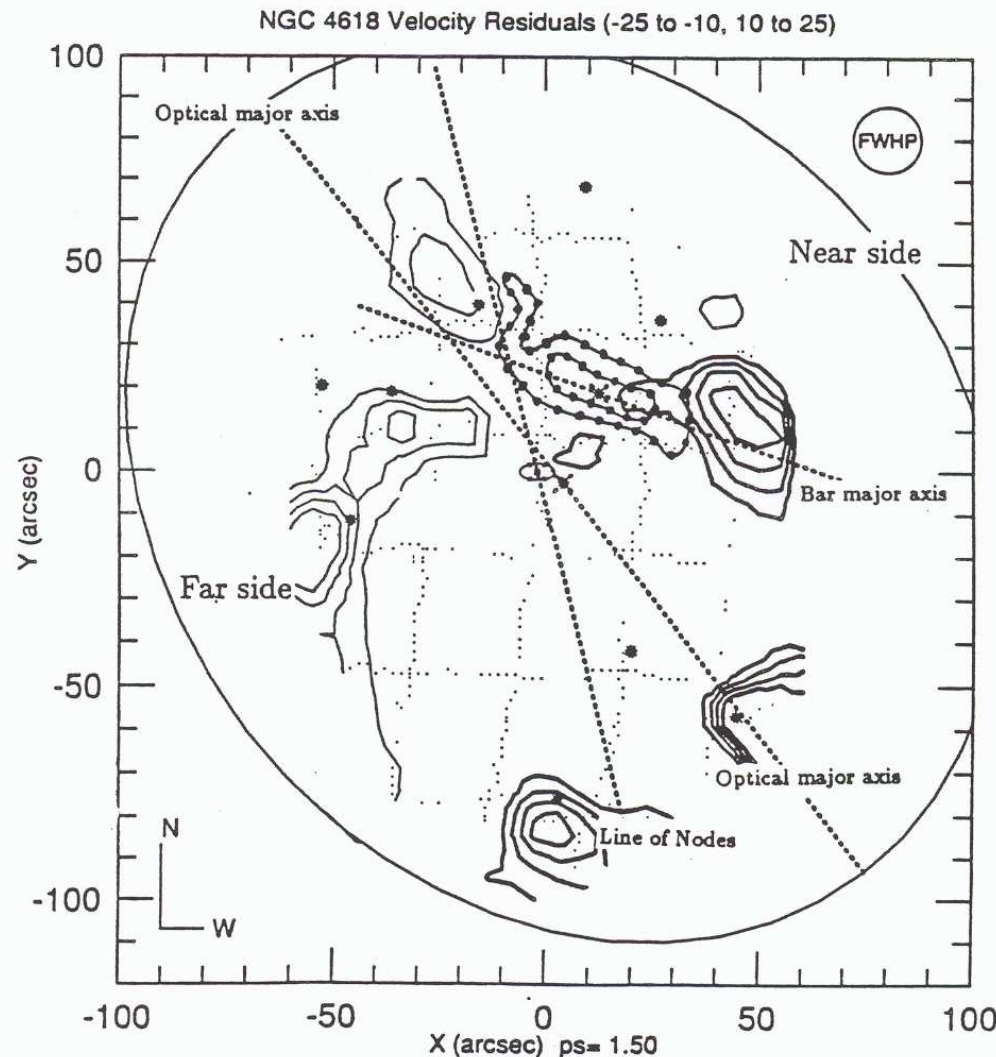
Topic	Primary Instrument	Key Observation	Magnitude or Flux	Target Density
Faint galaxy identification and morphology	NIRCam	Detect the SMC at $z = 5$ in rest-frame V	$L_{AB} = 30.3$ mag	$100 \text{ arcmin}^{-2}$
Metallicity determination	NIRSpec	Determine $R_{23}$ from emission line ratios for galaxy with $\text{SFR} = 3 M_{\odot}/\text{yr}$ at $z = 5$	$5 \times 10^{-19} \text{ erg s}^{-1} \text{ cm}^{-2}$	$100 \text{ arcmin}^{-2}$
Scaling relations	MIRI spectroscopy (short wavelength)	Measure stellar velocity dispersion for $R_{AB}=24.5$ Lyman Break galaxy at $z = 3$	$AB(9\mu\text{m}) = 21.3$ mag	$1 \text{ arcmin}^{-2}$
Obscured galaxies	MIRI spectroscopy (long wavelength)	Measure [NeVI] in ULIRG with Arp220 $L_{\text{bol}}$ assuming Circinus spectrum	$1.4 \times 10^{-19} \text{ W m}^{-2}$	Individual

# Quantitative Morphology – We can numerically describe and identify $m=1$ galaxies!



Odewahn et.al. 2002 ApJ, 568, 539

Fourier Decomposition is remarkably good in distinguishing and quantifying bars and (1-armed, 2-armed) spiral structure. JWST will be able to do this out to  $z=5$  at least, hence enabling to quantitatively trace galaxy assembly.



## H $\alpha$ Kinematics in NGC 4618 (Odewahn 1990)

Substantial departures  
from circular motion  
in  $m=1$  arms, OFTEN  
accompanied by large  
OB associations (SSC?)

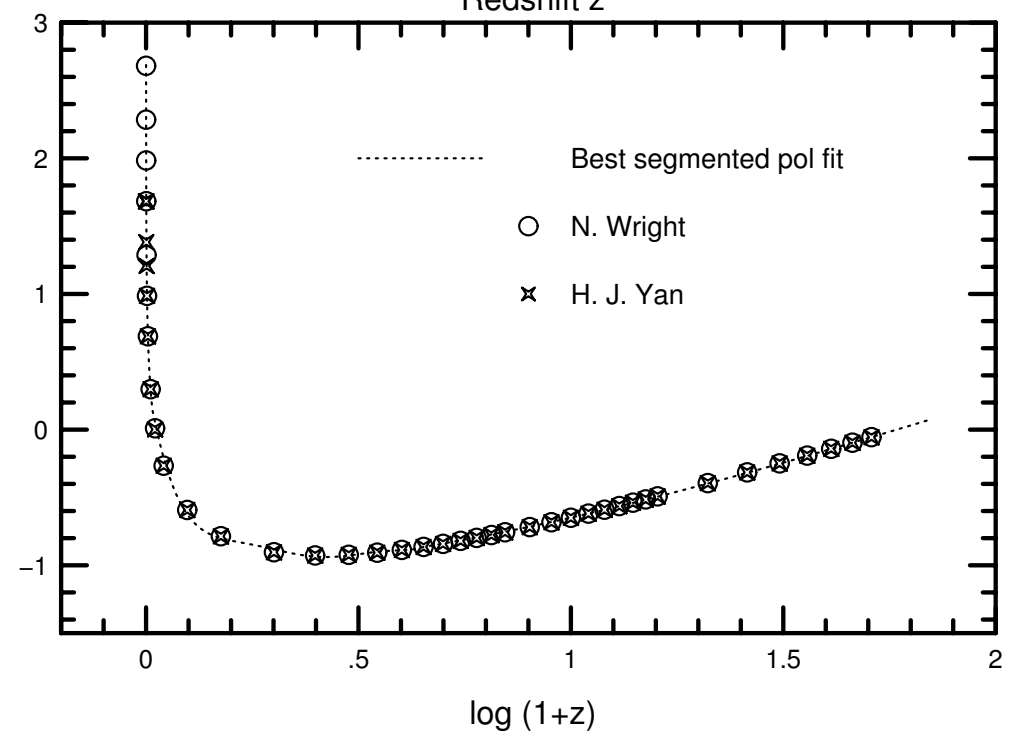
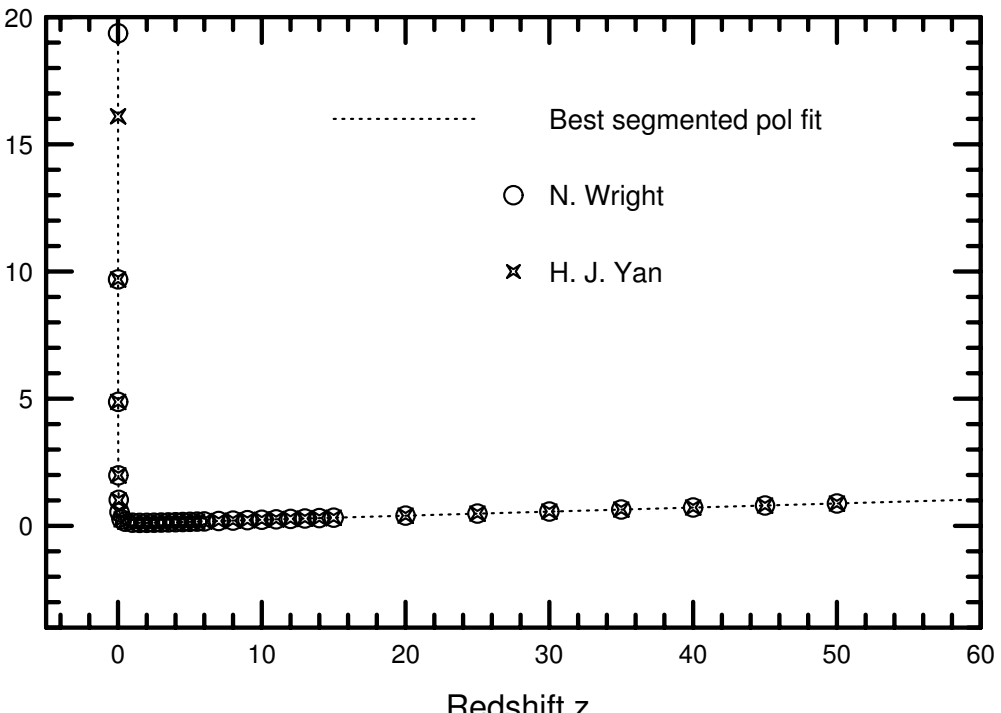
Spatially resolved NIRSpec and MIRI integral-field spectra of distant galaxies when compared to the quantitative structure from NIRCam Fourier Decompositions, will directly trace the physical causes of locally enhanced star-formation: infall, bulk velocities in excess of regular rotation, etc.

## (5) Details on JWST image simulations:

- All based on HST/WFPC2 F300W images from the HST mid-UV survey of nearby galaxies (Windhorst et al. 2002,ApJ Suppl. 143, 113).
- WMAP COSMOLOGY:  $H_0=71 \text{ km/s/Mpc}$ ,  $\Omega_m=0.27$ ,  $\Omega_\Lambda=0.73$ .
- INSTRUMENT: 6.0 m effective aperture, diffraction limited at  $\lambda \gtrsim 2.0 \mu\text{m}$ , JWST/NIRCam,  $0''.034/\text{pix}$ , read-noise=5.0 e<sup>-</sup>, dark-current=0.02 e<sup>-</sup>/s, NEP-Sky(1.6  $\mu\text{m}$ )=21.7 mag/( $''^2$ ) in L2, Zodi spectrum,  $t_{exp}=4 \times 900\text{s}$ .

Row	Telesc.	Redshift	$\lambda (\mu\text{m})$	FWHM ( $''$ )
1	HST	$z \sim 0$	$0.293 \mu\text{m}$	$0''.04$
	JWST	$z=1.0$	$0.586 \mu\text{m}$	$0''.084$
	JWST	$z=2.0$	$0.879 \mu\text{m}$	$0''.084$
2	JWST	$z=3.0$	$1.17 \mu\text{m}$	$0''.084$
	JWST	$z=5.0$	$1.76 \mu\text{m}$	$0''.084$
	JWST	$z=7.0$	$2.34 \mu\text{m}$	$0''.098$
3	JWST	$z=09.0$	$2.93 \mu\text{m}$	$0''.122$
	JWST	$z=12.0$	$3.81 \mu\text{m}$	$0''.160$
	JWST	$z=15.0$	$4.69 \mu\text{m}$	$0''.197$

Theta-z relation for  $H_0=71$ ,  $\Omega_m=0.27$ ,  $\Omega_\Lambda=0.73$



Angular size vs. redshift relation in a Lambda dominated cosmology of  $H_0 = 71 \text{ km s}^{-1} \text{ Mpc}^{-1}$ ,  $\Omega_m=0.27$ ,  $\Omega_\Lambda=0.73$ .

In the top panel the relation is nearly linear in  $1/z$  for  $z \lesssim 0.05$  (the small angle approximation) and linear in  $z$  for  $z \gtrsim 3$  (the Lambda dominated universe).

All curvature occurs in the range  $0.05 \lesssim z \lesssim 3$ , which is coded up in the IRAF script that does the JWST simulations.

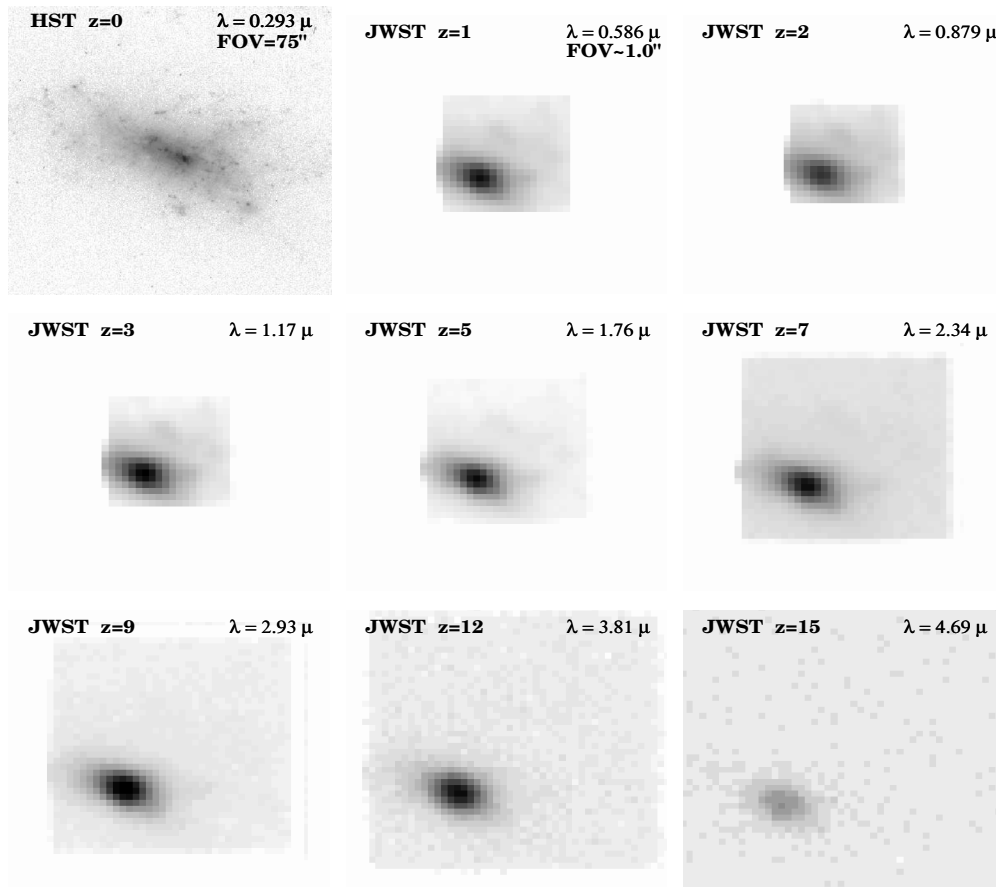


**Fig. 4.01.** JWST simulations based on HST/WFPC2 F300W images of the dwarf irregular NGC1140 ( $z=0.0050$ ). This compact high SB object would be visible to  $z\simeq15$ , but hard to classify at all  $z\geq1$ .

ASSUMPTIONS: COSMOLOGY:  $H_0=71$  km/s/Mpc,  $\Omega_m=0.27$ , and  $\Omega_\Lambda=0.73$ .

INSTRUMENT: 6.0 m effective aperture, JWST/NIRCam,  $0.034''/\text{pix}$ ,  $RN=5.0 \text{ e}^-$ ,  $\text{Dark}=0.020 \text{ e}^-/\text{sec}$ , NEP  $H\text{-band Sky}=21.7 \text{ mag/arcsec}^2$  in L2, Zodiacial spectrum,  $t_{exp}=1.0 \text{ hrs}$ , read-out every 900 sec.

**Row 1:**  $z=0.0$  (HST  $\lambda=0.293\mu\text{m}$ , FWHM= $0.04''$ ),  $z=1.0$  (JWST  $\lambda=0.586\mu\text{m}$ , FWHM= $0.084''$ ), and  $z=2.0$  (JWST  $\lambda=0.879\mu\text{m}$ , FWHM= $0.084''$ ).

**Row 2:**  $z=3.0$  (JWST  $\lambda=1.17\mu\text{m}$ , FWHM= $0.084''$ ),  $z=5.0$  (JWST  $\lambda=1.76\mu\text{m}$ , FWHM= $0.084''$ ), and  $z=7.0$  (JWST  $\lambda=2.34\mu\text{m}$ , FWHM= $0.098''$ ).

**Row 3:**  $z=9.0$  (JWST  $\lambda=2.93\mu\text{m}$ , FWHM= $0.122''$ ),  $z=12.0$  (JWST  $\lambda=3.81\mu\text{m}$ , FWHM= $0.160''$ ), and  $z=15.0$  (JWST  $\lambda=4.69\mu\text{m}$ , FWHM= $0.197''$ )

The compact high-SB dwarf irregular galaxy NGC1140 ( $z=0.0050$ ).

With JWST, this object would be visible to  $z\simeq15$ , but it will be hard to classify at all redshifts  $z\geq1$ .

Note that the object indeed reaches a minimum angular size at  $z\simeq1.7$ .

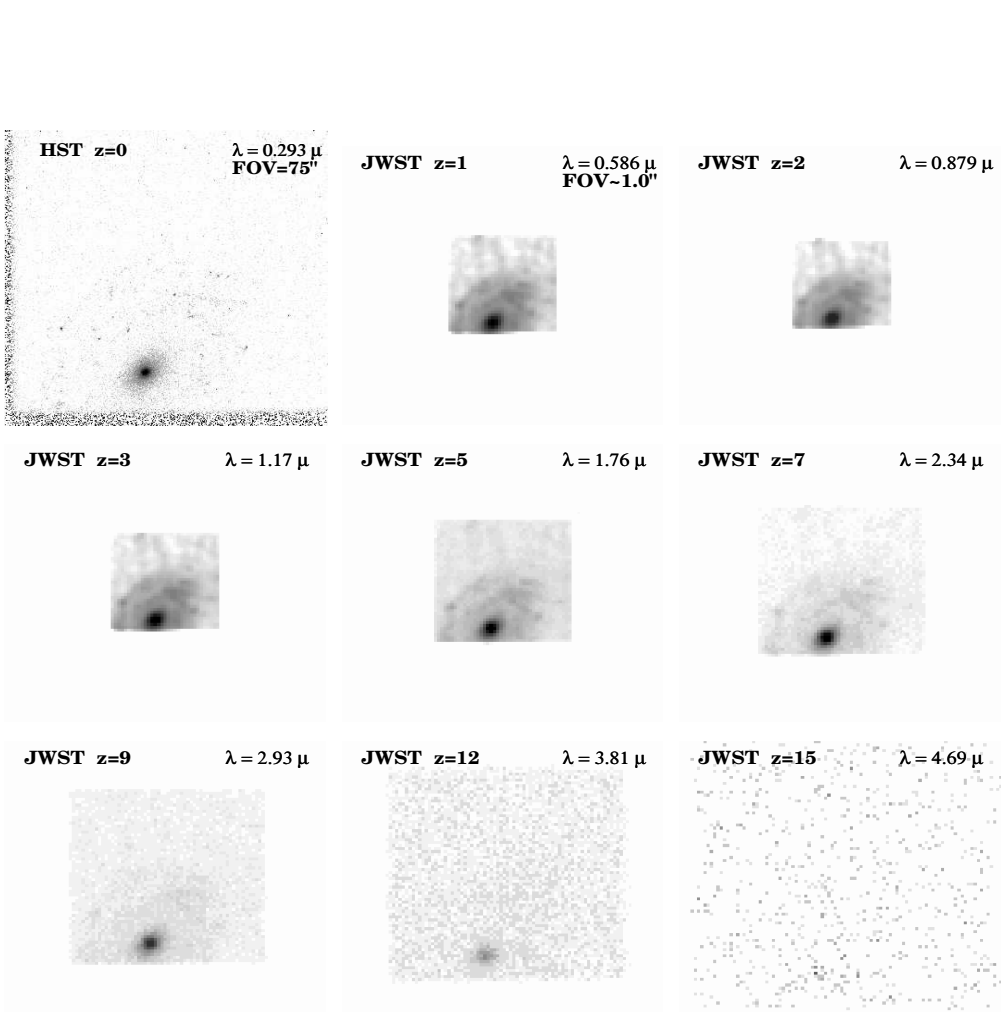


**Fig. 4.02.** JWST simulations based on HST/WFPC2 F300W images of the mid-type spiral NGC2551 (0.0078). Such an object would be visible to  $z \approx 10$ , but only recognizable to  $z \approx 7$ .

ASSUMPTIONS: COSMOLOGY:  $H_0=71$  km/s/Mpc,  $\Omega_m=0.27$ , and  $\Omega_\Lambda=0.73$ .

INSTRUMENT: 6.0 m effective aperture, JWST/NIRCam,  $0.034''/\text{pix}$ ,  $RN=5.0\text{ e}^-$ ,  $\text{Dark}=0.020\text{ e}^-\text{/sec}$ , NEP H-band Sky= $21.7\text{ mag/arcsec}^2$  in L2, Zodiacal spectrum,  $t_{\text{exp}}=1.0\text{ hrs}$ , read-out every 900 sec.

**Row 1:**  $z=0$  (HST  $\lambda=0.293\mu\text{m}$ , FWHM= $0.04''$ ),  $z=1.0$  (JWST  $\lambda=0.586\mu\text{m}$ , FWHM= $0.084''$ ), and  $z=2.0$  (JWST  $\lambda=0.879\mu\text{m}$ , FWHM= $0.084''$ ).

**Row 2:**  $z=3.0$  (JWST  $\lambda=1.17\mu\text{m}$ , FWHM= $0.084''$ ),  $z=5.0$  (JWST  $\lambda=1.76\mu\text{m}$ , FWHM= $0.084''$ ), and  $z=7.0$  (JWST  $\lambda=2.34\mu\text{m}$ , FWHM= $0.098''$ ).

**Row 3:**  $z=9.0$  (JWST  $\lambda=2.93\mu\text{m}$ , FWHM= $0.122''$ ),  $z=12.0$  (JWST  $\lambda=3.81\mu\text{m}$ , FWHM= $0.160''$ ), and  $z=15.0$  (JWST  $\lambda=4.69\mu\text{m}$ , FWHM= $0.197''$ )

The mid-type spiral NGC2551 ( $z=0.0078$ ) would be visible out to  $z \approx 10$ , but only recognizable out to  $z \approx 7$ .

Its disk is in principle visible to  $z \gtrsim 5-7$ . Hence, if such objects are not seen by JWST at  $z \lesssim 3$ , then disks likely form at  $z \lesssim 3$ .

With HST we have seen glimpses of this, but with JWST these will become robust conclusions.

ST z=0

$\lambda = 0.293 \mu$   
**FOV=75"**

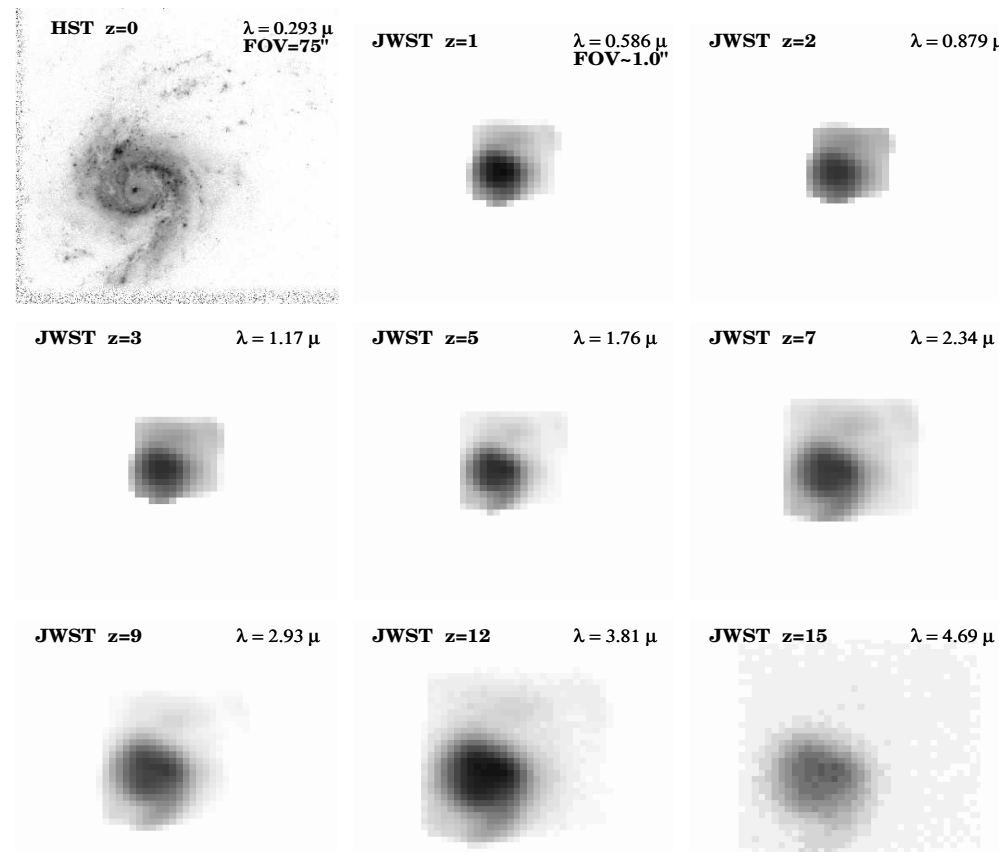


**Fig. 4.03.** JWST simulations based on HST/WFPC2 F300W images of the high-SB starbursting dwarf spiral galaxy NGC3310 (0.0033). The minimum in the  $\Theta$ -z relation at  $z \simeq 1.7$  and the JWST diffraction limit at  $\lambda \geq 2.2 \mu\text{m}$  — combined with the object's very high rest-frame UV SB — conspire to improve the effective JWST resolution on the mid-UV morphology of this object from  $z \simeq 2$  to  $z \simeq 7$ .

ASSUMPTIONS: COSMOLOGY:  $H_0=71 \text{ km/s/Mpc}$ ,  $\Omega_m=0.27$ , and  $\Omega_\Lambda=0.73$ . INSTRUMENT: 6.0 m effective aperture, JWST/NIRCam,  $0.034''/\text{pix}$ ,  $RN=5.0 \text{ e}^-$ ,  $\text{Dark}=0.020 \text{ e}^-/\text{sec}$ , NEP H-band Sky=21.7 mag/arcsec<sup>2</sup> in L2, Zodiocal spectrum,  $t_{exp}=1.0 \text{ hrs}$ , read-out every 900 sec.

**Row 1:**  $z=0.0$  (HST  $\lambda=0.293 \mu\text{m}$ , FWHM=0.04''),  $z=1.0$  (JWST  $\lambda=0.586 \mu\text{m}$ , FWHM=0.084''), and  $z=2.0$  (JWST  $\lambda=0.879 \mu\text{m}$ , FWHM=0.084''). **Row 2:**  $z=3.0$  (JWST  $\lambda=1.17 \mu\text{m}$ , FWHM=0.084''),  $z=5.0$  (JWST  $\lambda=1.76 \mu\text{m}$ , FWHM=0.084''), and  $z=7.0$  (JWST  $\lambda=2.34 \mu\text{m}$ , FWHM=0.098''). **Row 3:**  $z=9.0$  (JWST  $\lambda=2.93 \mu\text{m}$ , FWHM=0.122''),  $z=12.0$  (JWST  $\lambda=3.81 \mu\text{m}$ , FWHM=0.160''), and  $z=15.0$  (JWST  $\lambda=4.69 \mu\text{m}$ , FWHM=0.197'')

The very high-SB, compact starbursting dwarf spiral galaxy NGC3310 ( $z=0.0033$ ).

The minimum in the  $\Theta$ -z relation at  $z \simeq 1.7$  and the JWST diffraction limit at  $\lambda \geq 2.2 \mu\text{m}$  — combined with the object's very high rest-frame UV-SB — conspire to improve the effective JWST resolution on the mid-UV morphology of this object from  $z \simeq 2$  to  $z \simeq 7$ .

A rather exceptional case of where nasty cosmology doesn't appear to cost you prohibitive sensitivity, but gains you resolution!

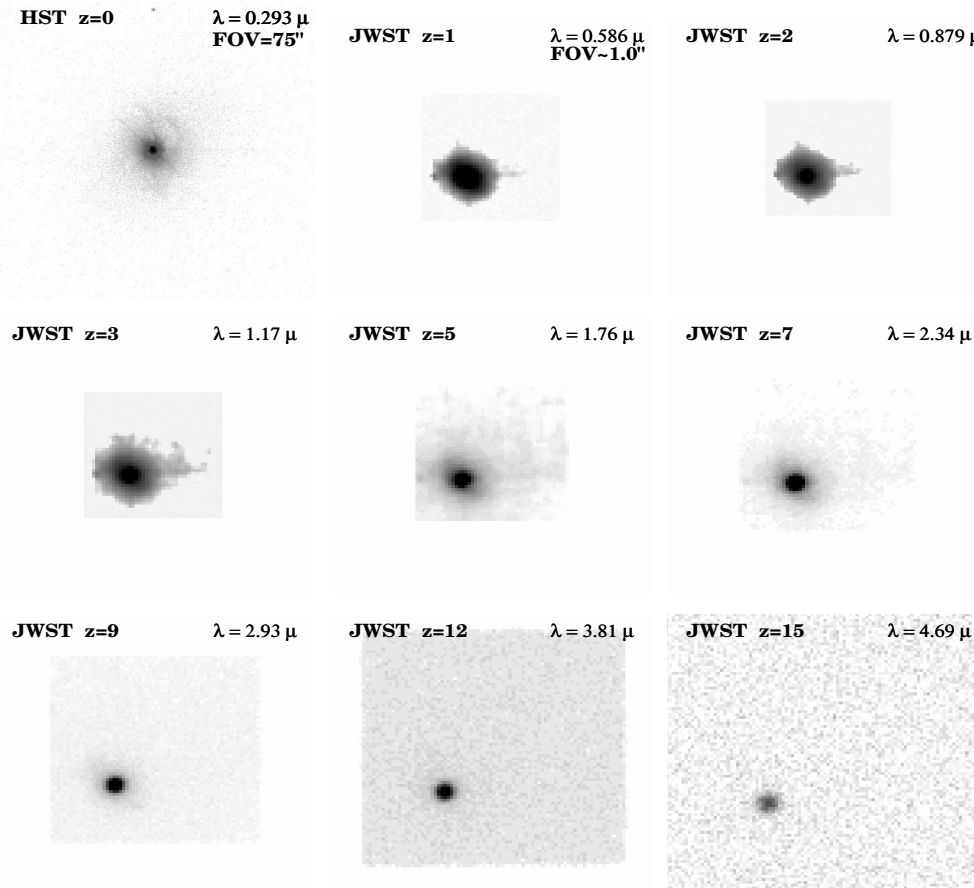


**Fig. 4.04.** JWST simulations based on HST/WFPC2 F300W images of the Seyfert galaxy NGC3516 (0.0088). Note that the faint nebulosity surrounding the AGN in the mid-UV at  $z=0$  essentially disappears at  $z \geq 7$ , so that at high redshifts such objects would look like a pure AGN.

ASSUMPTIONS: COSMOLOGY:  $H_0=71$  km/s/Mpc,  $\Omega_m=0.27$ , and  $\Omega_\Lambda=0.73$ .

INSTRUMENT: 6.0 m effective aperture, JWST/NIRCam,  $0.034''/\text{pix}$ ,  $RN=5.0\text{ e}^-$ ,  $\text{Dark}=0.020\text{ e}^-\text{/sec}$ , NEP H-band Sky=21.7 mag/arcsec<sup>2</sup> in L2, Zodiacal spectrum,  $t_{exp}=1.0$  hrs, read-out every 900 sec.

**Row 1:**  $z=0.0$  (HST  $\lambda=0.293\mu\text{m}$ , FWHM= $0.04''$ ),  $z=1.0$  (JWST  $\lambda=0.586\mu\text{m}$ , FWHM= $0.084''$ ), and  $z=2.0$  (JWST  $\lambda=0.879\mu\text{m}$ , FWHM= $0.084''$ ). **Row 2:**  $z=3.0$  (JWST  $\lambda=1.17\mu\text{m}$ , FWHM= $0.084''$ ),  $z=5.0$  (JWST  $\lambda=1.76\mu\text{m}$ , FWHM= $0.084''$ ), and  $z=7.0$  (JWST  $\lambda=2.34\mu\text{m}$ , FWHM= $0.098''$ ). **Row 3:**  $z=9.0$  (JWST  $\lambda=2.93\mu\text{m}$ , FWHM= $0.122''$ ),  $z=12.0$  (JWST  $\lambda=3.81\mu\text{m}$ , FWHM= $0.160''$ ), and  $z=15.0$  (JWST  $\lambda=4.69\mu\text{m}$ , FWHM= $0.197''$ )

The Seyfert galaxy NGC3516 ( $z=0.0088$ ) has a faint nebulosity surrounding its AGN in the mid-UV, while at longer wavelengths the surrounding elliptical galaxy is present (not shown here).

The nebulosity surrounding the AGN is essentially SB-dimmed away at  $z \geq 7$ , so that at high redshifts these objects would look like purely stellar objects (“quasars”).

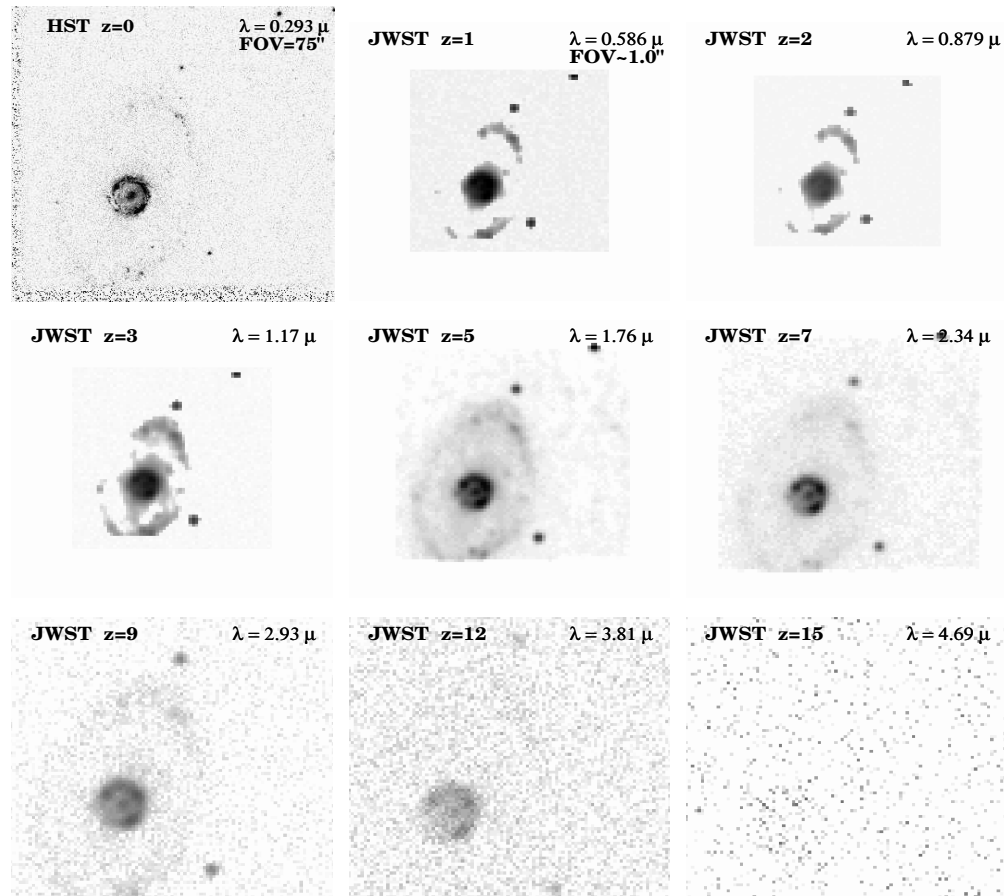


**Fig. 4.05.** JWST simulations based on HST/WFPC2 F300W images of the barred ring galaxy NGC6782 (0.0125). Note again that for  $z \simeq 2\text{--}7$ , the effective resolution on the bright star-forming ring improves with increasing redshift, until the  $(1+z)^4$ -dimming completely kills it for  $z \gtrsim 10$ .

ASSUMPTIONS: COSMOLOGY:  $H_0=71$  km/s/Mpc,  $\Omega_m=0.27$ , and  $\Omega_\Lambda=0.73$ .

INSTRUMENT: 6.0 m effective aperture, JWST/NIRCam,  $0.034''/\text{pix}$ ,  $RN=5.0 \text{ e}^-$ ,  $\text{Dark}=0.020 \text{ e}^-/\text{sec}$ , NEP H-band Sky=21.7 mag/arcsec<sup>2</sup> in L2, Zodiacal spectrum,  $t_{exp}=1.0$  hrs, read-out every 900 sec.

**Row 1:**  $z=0$  (HST  $\lambda=0.293\mu\text{m}$ , FWHM=0.04''),  $z=1.0$  (JWST  $\lambda=0.586\mu\text{m}$ , FWHM=0.084''), and  $z=2.0$  (JWST  $\lambda=0.879\mu\text{m}$ , FWHM=0.084''). **Row 2:**  $z=3.0$  (JWST  $\lambda=1.17\mu\text{m}$ , FWHM=0.084''),  $z=5.0$  (JWST  $\lambda=1.76\mu\text{m}$ , FWHM=0.084''), and  $z=7.0$  (JWST  $\lambda=2.34\mu\text{m}$ , FWHM=0.098''). **Row 3:**  $z=9.0$  (JWST  $\lambda=2.93\mu\text{m}$ , FWHM=0.122''),  $z=12.0$  (JWST  $\lambda=3.81\mu\text{m}$ , FWHM=0.160''), and  $z=15.0$  (JWST  $\lambda=4.69\mu\text{m}$ , FWHM=0.197'')

The barred ring galaxy NGC6782 (0.0125) shows that at  $z \simeq 2$  to  $z \simeq 7$ , the effective resolution on its high-SB bright star-forming ring improves with increasing redshift, until the  $(1+z)^4$ -dimming completely kills it for  $z \gtrsim 10\text{--}12$ .

Another good case showing why cosmology is not “WYSIWYG”.